MINIMUM VARIANCE ORBIT DETERMINATION PROGRAM

FIRST
QUARTERLY STATUS
REPORT

22 July 1963 to 22 October 1963

MINIMUM VARIANCE ORBIT DETERMINATION PROGRAM

FIRST
QUARTERLY STATUS
REPORT

22 July 1963 to 22 October 1963

Sperry Report No. AB-1210-0018

Prepared for: NATIONAL AERONAUTICS AND SPACE ADMINISTRATION
GODDARD SPACE FLIGHT CENTER
GREENBELT, MARYLAND

Contract No. NAS5-3509

Prepared by: Sperry Rand Systems Group
Sperry Gyroscope Company
Great Neck, New York

8 November 1963

Copy No. 01

TABLE OF CONTENTS

1.0. SUMMARY OF FIRST QUARTERLY STATUS,

ORBIT DETERMINATION PROGRAM

In this report are presented detailed technical summaries of the effort accomplished on Phase II of the Orbit Determination Program for the period July 22 to October 22, 1963, inclusive. Efforts carried out under Phase I which are applicable to the precision version of the Program are reported here as well. 1827

Section 2.0 exhaustively defines the coordinate transformations which have been or will be included in MINIVAR. These transformations have been taken from the astronomical literature and their primary purpose is to reduce positions and velocities specified in moving coordinate systems to corresponding quantities in an inertial coordinate system. The inertial system is specified by the mean equator and equinox obtaining at $o^h.o$ January 1 of the year subsequent to the year in which the trajectory of interest takes place. Astronomical ephemerides used in the Program are referenced to this base date system, and all trajectory computation takes place in this system. In addition to position and velocity transformations, provision has been made for transforming the earth's gravitational force field into the same inertial frame. Libration transformations have been included for the two-fold purpose of specifying vehicle position and velocity with respect to selonographic coordinates rigidly attached to the lunar surface, and transforming the moon's gravitational force field to the base date inertial reference. The work reported in this Section was developed under Phase I. Author

Some of the transformations reported in Section 2.0, particularly those dealing with precession and nutation, are approximations. The same astronomical literature from which these approximations were obtained, however, report more accurate versions for the elements of the transformation matrices. In Section 3.0, the equations for these higher accuracy quantities have been tabulated. In the case of nutation particularly, the amount of computation required to obtain the increased accuracy is quite large, and, before including such expressions in the program tests will be made to determine whether or not the increased accuracy affects the desired Program precision.

Section 4.0 derives an equation for computing timing signal delay from WWV to a range-and-range-rate tracking station. An error analysis is included to illustrate the error magnitudes to be expected in a few typical cases.

Timing errors in Minitrack and range-and-range-rate systems data are described in Section 5.0, and methods for correcting these errors are outlined. A technique for resolving range ambiguities in R&R data is described.

The work reported in Sections 4.0 and 5.0 was carried out under Phase I.

Results from a comprehensive evaluation of precision in FORTRAN IV

single and double precision subroutines are given in Section 6.0. Common routines such as sine, cosine, arctangent, square root, and exponential were tested; the test results were generally in close agreement with the published precisions for these routines.

Recommendations are made in Section 7.0 for storing atmospheric models for the Earth, Venus, Mars and Jupiter. Interpolation procedures are suggested, and, for the lower and upper Earth atmosphere models, characteristics for a transition region are recommended to overcome discontinuities in both the models and the applicable drag equations.

Matrix inversions are minimized by the Kalman filtering process; nonetheless, at least one matrix (Y) must be inverted in order to compute the optimum weighting matrix for the residuals. Section 8.0 describes a method whereby a matrix having an order up to 8 x 8 may be inverted through use of an approximation to the true inverse and an iteration procedure for refining this estimate.

Sections 9.0 and 10.0 are both related to the use of two-body trajectories in the Orbit Determination Program. A central-difference numerical differentiation formula is derived in Section 9.0; the uses of this formula are to be:

a. a measure of the precision attainable in computing the elements of the two-body state transition matrix, whether by means of the variational parameters now used in MINIVAR or by some other technique;

b. a method for obtaining the elements of the true transition matrix in those instances for which the two-body approximation is inadequate.

Section 10.0 treats the problem of accurately representing two-body motion, with particular attention being given to a universal representation applicable to all conics. Herrick's variables offer promise in this direction, and two methods are under consideration for overcoming difficulties arising from large values of the independent variable. One method suggested by Herrick, employs a "shifted epoch" to maintain reasonable values of the time-dependent argument; the other approach calls for the use of continued fractions rather than infinite series in representing the variables so as to delimit the number of terms which must be carried for a specified accuracy. Section 10.0 also describes a two-body representation in terms of range angle or differential true anomaly. A program exists in this formulation which computes not only the conic but also the elements of the state transition matrix.

Bias errors to be included in MINIVAR are discussed in Section 11.0. Among these errors are station location errors, uncertainty in the knowledge of Earth's mass and oblateness terms, and uncertainties in the velocity of light and the astronomical unit. Section 11.0 discusses augmentation of the state transition matrix and the point transformation matrices associated with the variational parameters.

Another aspect of the two-body problem is treated in Section 12.0.

A program is described whereby the effect of errors in the elements of the state transition matrix on the elements of the Kalman filter K may be computed. It is desirable to maintain the same precision in K as that contained in the residual, $(y_c - y_o)$; consequently, a computer study based on this program will be run to determine to what precision the elements of the transition matrix should be computed to obtain a given precision in K.

The executive routine, as described in Section 13.0, is based upon a concept of close communication with IBSYS. This concept is currently being revised, and, consequently not all of the work here reported is directly applicable to the final system. It is reported, however, for the sake of completeness.

A brief comparision of the oblateness terms used in ITEM, MINIVAR and by JPL, based upon work by Kaula, is given in Section 14.0. The conclusion, based on this comparision, is that Kaula's recommended notation and nominal values will be included in the Phase II Program.

Correction formulae for electromagnetic propagation through both the troposphere and ionosphere are contained in Section 15.0. An exponentially-decaying density is assumed for the troposphere, whereas a three-parameter model is used for the ionosphere; both models are numerically integrated to compute range and range-rate corrections in the troposphere. Coordinate systems and transformations required for making the corrections are described. This work was carried out under Phase I, but is directly applicable to the high precision version of the Orbit Determination Program.

2.0. TRANSFORMATION OF PLANETARY COORDINATES, PHASE I

J. F. BELLANTONI

Table of Contents

Appendices

1. Derivation of Precession Transformation to a Variable Base Date
2. Derivation of expression for Triaxial Lunar Potential
3. Alternate Subroutine DATE

2.1. INTRODUCTION

This report describes the transformation of vehicle initial conditions and earth and lunar oblateness attractions to the "base date" coordinate system used for trajectory calculations in MINIVAR*. The "base date" system is determined by the direction of the vernal equinox of 0.0 January 1 of the year subsequent to the launch year. It has been chosen as the basis for calculation because the planetary and solar coordinates are written on tapes in that coordinate system. Rather than transform the tape information the vehicle initial conditions and the oblateness accelerations are transformed into the base date system.

1. Vehicle initial conditions that are inserted in an earth referenced system, such as latitude, longitude, altitude, are transformed first to a system determined by the vernal equinox of date. This system (true) differs from the base date system by the earth's nutation and precession. Transformation by the nutation matrix [N] and the precession matrix [A] thereupon brings the initial conditions into the base date system.

2. The oblateness attraction of the earth is calculated from a knowledge of $\bar{R}$, the position of the vehicle from the center of the earth, expressed in the true earth system. Since vehicle position as calculated in the trajectory portion is in base date components these components must be transformed via precession and nutation into the true earth system. The resultant attraction is then transformed back into the base date system.

   The oblateness attraction of the moon has not been employed previously in MINIVAR. It is calculated from the vehicle position with respect to the moon's center and the lunar oblateness matrix; the latter takes account of spherical harmonics of potential of degree -3 based on the three lunar moments of inertia.

The transformations described in this report are also employed in calculation of the observations and the matrix of their partial derivatives with respect to the state variables. These applications are not discussed here.

The subroutines here described are generally single precision; investigation of double precision has been reserved for phase II.

The transformations of lunar-based initial conditions described herein have not been programmed in phase I. It is presently planned to incorporate them in phase II.

---

*The "base date" employed here is to be distinguished from the "base time" of reference 8. The latter is 0.0 31 December of the year prior to launch; it is used as an arbitrary reference point for input data, observation time and planetary tape in the Minimum Variance Orbit Determination Program.

No attempt is here made to derive basic astronomical transformations such as precession, nutation, libration or the Greenwich hour angle of the vernal equinox, representing, as they do, years* of assiduous labor by experts in celestial mechanics. Rather, those results that apply to the present orbit determination program are presented in a form that may be programmed readily.

2.2. DEFINITION OF COORDINATE SYSTEMS

The precession, nutation, libration and other transformations to be used in the Orbit Determination Program all represent rigid rotation of right-handed cartesian coordinate systems. Hence, the matrices are real, orthogonal and have determinants equal to +1. The coordinate systems involved are defined in this section, the transformations are defined in the following section.

Unit vectors are characterized by the circumflex accent ^ .

$\hat{X}_B \hat{Y}_B \hat{Z}_B$ $\hat{X}_B$ along mean vernal equinox of base date (intersection of ecliptic of base date and mean equatorial plane of base date).
$\hat{Z}_B$ normal to mean equatorial plane of base date, positive in northern hemisphere.
$\hat{Y}_B$ such that $\hat{X}_B \hat{Y}_B \hat{Z}_B$ is right handed orthogonal.

$\hat{X}_Q \hat{Y}_Q \hat{Z}_Q$ $\hat{X}_Q$ along mean vernal equinox of date (intersection of mean equator of date and ecliptic of date).
$\hat{Z}_Q$ normal to mean equator of date, positive in northern hemisphere.
$\hat{Y}_Q$ normal to $\hat{X}_Q$ and $\hat{Z}_Q$ so that $\hat{X}_Q \hat{Y}_Q \hat{Z}_Q$ forms a right handed system.

$\hat{X}_E \hat{Y}_E \hat{Z}_E$ $\hat{X}_E$ along true vernal equinox of date (intersection of true equatorial plane and ecliptic of date).
$\hat{Z}_E$ normal to true equator, positive toward northern hemisphere.
$\hat{Y}_E$ normal to $\hat{X}_E \hat{Z}_E$ and such that $\hat{X}_E \hat{Y}_E \hat{Z}_E$ form a right handed system.

$\hat{X}_M \hat{Y}_M \hat{Z}_M$ $\hat{X}_M$ along the (A) principle axis of moon, positive on earth side, $\hat{Z}_M$ along the (C) principle axis of moon positive in direction of rotation of moon with respect to space;
$\hat{Y}_M$ along the (B) principle axis of moon, to form right handed system with $\hat{X}_M$ and $\hat{Z}_M$.

$\hat{X}_G \hat{Y}_G \hat{Z}_G$ $\hat{X}_G$ in true equator of earth and in Greenwich Meridian: $\hat{Z}_G$ normal to true equator, positive toward north pole; $\hat{Y}_G$ to form right handed system with $\hat{X}_G$ and $\hat{Z}_G$.

---

*A precession formula was first used in the Nautical Almanac in 1854; a nutation formula in 1767. (See p. 181 of reference 3.) The Present-day formulas are refinements of the publications of S. Newcomb in 1897.

$\lambda_E \phi_E R_E$ Geocentric rt. ascension (apparent siderial time); geocentric angle, or declination of line from earth center to vehicle; geocentric distance from vehicle. See Figure I.

$\hat{\lambda}_E \hat{\phi}_E \hat{R}_E$ $\hat{\lambda}_E$ normal to vehicle's local meridian, positive eastward; $\hat{R}_E$ along geocentric radius vector to vehicle; $\hat{\phi}_E$ normal to $\hat{\lambda}_E$ and $\hat{R}_E$ and such that $\hat{\lambda}_E \hat{\phi}_E \hat{R}_E$ form a right handed system. See Figure I.

$\hat{\lambda}_G \hat{\phi}_G \hat{h}_G$ local geographic system: $\hat{\lambda}_G$ normal to meridian, towards east, ($\hat{\lambda}_G = \hat{\lambda}_E$); $\hat{h}_G$ normal to ellipsoid through position of vehicle; $\hat{\phi}_G$ normal to $\hat{\lambda}_G$ and $\hat{R}_G$ such that $\hat{\lambda}_G \hat{\phi}_G \hat{h}_G$ is right handed.

$\lambda_G \phi_G h_G$ Geographic longitude, positive easterly from Greenwich meridian through 360 degrees; geographic latitude (angle between equatorial plane and normal to ellipsoid through vehicle position); altitude above ellipsoid. See Figure II.

$\hat{\lambda}_M \hat{\phi}_M \hat{R}_M$ $\hat{\lambda}_M$ normal to local moon meridian; $\hat{R}_M$ along outward radial from center of moon to vehicle; $\hat{\phi}_M$ normal to $\hat{R}_M$ and $\hat{\lambda}_M$. See Figure III.

$\lambda_M \phi_M R_M$ selenocentric longitude, measured in the $\hat{X}_M \hat{Y}_M$ plane in the sense of positive rotation about $\hat{Z}_M$; selenocentric declination; selenocentric distance. See Figure III.

$V_{A_G} \gamma_G$ vehicle speed relative to $X_G Y_G Z_G$ frame; azimuth, flight path angle relative to $\hat{\lambda}_G \hat{\phi}_G \hat{h}_G$ system. See Figure IV.

2.3. LIST OF TRANSFORMATIONS

The coordinate system under From and To are defined in Section 2.2 of this report. The matrices used are given in Section 2.4.

SYMBOL	NAME	ACRONYM	FROM	TO
[A]	Precession	PREC	$\hat{X}_Q \hat{Y}_Q \hat{Z}_Q$	$\hat{X}_B \hat{Y}_B \hat{Z}_B$
[N]	Nutation	NUTA	$\hat{X}_E \hat{Y}_E \hat{Z}_E$	$\hat{X}_Q \hat{Y}_Q \hat{Z}_Q$
[L]	Libration	LIBRA	$\hat{X}_M \hat{Y}_M \hat{Z}_M$	$\hat{X}_E \hat{Y}_E \hat{Z}_E$
[γ]	Gamma Matrix	GAMMAT	$\hat{X}_G \hat{Y}_G \hat{Z}_G$	$\hat{X}_E \hat{Y}_E \hat{Z}_E$
[G]	Geographic to Greenwich Transformation	GENMAT (λ_G, ϕ_G)	$\hat{\lambda}_G \hat{\phi}_G \hat{h}_G$	$\hat{X}_G \hat{Y}_G \hat{Z}_G$
[D,RA]	Declination, Right Ascension	GENMAT (λ_E, ϕ_E)	$\hat{\lambda}_E \hat{\phi}_E \hat{R}_E$	$\hat{X}_E \hat{Y}_E \hat{Z}_E$
[S]	Selenographic	GENMAT (λ_M, ϕ_M)	$\hat{\lambda}_M \hat{\phi}_M \hat{R}_M$	$\hat{X}_M \hat{Y}_M \hat{Z}_M$

Since all the above transformations are orthogonal, the inverse of any is simply its transpose.

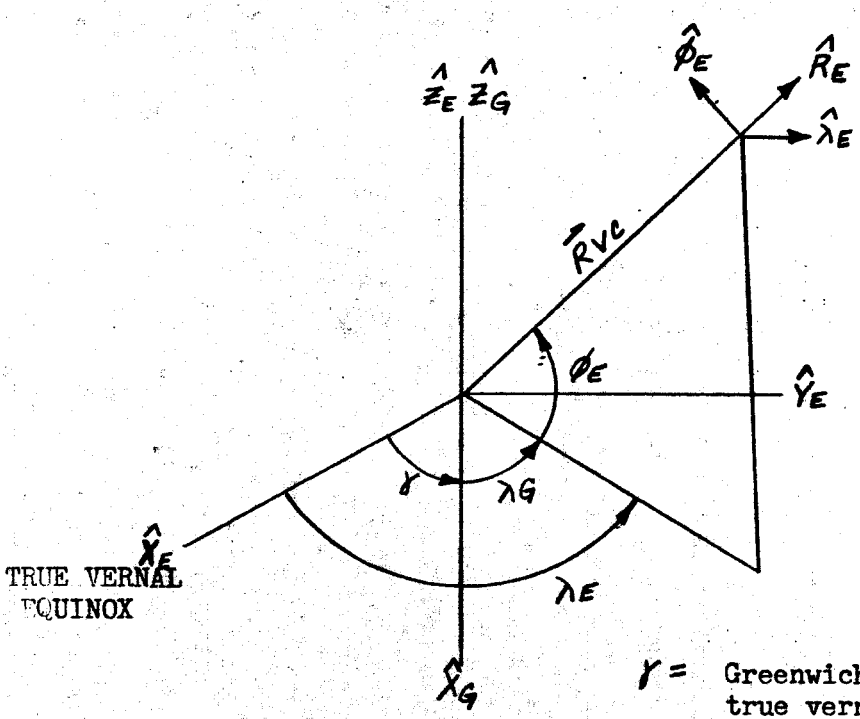

FIGURE I
GEOCENTRIC
COORDINATES

IN TRUE
EQUATOR

γ = Greenwich hour angle of true vernal equinox of date

$\vec{R}_E = \vec{R}_{VC}$ for earth as dominant body.

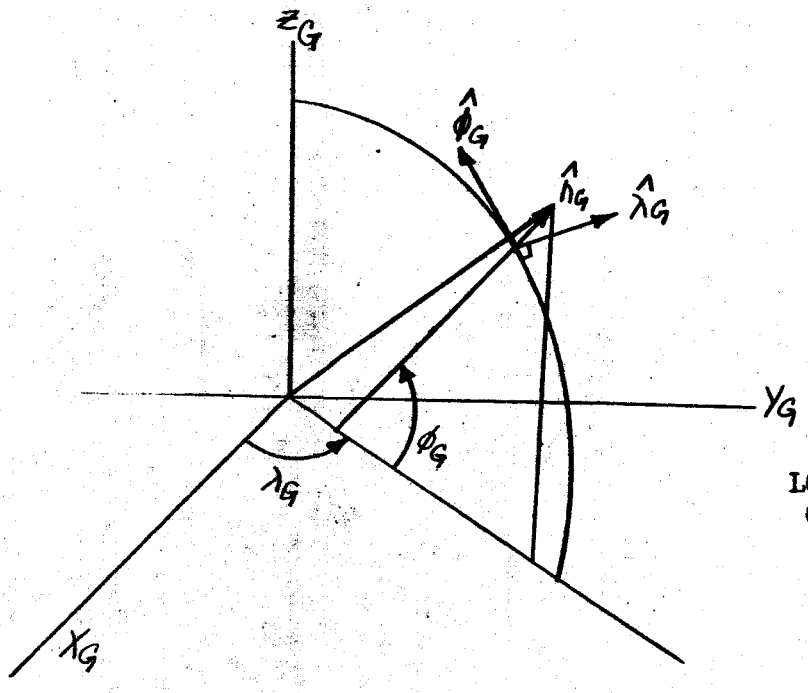

FIGURE II
LOCAL GEOGRAPHIC
COORDINATES

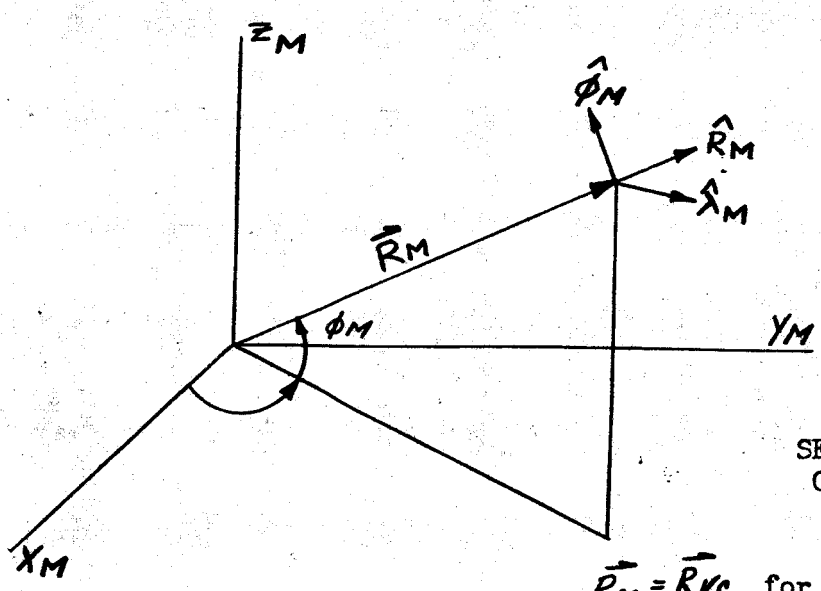

FIGURE III
SELENOCENTRIC
COORDINATES

$\vec{R}_M = \vec{R}_{VC}$ for moon as dominant body

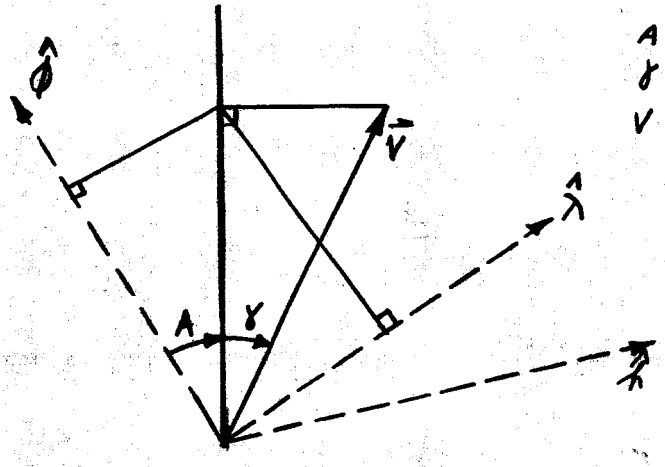

FIGURE IV
AZIMUTH AND
FLIGHT PATH
ANGLES

A positive CW from north

γ positive up from plane $\hat{\phi}$ $\hat{\lambda}$

V always positive, being $|\vec{V}|$

2.4. DESCRIPTION OF SUBROUTINES

2.4.1. Subroutines for Transformations

2.4.1.1. PREC: Precession

The spin axis of the earth is slowly precessing in inertial space due to lunar and solar attractions on the terrestrial bulge; the plane of the earth's orbit about the sun (ecliptic) moves slowly because of planetary attractions. As a result the intersection of the earth's mean equator and the ecliptic (termed the vernal equinox, γ) undergoes a gradual rotation is space. Therefore, the $\hat{X}_Q \hat{Y}_Q \hat{Z}_Q$ coordinate system as defined in Section 2.3 is rotating with respect to the $\hat{X}_B \hat{Y}_B \hat{Z}_B$ system. Figure V illustrates this rotation of the equinox with respect to its position at base date. The transformation from $\hat{X}_Q \hat{Y}_Q \hat{Z}_Q$ to $\hat{X}_B \hat{Y}_B \hat{Z}_B$ is [A]:

$$[A] = \begin{bmatrix} 1 & 0 & 0 \\ 0 & 1 & 0 \\ 0 & 0 & 1 \end{bmatrix} + \begin{bmatrix} a_{11} & a_{21} & a_{31} \\ a_{12} & a_{22} & a_{32} \\ a_{13} & a_{23} & a_{33} \end{bmatrix} X \begin{bmatrix} \Delta a_{11} & \Delta a_{12} & \Delta a_{13} \\ \Delta a_{21} & \Delta a_{22} & \Delta a_{23} \\ \Delta a_{31} & \Delta a_{32} & \Delta a_{33} \end{bmatrix}$$

$$a_{11} = 1.000\,000\,0 - 0.000\,296\,970\,T_B^2 - 0.000\,000\,130\,T_B^3$$

$$a_{12} = 0.022\,349\,88\,T_B + 0.000\,767\,00\,T_B^2 - 0.000\,002\,21\,T_B^3$$

$$a_{13} = 0.009\,717\,11\,T_B - 0.000\,002\,07\,T_B^2 - 0.000\,000\,96\,T_B^3$$

$$a_{21} = -a_{12}$$

$$a_{22} = 1.000\,0000 - 0.000\,249\,76\,T_B^2 - 0.000\,000\,15\,T_B^3$$

$$a_{23} = -0.000\,108\,59\,T_B^2 - 0.000\,000\,030\,T_B^3$$

$$a_{31} = -a_{13}$$

$$a_{32} = a_{23}$$

$$a_{33} = 1.000\,000\,0 - 0.000\,047\,21\,T_B^2 + 0.000\,000\,020\,T_B^3$$

and

$$\Delta a_{11} = -0.000\,296\,97\,\hat{c}_2 - 0.000\,000\,390\,\hat{c}_3$$

$$\Delta a_{12} = 0.022\,349\,88\,\hat{c}_1 + 0.000\,006\,76\,\hat{c}_2 - 0.000\,006\,63\,\hat{c}_3$$

$$\Delta a_{13} = 0.009\,717\,11\,\hat{c}_1 - 0.000\,002\,07\,\hat{c}_2 - 0.000\,002\,88\,\hat{c}_3$$

$$\Delta a_{21} = -\Delta a_{12}$$

$$\Delta a_{22} = -0.000\,249\,76\,\hat{c}_2 - 0.000\,000\,450\,\hat{c}_3$$

$$\Delta a_{23} = -0.000\,108\,59\,\hat{c}_2 - 0.000\,000\,090\,\hat{c}_3$$

$$\Delta a_{31} = -\Delta a_{13}$$

$$\Delta a_{32} = \Delta a_{23}$$

$$\Delta a_{33} = -0.000\,047\,21\,\hat{c}_2 + 0.000\,000\,060\,\hat{c}_3$$

and

$$\hat{c}_1 = \Delta T$$

$$\hat{c}_2 = \Delta T\,(2T_B + \Delta T)$$

$$\hat{c}_3 = \Delta T\left(T_B^2 + T_B\Delta T + \tfrac{1}{3}\Delta T^2\right)$$

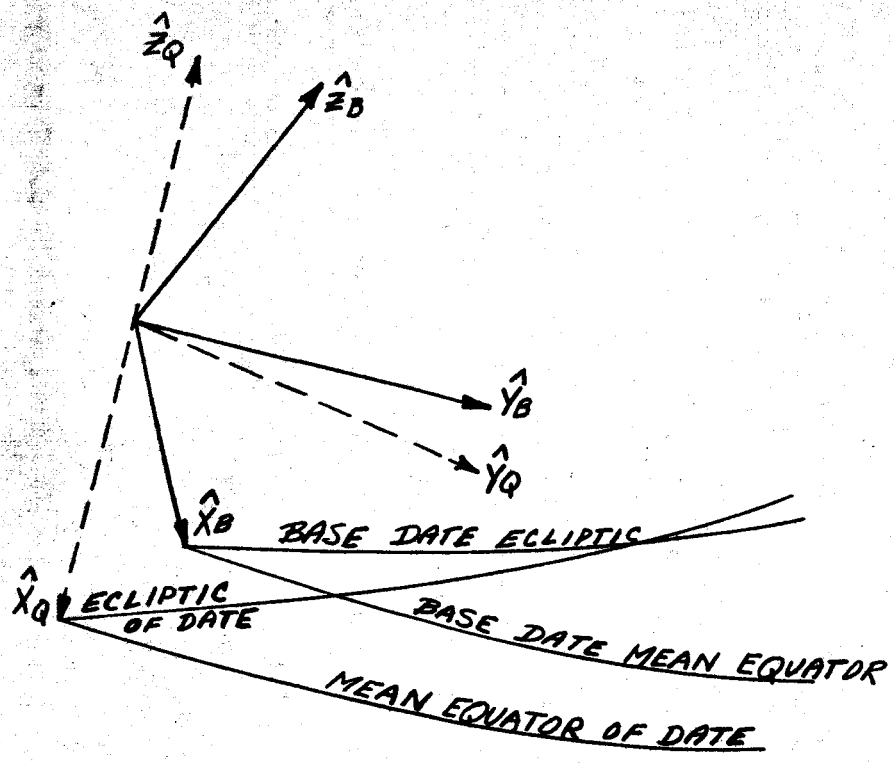

FIGURE V
PRECESSION OF EQUINOXES

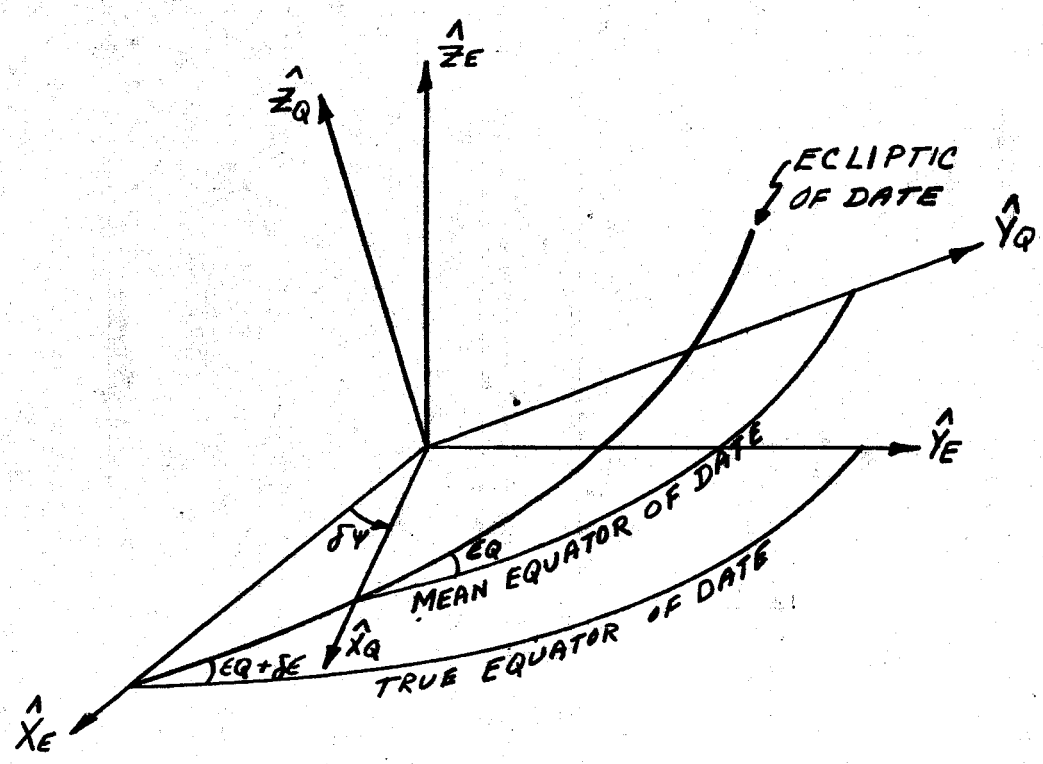

FIGURE VI
NUTATION ANGLES

The quantities ΔT and T_B are calculated in the subroutine DATE, described in Section 2.4.2.1 below. T_B is the number of days from Jan. 0.0, 1950 to the base date, divided by 36525. ΔT is the number of days from the base date to the present time, divided by 36525. The base date depends on the launch date of a particular trajectory, being 0.0 Jan. 1 of the subsequent year.

The above form of the transformation is derived in Appendix 1 from the forms given in the literature (see References 1, 2, 3).

The elements of the [A] matrix are computed whenever needed, except that if [A] has been computed within the previous 1322 seconds, the previous value is used.

2.4.1.2. NUTA: Nutation

The oscillatory motion of the $\hat{X}_E \hat{Y}_E \hat{Z}_E$ system about its mean position ($\hat{X}_Q \hat{Y}_Q \hat{Z}_Q$) is given by the transformation from $\hat{X}_E \hat{Y}_E \hat{Z}_E$ to $\hat{X}_Q \hat{Y}_Q \hat{Z}_Q$.

$$[N] = \begin{bmatrix} 1 & -\delta\psi \cos\epsilon_Q & -\delta\psi \sin\epsilon_Q \\ \delta\psi \cos\epsilon_Q & 1 & -\delta\epsilon \\ \delta\psi \sin\epsilon_Q & \delta\epsilon & 1 \end{bmatrix}$$

where $\delta\psi$, $\delta\epsilon$ and ϵ_Q are obtained from subroutine EXPR. The geometric significance of $\delta\psi$, $\delta\epsilon$ and ϵ_Q is shown in Figure VI.

The [N] matrix above is an approximation, valid to about 0.5×10^{-8}. The exact transformation is given in reference 1, pp 67-68. Fuller discussions of nutation may be found in references 5 and 6.

The nutation terms are recomputed if needed and if the prior values are more than 0.1 day old.

2.4.1.3. LIBRA: Libration

The transformation from the moon-fixed axes $\hat{X}_M \hat{Y}_M \hat{Z}_M$ to the $X_E Y_E Z_E$ axes, pictured in Figure VII, is given by [L]:

$$[L] = \begin{bmatrix} l_{11} & l_{12} & l_{13} \\ l_{21} & l_{22} & l_{23} \\ l_{31} & l_{32} & l_{33} \end{bmatrix}$$

where the l's are given in terms of the three angles Ω, Λ, i :

FIGURE VII LIBRATION ANGLES

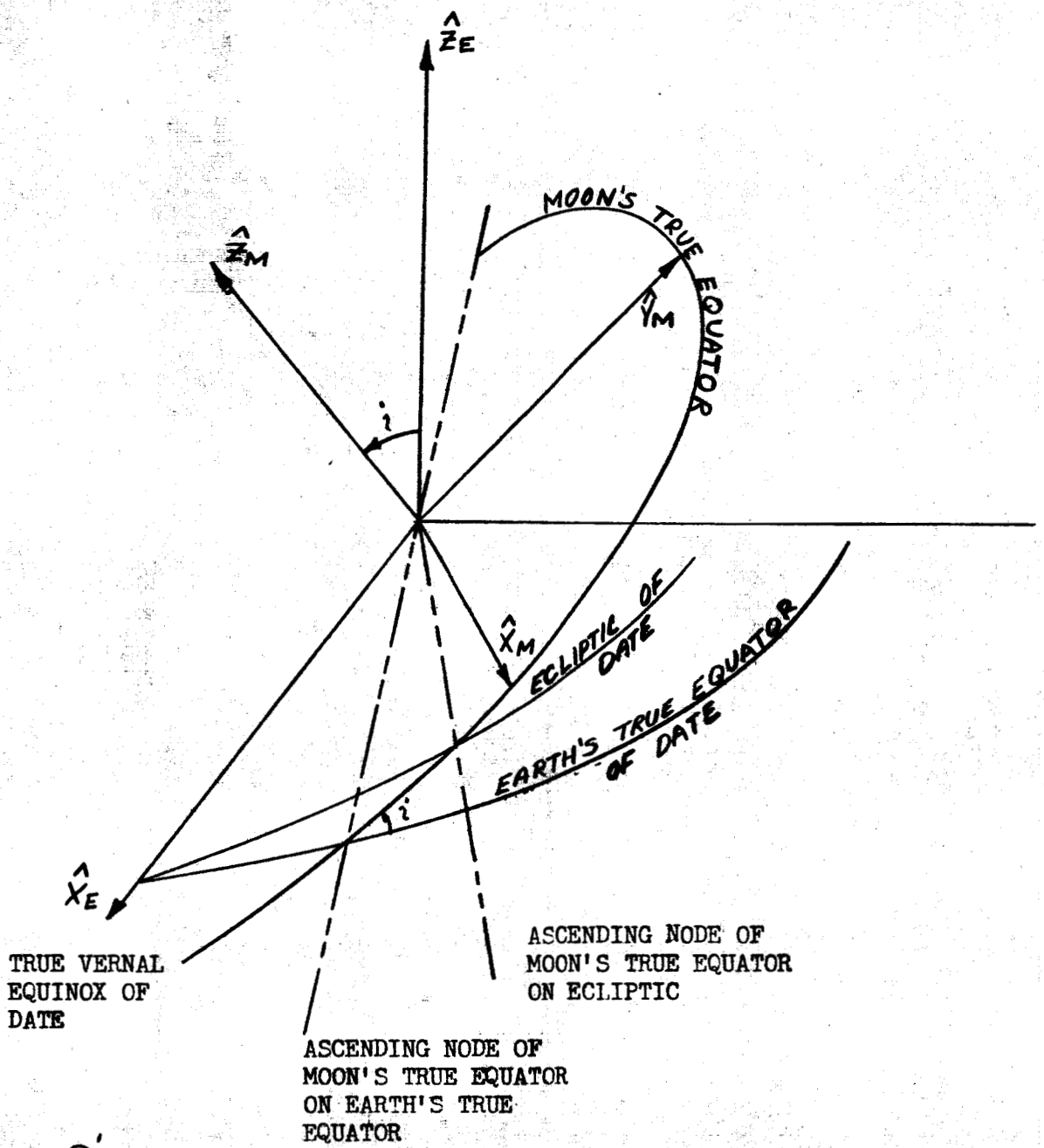

Ω' = Right Ascension of Ascending Node of Moon's True Equator.

Λ = Anomaly from Ascending Node of Moon's True Equator on the Earth's True Equator to the Moon's Axis $\hat{X}_M$.

i = Inclination of Moon's True Equator to Earth's True Equator

and

$$q = 215^\circ.540\,13 + 13^\circ.064\,992\,(d-d_{50})$$
$$g' = 358^\circ.009\,067 + 0^\circ.985\,600\,5\,(d-d_{50})$$
$$\omega = 196^\circ.745\,632 + 0^\circ.164\,358\,6\,(d-d_{50})$$
$$\epsilon_E = \epsilon_Q + \delta\epsilon$$

The quantities ϵ_Q, $\delta\epsilon$, $\delta\psi$, $\mathcal{I}$, Ω are obtained from the subroutine EXPR., the quantity $(d-d_{50})$ is obtained from the subroutine DATE.

The libration formulas are taken from reference 4, and may be found also in references 2 and 1.

The libration matrix is recomputed when needed, except that the prior values are used if they were calculated less than 0.01 days previously.

2.4.1.4. LIBRADT: Libration Rate

The time derivation of [L] is used in the transformation of initial conditions referenced to the moon.

In taking the derivative of the elements l_{ij}, the time rate of change of Ω' and of i are neglected in comparison to that of Λ:

$\frac{d\Omega'}{dt}$ = rate of precession of line of nodes $\sim$ 2π radians/18.5 years

$\frac{di}{dt}$ = rate of change of inclination $< \frac{d\Omega'}{dt}$

$\frac{d\Lambda}{dt} \sim$ rotation rate of moon $\sim$ 2π radians/27.5 days

With the above approximations one obtains

$$[\dot{L}] = \begin{bmatrix} \dot{l}_{11} & \dot{l}_{12} & \dot{l}_{13} \\ \dot{l}_{21} & \dot{l}_{22} & \dot{l}_{23} \\ \dot{l}_{31} & \dot{l}_{32} & \dot{l}_{33} \end{bmatrix} \dot{\Lambda}$$

$$\dot{l}_{11} = -(\sin\Lambda\cos\Omega' + \cos\Lambda\sin\Omega'\cos i)$$
$$\dot{l}_{12} = -(\cos\Lambda\cos\Omega' - \sin\Lambda\sin\Omega'\cos i)$$
$$\dot{l}_{13} = 0$$
$$\dot{l}_{21} = -(\sin\Lambda\sin\Omega' - \cos\Lambda\cos\Omega'\cos i)$$
$$\dot{l}_{22} = -(\cos\Lambda\sin\Omega' + \sin\Lambda\cos\Omega'\cos i)$$
$$\dot{l}_{23} = 0$$
$$\dot{l}_{31} = (\cos\Lambda\sin i)$$
$$\dot{l}_{32} = -(\sin\Lambda\sin i)$$
$$\dot{l}_{33} = 0$$

The expression for $\dot{\Lambda}$ is:

$$\dot{\Lambda} = \dot{\Delta} + \dot{\zeta} + \dot{\tau} - \dot{\Omega} - \dot{\sigma}$$

where

$$\dot{\Delta} = \frac{-(\dot{\Omega}+\dot{\sigma})\sin(\epsilon_0+\delta\epsilon)\cos(\Omega+\sigma+\delta\psi)}{\sin i \cos\Delta} \quad \text{RADIANS/SEC.}$$

$$\dot{\zeta} = 0.266\,170\,762 \times 10^{-5} - 0.124\,991\,71 \times 10^{-13} T \quad \text{RADIANS/SEC.}$$

$$\dot{\Omega} = -0.106\,969\,843\,5 \times 10^{-7} + 0.230\,153\,29 \times 10^{-13} T \quad \text{RADIANS/SEC.}$$

$$\dot{\tau} = -0.153\,527\,924\,6 \times 10^{-9} \cos g$$
$$+ 0.569\,494\,067 \times 10^{-10} \cos g'$$
$$+ 0.579\,473\,484 \times 10^{-11} \cos 2\omega \quad \text{RADIANS/SEC.}$$

$$\dot{\sigma} = -0.520\,642\,191 \times 10^{-7} \cos g$$
$$+ 0.181\,177\,445\,1 \times 10^{-7} \cos(g+2\omega)$$
$$- 0.106\,405\,785\,8 \times 10^{-7} \cos(2\omega+2g) \quad \text{RADIANS/SEC.}$$

The values of $\delta\epsilon$, $\delta\psi$, ϵ_Q, Ω come from subroutine EXPR; the value of T comes from DATE; the values of i, Δ, σ, q, g', ω come from LIBRA subroutine.

The above forms are those of reference 1, p. 70.

2.4.1.5. GAMMAT: Greenwich Hour Angle of the True Vernal Equinox

The subroutine GAMMAT computes the rotation matrix $[\gamma]$ that transforms a vector from the $\hat{X}_G \hat{Y}_G \hat{Z}_G$ system to the $\hat{X}_E \hat{Y}_E \hat{Z}_E$ system. (See Section 2.2 for definitions of the two coordinate systems.)

$$[\gamma] = \begin{bmatrix} \cos\gamma & -\sin\gamma & 0 \\ \sin\gamma & \cos\gamma & 0 \\ 0 & 0 & 1 \end{bmatrix}$$

where $\gamma = \gamma_M + \delta\alpha$ degrees

$$\gamma = 100^\circ.075\,542\,60 + 0^\circ.985\,647\,346\,0\,di + 2^\circ.901\,5 \times 10^{-13}(di)^2 + 0^\circ.417\,807\,462\,206\,t' \text{ MODULO } 360^\circ$$

$$di = IP[d - d_{50}] \quad \text{(DIMENSIONLESS)}$$

$$t' = [3600(t - t_e + HRS) + 60\,HMIN + SEC] - \left\{IP\left[\frac{3600(t - t_e + HRS) + 60\,HMIN + SEC}{86400}\right]\right\} 86400$$

$$\omega_e = \frac{0.004\,178\,074\,62}{(1 + 5.21 \times 10^{-13}\, di)} \quad \text{DEGREES/SEC.}$$

and

$$\delta\alpha = \delta\psi \cos\epsilon_Q$$

IP(4) = INTEGRAL PART OF (4)

The inputs $\delta\psi$, ϵ_Q are obtained from EXPR, and the inputs $(d-d_{50})$, $(t-t_l)$ are obtained from DATE. The values for HRS, HMIN and SEC are launch date inputs to MINIVAR.

The entire subroutine is programmed in double precision in order to avoid loss of accuracy in γ_M (because of the mod 360°) and in t' (because of subtraction of large, nearly equal numbers).

The expression for γ is given in references 1 and 2.

2.4.1.6. GENMAT: General Purpose Orthogonal Transformation

The transformations [G], [DRA] and [S] defined in Section 2.3 all have the same form:

$$[G] = \begin{bmatrix} -\sin\lambda_G & -\sin\phi_G\cos\lambda_G & \cos\phi_G\cos\lambda_G \\ \cos\lambda_G & -\sin\phi_G\sin\lambda_G & \cos\phi_G\sin\lambda_G \\ 0 & \cos\phi_G & \sin\phi_G \end{bmatrix}$$

where λ_G and ϕ_G are geodetic longitude and latitude of the sub-vehicle point or of the observation station.

For [DRA], the right ascension λ_E of the vehicle or station replaces λ_G, and the declination ϕ_E replaces ϕ_G.

For [S], the lunar longitude λ_M of the vehicle replaces λ_G and lunar latitude ϕ_M replaces ϕ_G.

The above transformations may be obtained by inspectión of Figures I, II, and III.

2.4.2. Subsidiary Subroutines

2.4.2.1. DATE: Subroutine for time quantities

The subroutine DATE produces the time parameters for use in other subroutines. The inputs are calander date of launch and time since launch. The output quantities are T, T_B, ΔT and $d-d_{50}$. The program is purely procedural. It is limited to launch dates between 1960 and 1970.

NYEARP = year of launch
DAYS = day of year on which launch occurs. (ex: DAYS = 31 for launch on 31 Jan.)

HRS = number of hours fully expired from beginning of day of launch to time of launch.

HMIN = number of minutes fully expired from beginning of hour of launch to time of launch

SEC = number of seconds and fractional parts of a second expired from beginning of minute of launch to time of launch

$t-t_\ell$ = hours and fractions thereof from launch time to present time of trajectory calculation.

Procedure:

1. Calculate I: (I) = NYEARP - 1959
2. Lookup YR(I) and YR (I + 1) from Table:

(I)	Y(I)
0	3562
1	4018
2	4383
3	4748
4	5113
5	5479
6	5844
7	6209
8	6574
9	6940
10	7305

3. Calculate Output Quantities $T_B, d-d_{50}, T, \Delta T$:

$$T_B = YR(I+1)/36525 \quad \text{(DIMENSIONLESS)}$$

$$d-d_{50} = YR(I) + DAYS - 1 + HRS/24 + HMIN/1440 + SEC/86400 + (t-t_\ell)/24 \quad \text{(DIMENSIONLESS)}$$

$$T = (d-d_{50})/36525 \quad \text{(DIMENSIONLESS)}$$

$$\Delta T = T - T_B \quad \text{(DIMENSIONLESS)}$$

These outputs are recalculated as demanded by other subroutines.

2.4.2.2. EXPR: Long expressions for $\delta\psi$, $\delta\epsilon$, ϵ_0 , Ω , $\mathbb{C}$:

This subroutine takes in T and ($d - d_{50}$) from the subroutine DATE and puts out nutation in longitude $\delta\psi$, nutation in obliquity $\delta\epsilon$, mean obliquity ϵ_0 , mean longitude of descending node of moon's mean equator on ecliptic Ω and mean longitude of moon $\mathbb{C}$, for use in [N], [L] and [L]. The entire subroutine is repeated upon demand by other subroutines.

$$\epsilon_0 = 23^\circ.445\,787\,4 - 0^\circ.013\,013\,76\,T - 0^\circ.885\,5 \times 10^{-6} T^2 + 0^\circ.503 \times 10^{-6} T^3$$

$$\delta\epsilon = \Delta\epsilon + d\epsilon \quad \text{DEGREES}$$

$$\Delta\epsilon = 0^\circ.255\,833 \times 10^{-2} \cos\Omega - 0^\circ.25 \times 10^{-4} \cos 2\Omega + 0^\circ.153\,055\,5 \times 10^{-3} \cos 2L + 0^\circ.611\,11 \times 10^{-5} \cos(3L - \Pi) - 0^\circ.25 \times 10^{-5} \cos(L + \Pi) - 0^\circ.194\,444 \times 10^{-5} \cos(2L - \Omega) - 0^\circ.8333 \times 10^{-6} \cos(2\Pi' - \Omega)$$

$$d\epsilon = 0^\circ.244\,44 \times 10^{-4} \cos 2\mathbb{C} + 0^\circ.5 \times 10^{-5} \cos(2\mathbb{C} - \Omega) + 0^\circ.305\,55 \times 10^{-5} \cos(3\mathbb{C} - \Pi') - 0^\circ.138\,88 \times 10^{-5} \cos(\mathbb{C} + \Pi') - 0^\circ.8333 \times 10^{-6} \cos(\mathbb{C} - \Pi' + \Omega) + 0^\circ.8333 \times 10^{-6} \cos(\mathbb{C} - \Pi' - \Omega) + 0^\circ.5555 \times 10^{-6} \cos(3\mathbb{C} - 2L + \Pi') + 0^\circ.5555 \times 10^{-6} \cos(3\mathbb{C} - \Pi' - \Omega)$$

$$\Omega = 12^\circ.112\,790\,2 - 0^\circ.052\,953\,922\,2\,(d - d_{50}) + 0^\circ.207\,95 \times 10^{-2} T + 0^\circ.2081 \times 10^{-2} T^2 + 0^\circ.2 \times 10^{-5} T^3$$

$$\mathbb{C} = 64^\circ.375\,451\,67 + 13^\circ.176\,396\,526\,8\,(d - d_{50}) - 0^\circ.113\,157\,5 \times 10^{-2} T - 0^\circ.113\,015 \times 10^{-2} T^2 + 0^\circ.19 \times 10^{-5} T^3$$

$$\delta\psi = \Delta\psi + d\psi \quad \text{DEGREES}$$

$$\begin{aligned}\Delta\psi = -[&0^\circ.478\,956\,11 \times 10^{-2} + 0^\circ.472\,22 \times 10^{-5} T]\sin\Omega \\ &+ 0^\circ.580\,560 \times 10^{-4} \sin 2\Omega - 0^\circ.353\,33 \times 10^{-3} \sin 2L \\ &+ 0^\circ.350 \times 10^{-4} \sin(L - \Pi) - 0^\circ.138\,88 \times 10^{-4} \sin(3L - \Pi) \\ &+ 0^\circ.583\,33 \times 10^{-5} \sin(L + \Pi) + 0^\circ.3333 \times 10^{-5} \sin(2L - \Omega) \\ &+ 0^\circ.138\,88 \times 10^{-5} \sin(2\Pi' - \Omega) + 0^\circ.111\,11 \times 10^{-5} \sin(2L - 2\Pi')\end{aligned}$$

$$\begin{aligned}d\psi = &- 0^\circ.566\,66 \times 10^{-4} \sin(2\mathbb{C}) + 0^\circ.188\,88 \times 10^{-4} \sin(\mathbb{C} - \Pi') \\ &+ 0^\circ.833\,33 \times 10^{-6} \sin 2(\mathbb{C} - \Pi') - 0^\circ.944\,44 \times 10^{-5} \sin(2\mathbb{C} - \Omega) \\ &- 0^\circ.722\,2 \times 10^{-5} \sin(3\mathbb{C} - \Pi') + 0^\circ.416\,66 \times 10^{-5} \sin(\mathbb{C} - 2L + \Pi') \\ &+ 0^\circ.305\,55 \times 10^{-5} \sin(\mathbb{C} + \Pi') + 0^\circ.166\,66 \times 10^{-5} \sin(2\mathbb{C} - 2L) \\ &+ 0^\circ.166\,66 \times 10^{-5} \sin(\mathbb{C} - \Pi' + \Omega) + 0^\circ.166\,66 \times 10^{-5} \sin(\mathbb{C} - \Pi' - \Omega) \\ &- 0^\circ.138\,88 \times 10^{-5} \sin(3\mathbb{C} - 2L + \Pi') - 0^\circ.111\,11 \times 10^{-5} \sin(3\mathbb{C} - \Pi' - \Omega)\end{aligned}$$

where T, T', L are obtained from

$$T = 282^\circ.080\,530\,28 + 0^\circ.470\,684 \times 10^{-4}(d-d_{50}) - 0^\circ.455\,25 \times 10^{-3} T + 0^\circ.457\,5 \times 10^{-3} T^2 + 0^\circ.3 \times 10^{-5} T^3$$

$$T' = 208^\circ.843\,987\,7 + 0^\circ.111\,404\,0803\,(d-d_{50}) - 0^\circ.010\,334\,T - 0^\circ.010\,343\,T^2 - 0^\circ.12 \times 10^{-4} T^3$$

$$L = 280^\circ.081\,210\,09 + 0^\circ.985\,647\,335\,4\,(d-d_{50}) + 0^\circ.302 \times 10^{-3} T + 0^\circ.302 \times 10^{-3} T^2$$

These expressions are taken from references 1 and 4; fuller discussion of them is given in reference 2 under the explanation of the ephemeris for the sun, and in reference 3.

2.4.3. Subroutines for Transforming Initial Conditions and for Transforming Oblateness Attractions

2.4.3.1. XFORM: Transformation of Initial Conditions

This subroutine calls upon all the previous subroutines as needed to convert vehicle initial position and velocity into the base date system of trajectory calculation. Initial conditions consist of three position coordinates and three velocity components. The velocity need not be specified in the same type of coordinates as position. However, if moon referenced coordinates are used to express the input conditions, either for position or velocity, the input $\bar{R}_{VC}$, should be position relative to the moon or velocity $\bar{V}_{VC}$, relative to the moon. The output then will be the position or velocity relative to $\hat{X}_B \hat{Y}_B \hat{Z}_B$, expressed in the base date system.

Table I gives in the left column the various forms that initial position or velocity information may take, and in the right column the calculation required to transfer it to the base date system. The symbols used are defined in the table, in what follows, or in Section 2.2. It has been assumed in the table that $[\dot{A}]$ and $[\dot{N}]$ are negligible in a single precision program. It may be noted that $[\dot{\gamma}] = [w_e][\gamma]$, where

$$[w_e] = \text{antisymmetric matrix corresponding to } (\bar{w}_e \times)$$

$$= w_e \begin{bmatrix} 0 & -1 & 0 \\ 1 & 0 & 0 \\ 0 & 0 & 0 \end{bmatrix}$$

in the $\hat{X}_E \hat{Y}_E \hat{Z}_E$ basis and w_e is obtained from subroutine GAMMAT.

TABLE I

VARIOUS FORMS FOR INITIAL CONDITIONS	INITIAL CONDITIONS $X_B\ Y_B\ Z_B, \dot{X}_B\ \dot{Y}_B\ \dot{Z}_B$ IN BASE DATE SYSTEM	
λ_E Right Ascension (RA) ϕ_E Declination (D) R_E Geocentric Dist.	$[A][N][DRA]\begin{bmatrix}0\\0\\R_E\end{bmatrix}$	*
$V_{\lambda E} = \bar{V}_{VC'}$ along $\hat{\lambda}_E$ $V_{\phi E} = \bar{V}_{VC'}$ along $\hat{\phi}_E$ $V_{RE} = \bar{V}_{VC'}$ along $\hat{R}_E$	$[A][N]\left\{[DRA]\begin{bmatrix}V_{\lambda E}\\V_{\phi E}\\V_{RE}\end{bmatrix} + [We][DRA]\begin{bmatrix}0\\0\\R_E\end{bmatrix}\right\}$	*
V magnitude of $\bar{V}_{VC'}$ γ_E flt. pth. angle $\bar{V}_{VC'}$ A_E azimuth angle $\bar{V}_{VC'}$	$[A][N]\left\{[DRA]\begin{bmatrix}V\cos\gamma_E\ \sin A_E\\V\cos\gamma_E\ \cos A_E\\V\sin\gamma_E\end{bmatrix} + [We][DRA]\begin{bmatrix}0\\0\\R_E\end{bmatrix}\right\}$	* N.B. 1.
λ_G Geodetic Longitude ϕ_G Geodetic Latitude h_G Geodetic Altitude	$[A][N][\gamma]\left\{[G]\begin{bmatrix}0\\0\\h_G+c\end{bmatrix} - \begin{bmatrix}0\\0\\\varepsilon^2 c\sin\phi_G\end{bmatrix}\right\} \triangleq [A][N][\gamma]\bar{R}_G$	*
$V_e = \bar{V}'_{VC}$ along east $V_m = \bar{V}'_{VC}$ along north $V_h = \bar{V}'_{VC}$ along vertical (up)	$[A][N]\left\{[\gamma][G]\begin{bmatrix}V_e\\V_m\\V_h\end{bmatrix} + [We][\gamma]\bar{R}_G\right\}$	* N.B. 1.

TABLE I continued

VARIOUS FORMS FOR INITIAL CONDITIONS	INITIAL CONDITIONS $X_B\ Y_B\ Z_B,\ \dot{X}_B\ \dot{Y}_B\ \dot{Z}_B$ IN BASE DATE SYSTEM	
$\sqrt{}$ magnitude of $\bar{V}_{Vc}$ γ_G flight path angle A_G azimuth	$[A][N]\left\{[\gamma][G]\begin{bmatrix} V\cos\gamma_G \sin A_G \\ V\cos\gamma_G \cos A_G \\ V\sin\gamma_G \end{bmatrix} + [\omega_e][\gamma]\bar{R}_G\right\}$	* N.B.1.
$X_E = \bar{R}'_{Vc}$ along $\hat{X}_E$ $Y_E = \bar{R}'_{Vc}$ along $\hat{Y}_E$ $Z_E = \bar{R}'_{Vc}$ along $\hat{Z}_E$	$[A][N]\begin{bmatrix} X_E \\ Y_E \\ Z_E \end{bmatrix}$	*
$\dot{X}_E = \bar{V}'_{Vc}$ along $\hat{X}_E$ $\dot{Y}_E = \bar{V}'_{Vc}$ along $\hat{Y}_E$ $\dot{Z}_E = \bar{V}'_{Vc}$ along $\hat{Z}_E$	$[A][N]\left\{\begin{bmatrix} \dot{X}_E \\ \dot{Y}_E \\ \dot{Z}_E \end{bmatrix} + [\omega_e]\begin{bmatrix} X_E \\ Y_E \\ Z_E \end{bmatrix}\right\}$	* N.B.1.
$X_M = \bar{R}'_{Vc}$ along $\hat{X}_M$ $Y_M = \bar{R}'_{Vc}$ along $\hat{Y}_M$ $Z_M = \bar{R}'_{Vc}$ along $\hat{Z}_M$	$[A][N][L]\begin{bmatrix} X_M \\ Y_M \\ Z_M \end{bmatrix}$	* *
$\dot{X}_M = \bar{V}'_{Vc}$ along $\hat{X}_M$ $\dot{Y}_M = \bar{V}'_{Vc}$ along $\hat{Y}_M$ $\dot{Z}_M = \bar{V}'_{Vc}$ along $\hat{Z}_M$	$[A][N][L]\begin{bmatrix} \dot{X}_M \\ \dot{Y}_M \\ \dot{Z}_M \end{bmatrix} + [A][N][\dot{L}]\begin{bmatrix} X_M \\ Y_M \\ Z_M \end{bmatrix}$	* *

TABLE I concluded

VARIOUS FORMS FOR INITIAL CONDITIONS	INITIAL CONDITIONS $X_B\ Y_B Z_B, \dot{X}_B \dot{Y}_B \dot{Z}_B$ IN BASE DATE SYSTEM	
λ_M Selenographic Longitude ϕ_M Selenographic Latitude R_M Selenocentric Dist.	$[A][N][L][S]\begin{bmatrix}0\\0\\R_M\end{bmatrix}$	* *
$V_{\lambda M} = V_{V'C}$ along $\hat{\lambda}_M$ $V_{\phi M} = \bar{V}'_{V'C}$ along $\hat{\phi}_M$ $V_{RM} = \bar{V}'_{V'C}$ along $\hat{R}_M$	$[A][N][L][S]\begin{bmatrix}V_{\lambda M}\\V_{\phi M}\\V_{RM}\end{bmatrix} + [A][N][\dot{L}][S]\begin{bmatrix}0\\0\\R_M\end{bmatrix}$	* *
V_M magnitude of $\bar{V}'_{V'C}$ γ_M flight path angle A_M azimuth angle	$[A][N][L][S]\begin{bmatrix}V_M\cos\gamma_M & \sin A_M\\ V_M\cos\gamma_M & \cos A_M\\ V_M\sin\gamma_M & \end{bmatrix} + [A][N][\dot{L}][S]\begin{bmatrix}0\\0\\R_M\end{bmatrix}$	* *

$\bar{R}'_{V'C}$ = vector from center of reference body to vehicle, expressed in any basis.

$\bar{V}'_{V'C}$ = velocity of vehicle relative to (rotating)reference body, expressed in any basis.

* programmed in phase I
** to be programmed in phase II
Note: It is also possible to input $X_B\ Y_B Z_B, \dot{X}_B \dot{Y}_B \dot{Z}_B$ directly.

Note: " $\bar{R}_{V'C}$ along $\hat{X}_E$" etc., means the dot product $\bar{R}_{V'C} \cdot \hat{X}_E$, etc. In the dot product $\hat{X}_E$ is expressed in the same basis as chosen for $\bar{R}_{V'C}$.

N.B.1: Options available for $\omega_e = 0$. These transformations imply that inertial velocity coordinates may be loaded as input.

Also,

$$c = a_e \left(1 - \varepsilon^2 \sin^2 \phi_G\right)^{-1/2}$$

where a_e and ε^2 are input to the program as ERAD and EPSSQ (Sect. 6, card 1, columns 37-48 and 49-60). The values used are

a_e = earth radius = 1 ER = 0.6378165×10^3 KM
ε^2 = earth eccentricity, squared = $0.66934220 \times 10^{-2}$

The initial position may be input in kilometers (KM) or earth radii (ER) for distances and degrees (DG) for angles. The initial velocity may be input in kilometers per second (K/S) or earth radii per hour (ER/HR). Since the trajectory calculation is done in earth radii and earth radii per hour, conversion from KM and K/S to ER and ER/HR is performed. It is performed in subroutine INPUT, which precedes subroutine XFORM.

2.4.3.2. OBLATE: Calculation of Oblateness Attractions

2.4.3.2.1. Earth Oblateness Attraction

The subroutine OBLATE transforms the vehicle position vector $\bar{R}_{VC}$ relative to the earth's center into the true earth system $\hat{X}_E$ $\hat{Y}_E$ $\hat{Z}_E$. The oblateness attraction given in equations 6 and 7 of reference 7, is then calculated using the transformed values of R_{VC}. The resultant attraction vector is then expressed in the base date system. The formulas employed are, in effect,

$$\left(\bar{F}_2\right)_B = [A][N]\left\{b(z_E)\bar{R}_E + c(z_E)\hat{Z}_E\right\}$$

where $\vec{R}_E = [N]^{-1}[A]^{-1}\vec{R}_B$, $z_E = \hat{Z}_E \cdot \vec{R}_E$ and $b(z_E)$, $c(z_E)$ are given in equation 7), reference 7, with z_E for z and R_B for r.

The vector $(\vec{F}_2)_B$ is the earth oblateness attraction, due to the nutating, precessing earth, expressed in the base date system. It is used in place of $\vec{F}_2$ of equation 6) in reference 7, and is equal to $\vec{F}_2$ if precession and nutation are ignored.

2.4.3.2.2. Lunar Oblateness Attraction

Circumlunar trajectories are strongly influenced in the neighborhood of the moon by the lunar oblateness mass. Acceleration terms corresponding to lunar oblateness attraction were added as $\vec{F}_4$ to equation (1) of reference 7:

$$\vec{F}_4 \begin{cases} = 0 \text{ if } |\vec{R}_M| \geq 40{,}000 \text{ KM. otherwise} \\ = -\frac{5}{2}\gamma' \frac{\vec{R}_M}{R_M^7}\left\{\vec{R}_M \cdot [V_M]_B \cdot \vec{R}_M\right\} + \gamma' \frac{\vec{R}_M}{R_M^5} \cdot [V]_B \text{ (KM/SEC)} \end{cases}$$

where $\gamma' = 0.6671 \times 10^{-19}\ KM^3/(KG - SEC^2)$

$\vec{R}_M = \vec{R}_{VC} - \vec{R}_{ME}$ (KM)

$$[\gamma_M]_B = [A][N][L] \begin{bmatrix} 7.3 & 0 & 0 \\ 0 & 1.9 & 0 \\ 0 & 0 & -9.2 \end{bmatrix} [L]^{-1}[N]^{-1}[A]^{-1} \times 10^{25} \quad (KG - KM^2)$$

The vector $\vec{R}_{VC}$ is vehicle position relative to earth in the base date system, obtained from the trajectory calculation. The vector $\vec{R}_{ME}$ is moon position relative to the earth, obtained from core storage as XME, YME, ZME in earth radii. In phase II of the Orbit Determination Program $\vec{R}_{VC}$ may be vehicle position relative a reference body (c) other than earth. In that case the equation for $\vec{R}_M$ is $\vec{R}_M = \vec{R}_{VC} + \vec{R}_{CE} - \vec{R}_{ME}$. In either case the lunar oblateness term is appreciable only if R_M is less than about 40,000 KM.

The previous value for $[\gamma_M]_B$ is used if it was computed not more than 840 sec. prior to demand.

The dimensions of $\vec{F}_4$ as shown above are KM/SEC^2. They are converted to ER/HR^2 before addition to the other perturbation terms.

The derivation of the equations for $\vec{F}_4$ is given in Appendix 2.

2.4.4. List of Inputs and Outputs for Subroutines

Subroutine	Inputs	Outputs
PREC:	$T_B, \Delta T$	[A]
NUTA:	$\delta\psi, \delta\epsilon, \epsilon_Q$	[N]
LIBRA:	$\delta\psi, \delta\epsilon, \epsilon_Q, \mathbb{C}, \Omega$ $(\alpha - \alpha_{50})$	[L], $i, \Delta, \sigma, \vartheta, \vartheta', \omega$
LIBRADT:	$\delta\psi, \delta\epsilon, \epsilon_Q, \Omega, T, \dot{i}, \dot{\Delta}$ $\dot{\sigma}, \dot{\vartheta}, \dot{\vartheta}', \dot{\omega}$	$[\dot{L}]$
GAMMAT:	HRS, HMIN, SEC $\delta\psi, \epsilon_Q, \alpha - \alpha_{50}, t - t_E$	$[\gamma]$
GENMAT (λ_G, ϕ_G)	λ_G, ϕ_G	[G]
GENMAT (λ_E, ϕ_E)	λ_E, ϕ_E	[D, RA]
GENMAT (λ_M, ϕ_M)	λ_M, ϕ_M	[S]
DATE	NYEARP, DAYS, HRS HMIN, SEC,	$T_B, T, \Delta T, \alpha - \alpha_{50}$

EXPR	$T, d-d_{50}$	$\delta\psi, \delta\epsilon, \epsilon_Q, \Omega, \alpha$
XFORM	a_e, e^2	$\vec{R}_B, \vec{V}_B$
	$\lambda_E, \phi_E, R_E, V_{\lambda E}, V_{\phi E}, V_{RE}$	
	$V, \gamma_E, A_E, \lambda_G, \phi_G, h_G$	
	$V_e, V_n, V_h, V, \gamma_G, A_G$	
	$X_E, Y_E, Z_E, \dot{X}_E, \dot{Y}_E, \dot{Z}_E$	
	$X_M, Y_M, Z_M, \dot{X}_M, \dot{Y}_M, \dot{Z}_M$	
	$\lambda_M, \phi_M, R_M, V_{\lambda M}, V_{\phi M}, V_{RM}$	
	V_M, γ_M, A_M	
	$[A], [N], [DRA], [\gamma], [G]$	
	$[L], [\dot{L}]$	
OBLATE:	$[A], [N], \vec{R}_{VC}$	$\vec{F}_2$
	$[A], [N], [L], \vec{R}_{VC}, \vec{R}_{CE}, \vec{R}_{ME}$	$\vec{F}_4$

~~2.5.~~ REFERENCES

1. D. B. Holdridge, "Space Trajectories Program for the IBM 7090 Computer," J. P. L. Technical Report TR. 32-223, March 2, 1962.

2. The American Ephemeris and Nautical Almanac, for the year 1960, U. S. Government Printing Office, Washington D.C.

3. Explanatory Supplement to the Astronomical Ephemeris and the American Ephemeris and Nautical Almanac, Issued by H. M. Nautical Almanac Office, London, 1961.

4. Kalensher, B. E., "Selenographic Coordinates," J. P. L. Technical Report TR 32-41, February 24, 1961.

5. Astr. Paper Amer. Eph., Vol. XV, Part I p. 153, 1953.

6. Sterne, T. E., "An Introduction to Celestial Mechanics" Interscience Publishers, Inc., New York, 1960.

7. Woolston, D. S., and Mohan, John. Program Manual for Minimum Variance Precision Tracking and Orbit Prediction Program, NASA Goddard Space Flight Center Publication X-640-63-144, July 1, 1963.

8. Shaffer, Squires and Wolf, Interplanetary Trajectory Encke Method (ITEM) Program Manual, NASA Goddard Space Flight Center Publication X-640-63-71.

Appendix 1. Derivation of Precession Transformations to a Variable Base Date

The standard form of the precession matrix is a set of elements $a_{ij}(T)$ that are functions of the time T in Julian centuries of 36525 days from some standard time, usually 0^h.0 January 1, 1950 to the present epoch. This transformation $[a(T)]$ takes a vector from the present-time system to the January 1, 1950 system, i.e., through the small angle that the earth has precessed in the time T.

It is desired to refer vectors to some recent base date (say 0^h.0 January 1 of year subsequent to launch) rather than the 1950 date. Let

T_B = time in Julian centures from 0^h.0 January 1, 1950 to 0^h.0 January 1, of year after launch.

ΔT = time in Julian centuries from 0^h.0 January 1, of year after launch, to the present (trajectory) time.

$T = T_B + \Delta T$ = time in Julian centuries from 0.0 January 1, 1950 to trajectory time.

With the above notation, the desired transformation from the present system to the new base date is the product of $[a(T)]$, which transforms from the present date system to the 1950 date system, and $[a(T_B)]^{-1}$ which goes from the 1950 system to the base date system. Thus

$$[A(\Delta T)] \triangleq [a(T_B)]^{-1}[a(T)]$$
$$= [a(T_B)]^{-1}[a(T_B + \Delta T)]$$

Since $a_{ij}(T_B+\Delta T)$ is a polynomial of third degree in $(T_B+\Delta T)$ it is a simple matter to write it as a sum:

$$[a(T_B + \Delta T)] = [a(T_B)] + [\Delta a(\Delta T, T_B)]$$

So that

$$[A(\Delta T)] = [a(T_B)]^{-1}\{[a(T_B)] + [\Delta a(T_B, \Delta T)]\}$$
$$= [I] + [a(T_B)]^{-1}[\Delta a(T_B, \Delta T)]$$
$$= \begin{bmatrix} 1 & 0 & 0 \\ 0 & 1 & 0 \\ 0 & 0 & 1 \end{bmatrix} + \begin{bmatrix} a_{11} & a_{21} & a_{31} \\ a_{12} & a_{22} & a_{32} \\ a_{13} & a_{23} & a_{33} \end{bmatrix}_{T_B} \begin{bmatrix} \Delta a_{11} & \Delta a_{12} & \Delta a_{13} \\ \Delta a_{21} & \Delta a_{22} & \Delta a_{23} \\ \Delta a_{31} & \Delta a_{32} & \Delta a_{33} \end{bmatrix}_{T_B, \Delta T}$$

where the elements a_{ij} are $a_{ij}(T_B)$, the standard forms of the precession transformation elements evaluated at T_B.

The Δa_{ij} are obtained from their definition as follows:

$$a_{ij}(T_B+\Delta T) \triangleq a_{ij}(T_B) + \Delta a_{ij}(\Delta T, T_B)$$

$$\begin{aligned}\Delta a_{ij}(\Delta T, T_B) &= a_{ij}(T_B+\Delta T) - a_{ij}(T_B) \\ &= \mathring{a}_{ij} + \acute{a}_{ij}(T_B+\Delta T) + \mathring{a}_{ij}(T_B+\Delta T)^2 + \overset{3}{a}_{ij}(T_B+\Delta T)^3 \\ &\quad - \mathring{a}_{ij} - \acute{a}_{ij} T_B - \mathring{a}_{ij} T_B^2 - \overset{3}{a}_{ij} T_B^3 \\ &= \acute{a}_{ij}\Delta T + a^2_{ij}(2T_B\Delta T + \Delta T^2) \\ &\quad + a^3_{ij}(3T_B^2\Delta T + 3T_B\Delta T^2 + \Delta T^3) \\ &= a'_{ij}\mathcal{T}_1 + a^2_{ij}\mathcal{T}_2 + 3a^3_{ij}\mathcal{T}_3\end{aligned}$$

where $\mathcal{T}_1 \triangleq \Delta T$, $\mathcal{T}_2 \triangleq (2T_B\Delta T + \Delta T^2)$, and $\mathcal{T}_3 \triangleq (T_B^2\Delta T + T_B\Delta T^2 + \frac{1}{3}\Delta T^3)$

$$a_{ji}(x) \triangleq a^0_{ij} + a'_{ij}x + a^2_{ij}x^2 + a^3_{ij}x^3$$

The expanded forms for a_{ij} and Δa_{ij} are given in the body of this report under 2.4.1.1. PREC.

Appendix 2. Derivation of Triaxial Lunar Oblateness Terms in Base Date System

Let $\vec{R}_M$ be vehicle position relative to moon's center
d_M be element of lunar mass
$\vec{r}$ be position of d_M relative to moon's center
γ' be universal gravitation constant
M be total mass of moon

Then

V_M = lunar potential

$$= -\int_M \gamma' d_M \frac{1}{|\vec{R}_M - \vec{r}|}$$

$$= -\gamma' \int_M d_M \frac{1}{R_M} \left[1 - \frac{2\vec{r}\cdot\vec{R}_M}{R_M^2} + \frac{r^2}{R_M^2} \right]^{-1/2}$$

$$= -\gamma' \int_M \frac{d_M}{R_M} \left[1 + \frac{\vec{r}\cdot\vec{R}}{R_M^2} - \frac{1}{2}\frac{r^2}{R_M^2} + \frac{3}{4}\left(\frac{2\vec{r}\cdot\vec{R}_M}{R_M^2}\right)^2 + \cdots O\left(\frac{r^3}{R_M^3}\right) \cdots \right]$$

$$\cong -\frac{\gamma'}{R_M} \left[M + 0 - \frac{1}{2} \left(\int \frac{r^2 d_M}{R_M^2} - 3\hat{R}_M \cdot \int \frac{\vec{r}\vec{r}}{R_M^2} d_M \cdot \hat{R}_M \right) \right]$$

$$\cong -\frac{\gamma' M}{R_M} + \frac{\gamma'}{R_M^3}\frac{1}{2} \hat{R}_M \cdot \left[\int_M (r^2 \hat{\hat{I}} - 3\vec{r}\vec{r}) d_M \right] \cdot \hat{R}_M$$

$$\cong -\frac{\gamma' M}{R_M} - \frac{1}{2}\frac{\gamma'}{R_M^5} \vec{R}_M \cdot [V_M] \cdot \vec{R}_M$$

where $[V_M]$, the lunar oblateness dyadic is independent of vehicle position and may be written in terms of lunar constants in a principle lunar axis coordinate system as:

$$[V_M]_M = -\begin{bmatrix} 2A-B-C & 0 & 0 \\ 0 & 2B-A-C & 0 \\ 0 & 0 & 2C-A-B \end{bmatrix}$$

where $A = \int_M dm(Y^2+Z^2)$ = principal moment of inertia on $\hat{X}_M$
$B = \int_M dm(X^2+Z^2)$ = principal moment of inertia on $\hat{Y}_M$
$C = \int_M dm(Y^2+X^2)$ = principal moment of inertia on $\hat{Z}_M$

The (attractive) force on the vehicle due to the oblateness portion of the lunar potential is $\vec{F}_4$

$$\vec{F}_4 = -\nabla\left\{-\frac{1}{2}\gamma' R_M^{-5}\,\vec{R}_M\cdot[V_M]\cdot\vec{R}_M\right\}$$

$$= \frac{1}{2}\gamma'\left\{\nabla(R_M^{-5})\,\vec{R}_M\cdot[V_M]\cdot\vec{R}_M + R_M^{-5}\nabla\left[\vec{R}_M\cdot[V_M]\cdot\vec{R}_M\right]\right\}$$

Now

$$\nabla(R_M^{-5}) = -5R_M^{-6}\nabla R_M = -5R_M^{-6}\frac{\vec{R}_M}{R_M} = \frac{-5}{R_M^7}\vec{R}_M$$

$$\nabla\left\{\vec{R}_M\cdot[V_M]\cdot\vec{R}_M\right\} = \nabla\left\{\vec{R}_M\cdot\begin{bmatrix} V_{11} & 0 & 0\\ 0 & V_{22} & 0\\ 0 & 0 & V_{33}\end{bmatrix}\cdot\vec{R}_M\right\}$$

$$= \nabla\left\{V_{11}X_M^2 + V_{22}Y_M^2 + V_{33}Z_M^2\right\}$$

$$= 2V_{11}X_M\hat{X}_M + 2V_{22}Y_M\hat{Y}_M + 2V_{33}Z_M\hat{Z}_M$$

$$= 2[V_M]\cdot\vec{R}_M$$

where $\vec{R}_M$ was written in the cartesian system in which $[V_B]$ is diagonal. Thus $\vec{F}_4$ becomes

$$\vec{F}_4 = -\frac{5}{2}\frac{\gamma'}{R_M^7}\vec{R}_M\,\vec{R}_M\cdot[V_M]\cdot\vec{R}_M + \frac{\gamma'}{R_M^5}[V_M]\cdot\vec{R}_M$$

where $\vec{R}_M$ is assumed to be written in the same base system as $[V_M]$. Since $\vec{R}_M$ is the result of the trajectory calculation, it will be available in the base date $\hat{X}_B\ \hat{Y}_B\ \hat{Z}_B$ system. It is therefore necessary to write $[V_M]$ in that system. This may be done by the similarity transformation composed of precession, nutation and libration:

$$[V_M]_B = [A][N][L][V_M]_M[L]^{-1}[N]^{-1}[A]^{-1}$$

The values of γ', A, B, C employed are those given in reference 1, p. 79:

$$\gamma' = 0.6671 \times 10^{-19} \ KM^3/KG-SEC^2$$

$$A = 0.88746 \times 10^{29} \ KG-KM^2$$

$$B = 0.88746 \times 10^{29} \ KG-KM^2$$

$$C = 0.88801 \times 10^{29} \ KG-KM^2$$

The values of A, B, C, above agree with I_A, I_B and I_C given in reference 8, p. 7-2.

Appendix 3. Alternate Subroutine DATE

The following equations will accept a calander launch date and time and produce the required T_B, T, ΔT and $d-d_{50}$ for launch dates from A.D. 1950 to 2000. The inputs and outputs are identical to those described under DATE, Section 2.4.2.2 except that instead of DAYS, the following two quantities are input:

D_ℓ = day of mongh
M_ℓ = month of year.

For example, launch on January 30, 1963 at 2:30 P. M. would be input as NYEARP 1963.0 M_ℓ = 1.0, D_ℓ = 30.0, HRS = 14.0, HMIN = 30.0

(1) $d_B - d_\ell$ = integral number of days from 0.0 of launch date to base date, counting launch day but not base day.

$$= 365 + \lambda - (D_\ell - 1) - IP(B) - \delta$$

where $\alpha = (NYEARP - 1948)/4.0 + 0.01$

$$B = 30.608\, M_\ell - 32.408$$

$$\lambda = \begin{cases} 1 \text{ if } [\alpha - IP(\alpha)] < 0.011 \text{ and } M_\ell < 3 \\ 0 \text{ otherwise} \end{cases}$$

$$\delta = \begin{cases} IP(1.6\, M_\ell) \text{ if } M_\ell < 2.5 \\ 0 \text{ if } M_\ell > 2.5 \end{cases}$$

(2) $t_B - t_\ell$ = time from launch to base date, in hours

$$= 24.0\,(d_B - d_\ell) - HRS - \frac{HMIN}{60} - \frac{SEC}{3600}$$

(3) $$\Delta T = \frac{(t - t_\ell) - (t_B - t_\ell)}{(24.0)(36525)}$$

= time from base date to time of trajectory in Julian centuries of 36525 days.

(4) $$T_B = \frac{365.0\,(NYERP - 1949) + IP(\alpha)}{36525.0}$$

= Julian centuries from $0^h.0$ Jan. 1, 1950 to base date

(5) $$T = T_B + \Delta T$$

(6) $$(d - d_{50}) = 36525.0\, T$$

0-29-10 CA SAME

N64-18228

3.0. COORDINATE TRANSFORMATIONS, PHASE II

C. I. Smith

3.1. Precession Matrix A.

The precession matrix A transforms from a coordinate system defined by a mean equator and equinox of date to a coordinate system defined by the mean equator and equinox of base date. References 1, 3, and 4 give both exact and approximate formulations for the elements of A. Under Phase I, these approximate formulae have been programmed in single precision. For Phase II, a double precision program for these approximations is being written. To test the accuracy of the approximate formulation, the exact equations as given below will be written in double precision and a comparison will be made with the double precision approximations. If the results compare to ten places in a series of computations to be specified later, then the approximate equations will be accepted for use in the high-precision program.

Let χ_D = position components at epoch in the mean coordinate system of date;

χ_{1950} = position components in the mean coordinate system of 1950.0;

χ_B = desired position components in the mean base date system;

$A(\tau_B)$ = transformation from the 1950.0 mean system to the mean system of base date;

$A(D)$ = transformation from the 1950.0 mean system to the mean system of epoch.

Then,

$$\chi_B = A(\tau_B)\,\chi_{1950} \tag{1}$$

$$\chi_D = A(D)\,\chi_{1950} \tag{2}$$

Since the A matrix is orthogonal, it inverse may be replace by its transpose, so that

$$\chi_B = A(\tau_B)\,A^T(D)\,\chi_D \tag{3}$$

The following formulae are taken from Ref. 1. Matrix elements a_{ij} are given by:

$$
\begin{aligned}
a_{11} &= -\sin\zeta_0 \sin z + \cos\zeta_0 \cos z \cos\theta \\
a_{12} &= \sin\zeta_0 \cos z + \cos\zeta_0 \sin z \cos\theta \\
a_{13} &= \cos\zeta_0 \sin\theta \\
\\
a_{21} &= -\cos\zeta_0 \sin z - \sin\zeta_0 \cos z \cos\theta \\
a_{22} &= \cos\zeta_0 \cos z - \sin\zeta_0 \sin z \cos\theta \\
a_{23} &= -\sin\zeta_0 \sin\theta \\
\\
a_{31} &= -\cos z \sin\theta \\
a_{32} &= -\sin z \sin\theta \\
a_{33} &= \cos\theta
\end{aligned}
\qquad (4)
$$

The angular arguments of Equation (4) are obtained from the polynomials

$$
\begin{aligned}
\zeta_0 &= 0^\circ.640\,276\,94\,T + 0^\circ.838\,888 \times 10^{-4} T^2 + 0^\circ.497\,2 \times 10^{-5} T^3 \\
z &= 0^\circ.640\,276\,94\,T + 0^\circ.303\,611\,11 \times 10^{-3} T^2 + 0^\circ.5333 \times 10^{-5} T^3 \\
\theta &= 0^\circ.556\,749\,44\,T - 0^\circ.118\,3333 \times 10^{-3} T^2 - 0^\circ.115\,55 \times 10^{-4} T^3
\end{aligned}
\qquad (5)
$$

where T is measured in Julian centuries of 36,525 days from January 1.0, 1950. A tabulation of base dates in Julian centuries from 1950 to 1986 is given in Appendix A.

The precise velocity transformation is obtained by differentiating Equation (3):

$$
\dot{\psi}_B = A(T_B) A^T(D) \dot{\psi}_D + \left[A(T_B) \dot{A}^T(D) + \dot{A}(T_B) A^T(D) \right] \psi_D \qquad (6)
$$

Elements of the differentiated matrices are obtained by operating on Equations (4) and (5):

$$
\begin{aligned}
\dot{a}_{11} &= -[\cos\phi_0 \sin\chi + \sin\phi_0 \cos\chi \cos\theta]\dot{\phi}_0 \\
&\quad -[\sin\phi_0 \cos\chi + \cos\phi_0 \sin\chi \cos\theta]\dot{\chi} \\
&\quad -[\cos\phi_0 \cos\chi \sin\theta]\dot{\theta} \\
\dot{a}_{12} &= [\cos\phi_0 \cos\chi - \sin\phi_0 \sin\chi \cos\theta]\dot{\phi}_0 \\
&\quad -[\sin\phi_0 \sin\chi - \cos\phi_0 \cos\chi \cos\theta]\dot{\chi} \\
&\quad -[\cos\phi_0 \sin\chi \sin\theta]\dot{\theta} \\
\dot{a}_{13} &= -[\sin\phi_0 \sin\theta]\dot{\phi}_0 + [\cos\phi_0 \cos\theta]\dot{\theta}
\end{aligned}
\qquad \text{(7a)}
$$

$$
\begin{aligned}
\dot{a}_{21} &= [\sin\phi_0 \sin\chi - \cos\phi_0 \cos\chi \cos\theta]\dot{\phi}_0 \\
&\quad -[\cos\phi_0 \cos\chi - \sin\phi_0 \sin\chi \cos\theta]\dot{\chi} \\
&\quad +[\sin\phi_0 \cos\chi \sin\theta]\dot{\theta} \\
\dot{a}_{22} &= -[\sin\phi_0 \cos\chi + \cos\phi_0 \sin\chi \cos\theta]\dot{\phi}_0 \\
&\quad -[\cos\phi_0 \sin\chi + \sin\phi_0 \cos\chi \cos\theta]\dot{\chi} \\
&\quad +[\sin\phi_0 \sin\chi \sin\theta]\dot{\theta} \\
\dot{a}_{23} &= -[\cos\phi_0 \sin\theta]\dot{\phi}_0 - [\sin\phi_0 \cos\theta]\dot{\theta}
\end{aligned}
\qquad \text{(7b)}
$$

$$\left.\begin{aligned} \dot{a}_{31} &= [\sin z \sin\theta]\dot{z} - [\cos z \cos\theta]\dot{\theta} \\ \dot{a}_{32} &= -[\cos z \sin\theta]\dot{z} - [\sin z \cos\theta]\dot{\theta} \\ \dot{a}_{33} &= -[\sin\theta]\dot{\theta} \end{aligned}\right\} \qquad (7c)$$

$$\begin{aligned} \dot{\zeta}_o &= 0^\circ.640\,276\,94 + 1^\circ.677\,776 \times 10^{-4} T + 1^\circ.4916 \times 10^{-5} T^2 \\ \dot{z} &= 0^\circ.640\,276\,94 + 0^\circ.607\,222\,22 \times 10^{-3} T + 1^\circ.5999 \times 10^{-5} T^2 \\ \dot{\theta} &= 0^\circ.556\,749\,44 - 0^\circ.236\,666\,66 \times 10^{-3} T - 0^\circ.3465 \times 10^{-4} T^2 \end{aligned}$$

(8)

For Phase I, approximate elements are used for the precession matrix [A], and the matrix [$\dot{A}$] is assumed zero.

3.2 Nutation Matrix N.

Nutation in longitude and obliquity are described by the N matrix, the elements of which are:

$$\begin{aligned} N_{11} &= \cos\delta\psi & N_{21} &= \sin\delta\psi\cos\epsilon \\ N_{12} &= \sin\delta\psi\cos\bar{\epsilon} & N_{22} &= \cos\delta\psi\cos\epsilon\cos\bar{\epsilon} + \sin\epsilon\sin\bar{\epsilon} \\ N_{13} &= \sin\delta\psi\sin\bar{\epsilon} & N_{23} &= \cos\delta\psi\cos\epsilon\sin\bar{\epsilon} - \sin\epsilon\cos\bar{\epsilon} \end{aligned}$$

$$\begin{aligned} N_{31} &= \sin\delta\psi\sin\epsilon \\ N_{32} &= \cos\delta\psi\sin\epsilon\cos\bar{\epsilon} - \cos\epsilon\sin\bar{\epsilon} \\ N_{33} &= \cos\delta\psi\sin\epsilon\sin\bar{\epsilon} + \cos\epsilon\cos\bar{\epsilon} \end{aligned}$$

(9)

For Phase I, an approximation to this matrix is employed:

$$N = \begin{Bmatrix} 1 & -\delta\psi\cos\bar{\epsilon} & -\delta\psi\sin\bar{\epsilon} \\ \delta\psi\cos\bar{\epsilon} & 1 & -\delta\epsilon \\ \delta\psi\sin\bar{\epsilon} & \delta\epsilon & 1 \end{Bmatrix} \tag{10}$$

where, in Equations (9) and (10),

$\delta\psi$ = nutation in longitude;
$\delta\epsilon$ = nutation in obliquity;
$\bar{\epsilon}$ = mean obliquity;
$\epsilon = \bar{\epsilon} + \delta\epsilon$ = true obliquity.

In Phase I, the nutation in longitude is computed from

$$\delta\psi = \sum_{i=1}^{22} a_i(T)\sin\theta_i' \tag{11}$$

and the nutation in obliquity from

$$\delta\epsilon = \sum_{i=1}^{15} b_i\cos\phi_i' \tag{12}$$

where the arguments θ_i' and ϕ_i' are various combinations of the following angles:

Ω = longitude of the mean ascending node of the lunar orbit on the ecliptic, measured from the mean equinox of date;

$\mathbb{C}$ = mean longitude of the moon, measured in the ecliptic from the mean equinox of date to the mean ascending node of the lunar orbit, and then along the orbit;

Γ' = mean longitude of the lunar perigee, measured in the same manner as $\mathbb{C}$;

L = mean longitude of the sun;

Γ = mean longitude of the solar perigee.

The form of the nutation matrix represented by Equations (10), (11) and (12) have been programmed in single precision from the notes of J. Bellantoni. Double precision programming of this transformation is now being done.

More accurate forms of $\delta\psi$ and $\delta\epsilon$ are described in Ref. 1. Equations for these descriptions are given here for the purpose of obtaining a double precision program to be compared with the simpler, less accurate versions of $\delta\psi$ and $\delta\epsilon$ described above. More terms are included in the more accurate forms, and the arguments of the sine and cosine functions are combinations of different angles. In compact notation,

$$\delta\psi = \sum_{i=1}^{69} a_i(T) \sin\theta_i \tag{13}$$

$$\delta\epsilon = \sum_{i=1}^{40} b_i(T) \cos\phi_i \tag{14}$$

The sine and cosine arguments are combinations of

Ω = longitude of the mean ascending node of the lunar orbit on the ecliptic, measured from the mean equinox of date;

$D = \mathbb{C} - L$ = the mean elongation of the moon from the sun;

$\ell = \mathbb{C} - \Gamma'$ = the mean elongation of the moon from the lunar perigee;

$\ell' = L - \Gamma$ = the mean elongation of the sun from the solar perigee;

$F = \mathbb{C} - \Omega$ = the mean elongation of the moon from the ascending node of the lunar orbit.

For Phase II, these arguments are derived by updating the equations in the references from epoch 1900 to epoch 1950 and then combining the appropriate angles as shown above. To update, the variables are

d = 18,262.5 ephemeris days

T = 0.5 Julian centuries

Making these substitutions:

$$\ell = 215^\circ.531\,462 + 13^\circ.064\,992\,4665\,d + 0^\circ.009\,192\,T^2 + 0^\circ.000\,014\,4\,T^3 \tag{15}$$

$$l' = 358^\circ.000\,670 + 0^\circ.985\,600\,266\,9\,d - 0^\circ.000\,149\,T^2 - 0^\circ.000\,000\,33\,T^3 \quad (16)$$

$$F = 52^\circ.264\,140\,3 + 13^\circ.229\,350\,499\,0\,d - 0^\circ.003\,211\,T^2 - 0^\circ.000\,000\,3\,T^3 \quad (17)$$

$$D = 144^\circ.294\,235\,4 + 12^\circ.190\,749\,191\,4\,d - 0^\circ.001\,435\,T^2 + 0^\circ.000\,001\,9\,T^3 \quad (18)$$

$$\Omega = 12^\circ.112\,822\,4 - 0^\circ.052\,953\,922\,2\,d + 0^\circ.002\,077\,2\,T^2 + 0^\circ.000\,002\,24\,T^3 \quad (19)$$

Additionally, the mean obliquity, $\bar{\epsilon}$, is given by

$$\bar{\epsilon} = 23^\circ.445\,787\,4 - 0^\circ.013\,012\,5\,T - 0^\circ.000\,001\,64\,T^2 + 0^\circ.000\,000\,503\,T^3 \quad (20)$$

Coefficients and arguments for Equations (13) and (14) appear in Tables 1 and 2 respectively.

TABLE 1

NUTATION IN LONGITUDE

i	θ_i		$a_i(T)$ Degrees			Note 1
1	Ω	-47.8927	-0.04825	x	T	
2	2Ω	0.5800	+0.00006	x	T	
3	$-2\ell + 2F + \Omega$	0.013				
4	$2\ell - 2F$	0.0028				
5	$-2\ell' + 2F - 2D + \Omega$	-0.001				
6	$-2\ell + 2F + 2\Omega$	-0.0008				
7	$\ell - C - D$	-0.0006				
8	$2F - 2D + 2\Omega$	-3.536	-0.00036	x	T	
9	ℓ'	0.3499	-0.00086	x	T	
10	$\ell' + 2F - 2D + 2\Omega$	-0.138	+0.00033	x	T	
11	$-\ell' + 2F - 2D + 2\Omega$	0.0594	-0.0001	x	T	
12	$2F - 2D + \Omega$	0.0344	+0.00003	x	T	
13	$2\ell - 2D$	0.013				
14	$2F - 2D$	-0.0058				
15	$2\ell'$	0.0044	-0.00003	x	T	
16	$\ell' + \Omega$	-0.0042				
17	$2\ell' + 2F - 2D + 2\Omega$	-0.0042	+0.00003	x	T	
18	$-\ell' + \Omega$	-0.0028				
19	$-2\ell + 2D + \Omega$	-0.0014				
20	$-\ell' + 2F - 2D + \Omega$	-0.0014				
21	$2\ell - 2D + \Omega$	0.001				
22	$\ell' + 2F - 2D + \Omega$	0.0008				
23	$\ell - D$	-0.008				
24	$2F + 2\Omega$	-0.5658	-0.00006	x	T	
25	ℓ	0.188	+0.00003	x	T	
26	$2F + \Omega$	-0.0950	-0.0001	x	T	
27	$\ell + 2F + 2\Omega$	-0.0725				
28	$\ell - 2D$	-0.0414				

TABLE 1 (CONTINUED)

NUTATION IN LONGITUDE

i	Θ_i	$a_i(T)$ Degrees	Note 1
29	$-\ell+2F+2\Omega$	0.0317	
30	$2D$	0.017	
31	$\ell+\Omega$	0.016	
32	$-\ell+\Omega$	-0.016	
33	$-\ell+2F+2D+2\Omega$	-0.014	
34	$\ell+2F+\Omega$	-0.012	
35	$2F+2D+2\Omega$	-0.0089	
36	2ℓ	0.0078	
37	$\ell+2F-2D+2\Omega$	0.0072	
38	$2\ell+2F+2\Omega$	-0.0072	
39	$2F$	0.0069	
40	$-\ell+2F+\Omega$	0.0053	
41	$-\ell+2D+\Omega$	0.0039	
42	$\ell-2D+\Omega$	-0.0036	
43	$-\ell+2F+2D+\Omega$	-0.003	
44	$\ell+\ell'-2D$	-0.002	
45	$\ell'+2F+2\Omega$	0.002	
46	$\ell+2D$	0.002	
47	$2D+\Omega$	-0.002	
48	$-\ell'+2F+2\Omega$	-0.002	
49	$\ell+2F+2D+2\Omega$	-0.002	
50	$2\ell+2F-2D+2\Omega$	0.002	
51	$-2D+\Omega$	-0.001	
52	$2F+2D+\Omega$	-0.001	
53	$\ell+2F-2D+\Omega$	0.001	

TABLE 1 (CONTINUED)

NUTATION IN LONGITUDE

i	θ_i	$a_i(T)$ Degrees	Note 1
54	D	-0.001	
55	$l' - 2D$	-0.001	
56	$l - l'$	0.001	
57	$l - 2F$	0.001	
58	$2l + 2F + \Omega$	-0.001	
59	$l + 2F$	0.0008	
60	$l + l'$	-0.0008	
61	$l - l' + 2F + 2\Omega$	-0.0008	
62	$-2l + \Omega$	-0.0006	
63	$-l + 2F - 2D + \Omega$	-0.0006	
64	$2l + \Omega$	0.0006	
65	$-l' - l + 2F + 2D + 2\Omega$	-0.0006	
66	$-l' + 2F + 2D + 2\Omega$	-0.0006	
67	$l + 2\Omega$	-0.0006	
68	$l + l' + 2F + 2\Omega$	0.0006	
69	$3l + 2F + 2\Omega$	-0.0006	

Note 1: Multiply all a_i by 10^{-4}.

TABLE 2

NUTATION IN OBLIQUITY

i	ϕ_i	$b_i(T)$ Degrees			Note 1
1	Ω	25.584	+ 0.0025	×	T
2	2Ω	-0.251	+ 0.0001	×	T
3	$-2\ell + 2F + \Omega$	-0.0067			
4	$-2\ell' + 2F - 2D + \Omega$	0.0006			
5	$-2\ell + 2F + 2\Omega$	0.0006			
6	$2F - 2D + 2\Omega$	1.534	-0.00081	×	T
7	$\ell' + 2F - 2D + 2\Omega$	0.0599	-0.0002	×	T
8	$-\ell' + 2F - 2D + 2\Omega$	-0.026	+0.00008	×	T
9	$2F - 2D + \Omega$	-0.018			
10	$\ell' + \Omega$	0.002			
11	$2\ell' + 2F - 2D + 2\Omega$	0.002			
12	$-\ell' + \Omega$	0.001			
13	$-2\ell + 2D + \Omega$	0.0008			
14	$-\ell' + 2F - 2D + \Omega$	0.0008			
15	$2\ell - 2D + \Omega$	-0.0006			
16	$\ell' + 2F - 2D + \Omega$	-0.0006			
17	$2F + 2\Omega$	0.246	-0.0001	×	T
18	$2F + \Omega$	0.0508			
19	$\ell + 2F + 2\Omega$	0.0314	-0.00003	×	T
20	$-\ell + 2F + 2\Omega$	-0.014			
21	$\ell + \Omega$	-0.0086			
22	$-\ell + \Omega$	0.0083			
23	$-\ell + 2F + 2D + 2\Omega$	0.0061			
24	$\ell + 2F + \Omega$	0.0064			
25	$2F + 2D + 2\Omega$	0.0039			
26	$\ell + 2F - 2D + 2\Omega$	-0.0031			
27	$2\ell + 2F + 2\Omega$	0.0031			
28	$-\ell + 2F + 2\Omega$	-0.0028			
29	$-\ell + 2D + \Omega$	-0.002			
30	$\ell - 2D + \Omega$	0.002			

TABLE 2 (CONTINUED)

NUTATION IN OBLIQUITY

i	ϕ_i	$b_i(T)$ Degrees	Note 1
31	$-\ell + 2F + 2D + \Omega$	0.001	
32	$\ell' + 2F + 2\Omega$	-0.0008	
33	$2D + \Omega$	0.0008	
34	$-\ell' + 2F + 2\Omega$	0.0008	
35	$\ell + 2F + 2D + 2\Omega$	0.0008	
36	$2\ell + 2F - 2D + 2\Omega$	-0.0006	
37	$-2D + \Omega$	0.0008	
38	$2F + 2D + \Omega$	0.0008	
39	$\ell + 2F - 2D + \Omega$	-0.0008	
40	$2\ell + 2F + \Omega$	0.0006	

Note 1: Multiply all b_i by 10^{-4}.

3.3. Libration Matrix M.

The libration transformation is employed to determine the orientation of the moon with respect to the earth, thereby permitting a point on the moon's surface to be expressed in base date inertial coordinates, or permitting vehicle coordinates with respect to the earth to be expressed in selenographic coordinates. Equations (21) give the elements of the M matrix which transforms to a selenocentric coordinate system from a system based on the true equator and equinox of date. From Ref. 4:

$$
\begin{aligned}
M_{11} &= \cos\Omega'\cos\Lambda - \sin\Omega'\sin\Lambda\cos i \\
M_{21} &= \sin\Omega'\cos\Lambda + \cos\Omega'\sin\Lambda\cos i \\
M_{31} &= \sin\Lambda\sin i \\
M_{12} &= -\cos\Omega'\sin\Lambda - \sin\Omega'\cos\Lambda\cos i \\
M_{22} &= -\sin\Omega'\sin\Lambda + \cos\Omega'\cos\Lambda\cos i \\
M_{32} &= \cos\Lambda\sin i \\
M_{13} &= \sin\Omega'\sin i \\
M_{23} &= -\cos\Omega'\sin i \\
M_{33} &= \cos i
\end{aligned}
\qquad (21)
$$

The arguments of the trigonometric functions in (21) are obtained from:

$$
\begin{aligned}
\cos i &= \cos(\Omega+\sigma+\delta\psi)\sin\epsilon\sin(I+\rho) + \cos\epsilon\cos(I+\rho), \qquad 0<i<\tfrac{\pi}{2} \\
\sin\Omega' &= -\sin(\Omega+\sigma+\delta\psi)\sin(I+\rho)\csc i, \qquad -\tfrac{\pi}{2}<\Omega'<\tfrac{\pi}{2} \\
\sin\Delta &= -\sin(\Omega+\sigma+\delta\psi)\sin\epsilon\csc i \\
\cos\Delta &= -\sin(\Omega+\sigma+\delta\psi)\sin\Omega'\cos\epsilon \\
&\quad -\cos(\Omega+\sigma+\delta\psi)\cos\Omega', \qquad 0\le\Delta<2\pi
\end{aligned}
\qquad (22)
$$

$$\Lambda = \Delta + (\mathbb{C}+\tilde{c}) - (\Omega+\sigma)$$

$$\epsilon = \bar{\epsilon} + \delta\epsilon$$

In Ref. 3, the following values are given for σ, τ, ρ, I:

$$\begin{aligned}
\sigma \sin I &= -0^\circ.030\,2777 \sin g + 0^\circ.010\,2777 \sin(g+2\omega) \\
&\quad -0^\circ.003\,065\,55 \sin(2g+2\omega) \\
\tau &= -0^\circ.003\,333 \sin g + 0^\circ.016\,388\,8 \sin g' \\
&\quad +0^\circ.005 \sin 2\omega \\
\rho &= -0^\circ.029\,722\,2 \cos g + 0^\circ.010\,2777 \cos(g+2\omega) \\
&\quad -0^\circ.003\,055\,55 \cos(2g+2\omega) \\
I &= 1^\circ.535
\end{aligned} \tag{23}$$

where

$$\begin{aligned}
g &= 215^\circ.540\,13 + 13^\circ.064\,992 d \\
g' &= 358^\circ.009\,067 + 0^\circ.985\,600\,5 d \\
\omega &= 196^\circ.745\,632 + 0^\circ.164\,358\,6 d
\end{aligned} \tag{24}$$

Derivatives for the elements of (21) are also given in Ref. (3). In summary, these quantities are:

$$\begin{aligned}
\dot{M}_{11} &= (-\sin\Lambda\cos\Omega' - \cos\Lambda\sin\Omega'\cos i)\dot{\Lambda} \\
\dot{M}_{12} &= (-\sin\Lambda\sin\Omega' + \cos\Lambda\cos\Omega'\cos i)\dot{\Lambda} \\
\dot{M}_{13} &= (\cos\Lambda\sin i)\dot{\Lambda} \\
\dot{M}_{21} &= (-\cos\Lambda\cos\Omega' + \sin\Lambda\sin\Omega'\cos i)\dot{\Lambda} \\
\dot{M}_{22} &= (-\cos\Lambda\sin\Omega' - \sin\Lambda\cos\Omega'\cos i)\dot{\Lambda} \\
\dot{M}_{23} &= (-\sin\Lambda\sin i)\dot{\Lambda} \\
\dot{M}_{31} &= \dot{M}_{32} = \dot{M}_{33} = 0
\end{aligned} \tag{25}$$

$$\dot{\Lambda} = \dot{\Delta} + \dot{\zeta} + \dot{\tau} - \dot{\Omega} - \dot{\sigma}$$

$$\dot{\Delta} = \frac{-\cos(\Omega + \sigma + \delta\psi)\sin\epsilon\,(\dot{\Omega} + \dot{\sigma})}{\sin i \cos\Delta}$$

$$\dot{\zeta} = 0.266\,170\,762\,(10^{-5}) - 0.124\,991\,71\,(10^{-12})T \text{ RADIANS/SEC.}$$

$$\dot{\Omega} = -0.106\,969\,843\,5\,(10^{-7}) + 0.230\,153\,29\,(10^{-13})T \text{ RADIANS/SEC.}$$

$$\begin{aligned}\dot{\tau} = {} & -0.153\,527\,294\,6\,(10^{-9})\cos g \\ & +0.669\,494\,067\,(10^{-10})\cos g' \\ & +0.379\,473\,484\,(10^{-11})\cos 2\omega \text{ RADIANS/SEC.}\end{aligned} \tag{26}$$

$$\begin{aligned}\dot{\sigma} = {} & -0.520\,642\,191\,(10^{-7})\cos g \\ & +0.181\,177\,445\,1\,(10^{-7})\cos(g + 2\omega) \\ & -0.106\,405\,785\,8\,(10^{-7})\cos(2\omega + 2g) \text{ RADIANS/SEC.}\end{aligned}$$

Refinements in these expressions can be made by using the more accurate values of $\delta\psi$ and $\delta\epsilon$ from Section 3.2, and by using the more precise values of Ω, ζ and $\bar{\epsilon}$. Development of these refinements are to be postponed until the investigations of the A and N matrices are completed.

3.4. Greenwich Hour Angle Computation

As given in Ref. 3, GHA is computed from:

$$\gamma(T) = \gamma_M(T) + \delta\alpha \tag{27}$$

where

$$\begin{aligned}\gamma_M(T) = {} & 100^\circ.075\,542\,60 + 9^\circ.856\,473\,460\,(10^{-1})d \\ & + 2^\circ.901\,5\,(10^{-13})d^2 + \omega t \ (\text{MOD } 360^\circ), \quad 0 \le \gamma_M(T) < 2\pi\end{aligned} \tag{28}$$

$$\omega = \frac{0.004\,178\,074\,17}{1 + 5.21\,(10^{-13})d} \text{ DEGREES/SEC.}$$

$$d\alpha = \delta\psi\cos\bar{\epsilon} \tag{29}$$

Refinements in $\gamma(\tau)$ may be made by employing the more accurate values of $\delta\psi$ and $\bar{\epsilon}$ from Section 3.2.

3.5. Computation Program

Emphasis will be placed on first determining the precision provided by the A and N matrices before proceeding to $\dot{A}$, $\dot{N}$, $\dot{M}$, M, and the inverses. In this regard, the A and N matrices employed in Phase I are now being programmed in double precision. These same matrices will be re-programmed in double precision using the equations contained in this report. A comparison will be made between the results of the two programs to determine at what significant figure a discrepancy occurs. If the discrepancy arises beyond the ninth significant figure, then the Phase I equations in double precision are adequate for Phase II. If the discrepancy occurs before the ninth significant figure, then the more accurate equations are to be used.

REFERENCES

1. Explanatory Supplement to the Astronomical Ephemeris and the American Ephemeris and Nautical Almanac, H. M. Stationery Office, London, 1961.

2. The Astronomical Ephemeris for the Year 1962, H. M. Stationery Office, London, 1960.

3. Holdridge, D. B., "Space Trajectories Program for the IBM 7090 Computer", J. P. L. Technical Report No. 32-223, March 2, 1962.

4. Kalensher, B. E., "Selenographic Coordinates", J. P. L. Technical Report No. 32-41, February 1961.

Appendix A: REDUCTION FROM CIVIL DATE TO JULIAN CENTURIES

The transformations described previously employ Julian centuries and mean solar days as units of time, each day containing 86,400 mean solar seconds. In the ephemerides to be employed with the Orbit Determination Program, an inertial coordinate system is established at base dates obtaining at the center of a two-year file of planetary coordinates. Consequently, 0^h, January 1 of any year may be chosen as a base date, the choice being a function of the dates over which a particular mission is to be analyzed. Since the transformations are computed from a base epoch of 1950.0, it is necessary to convert from a given civil date to mean solar days and Julian centuries measured from 1950.0. Table A-1 gives accumulated days and Julian centuries from the base epoch to the base date for the years 1950 to 1986. The accumulated Julian centuries are tabulated in double precision.

Conversion from civil date to Julian centuries is computed for time after the base date from

$$T = T_B + \frac{1}{36525}\left\{ d + \frac{h}{24} + \frac{m}{1440} + \frac{s}{86400} \right\} \tag{A-1}$$

where T_B = base date in Julian centuries past 1950.0;
d = days from base date;
h = hours from midnight
m = minutes of the hour;
s = seconds of the minute.

so that the accumulated time from 1950.0 may be expressed as

$$T = T_B + \Delta T \tag{A-2}$$

If time relative to the base date is required, ΔT may be computed directly from Equation (A-1) if the desired civil date occurs after T_B. However, if the civil date occurs before T_B, the relative time $\Delta T'$ is computed from

$$\Delta T' = (T_B - T_{B^-}) - \Delta T \tag{A-3}$$

where T_{B^-} = base date previous to T_B;
$\Delta T'$ = time relative to T_B.

TABLE A-1

BASE DATES IN JULIAN CENTURIES FROM 1950.0

Year	Days Accumulated From 1950.0 to 0^h January 1	Julian Centuries Accumulated From 1950.0 to 0^h January 1
1950	0	0.000 000 000 000 000 0
1	365	0.009 993 155 373 032 2
2*	730	0.019 986 310 746 064 3
3	1096	0.030 006 844 626 967 8
4	1461	0.040 000 000 000 000 0
1955	1826	0.049 993 155 373 032 2
6*	2191	0.059 986 310 746 064 3
7	2557	0.070 006 844 626 967 8
8	2922	0.080 000 000 000 000 0
9	3287	0.089 993 155 373 032 2
1960*	3652	0.099 986 310 746 064 3
1	4018	0.110 006 844 626 967 8
2	4383	0.120 000 000 000 000 0
3	4748	0.129 993 155 373 032 2
4*	5113	0.139 986 310 746 064 3
1965	5479	0.150 006 844 626 967 8
6	5844	0.160 000 000 000 000 0
7	6209	0.169 993 155 373 032 2
8*	6574	0.179 986 310 746 064 3
9	6940	0.190 006 844 626 967 8
1970	7305	0.200 000 000 000 000 0
1	7670	0.209 993 155 373 032 2
2*	8035	0.219 986 310 746 064 3
3	8401	0.230 006 844 626 967 8
4	8766	0.240 000 000 000 000 0
1975	9131	0.249 993 155 373 032 2
6*	9496	0.259 986 310 746 064 3
7	9862	0.270 006 844 626 967 8
8	10227	0.280 000 000 000 000 0
9	10592	0.289 993 155 373 032 2
1980*	10957	0.299 986 310 746 064 3
1	11323	0.310 006 844 626 967 8
2	11688	0.320 000 000 000 000 0
3	12053	0.329 993 155 373 032 2
4*	12418	0.339 986 310 746 064 3
1985	12784	0.350 006 844 626 967 8
6	13149	0.360 000 000 000 000 0

* Leap Year

4.0 PROPAGATION DELAY FROM WWV

D.W. PROCTOR

The raw data from the R and R system is related to the time of the measurement at the ground station. These times are synchronized to WWV and include the time delay from WWV to the ground site. Since all computations must be made on the same time basis, propagation delay corrections from WWV to the site must be included in the computations. Because only three stations are involved, these corrections can be precomputed and stored as program constants for each station location.

A simple derivation of the time corrections is presented here together with a brief analysis of the errors which occur in using these equations.

4.1 Derivation of Time Delay

First, assume that the great circle arc between WWV and the ground station has been determined. Figure 1 illustrates some of the principle propagation paths that exist.

Essentially, the electromagnetic path bounces between the ionospheric maximum electron density layer and the earth's surface. Experience has indicated that the one-hop mode cannot exist for stations separated by more than 4000 km (39 degrees, great circle arc). One limitation to the number of hops which can be made is the attenuation of the signal at each reflection. The ultimate limit occurs when the angle between the ray striking the ionosphere and the tangent to the ionosphere becomes larger than a certain critical angle, after which the signal passes through and is not reflected.

When the signal can be received at a station in both the one-hop and two-hop modes, the two-hop signal is delayed slightly and is greatly attenuated by the additional number of imperfect reflections. Thus, the number of effective hops, m, is determined from

$$m = \left[\frac{GCD}{4000}\right] + 1 \qquad (1)$$

where [ ] indicates reduction to an integer, GCD = great circle distance (KM)

Figure 2 illustrates the geometry employed to compute the subsequent total range from which the propagation time is readily computed.

$$\theta' = \frac{\theta}{m} \qquad (2)$$

θ = total great circle arc
m = number of hops, from (1)
H = reflecting height
R_E = earth's radius

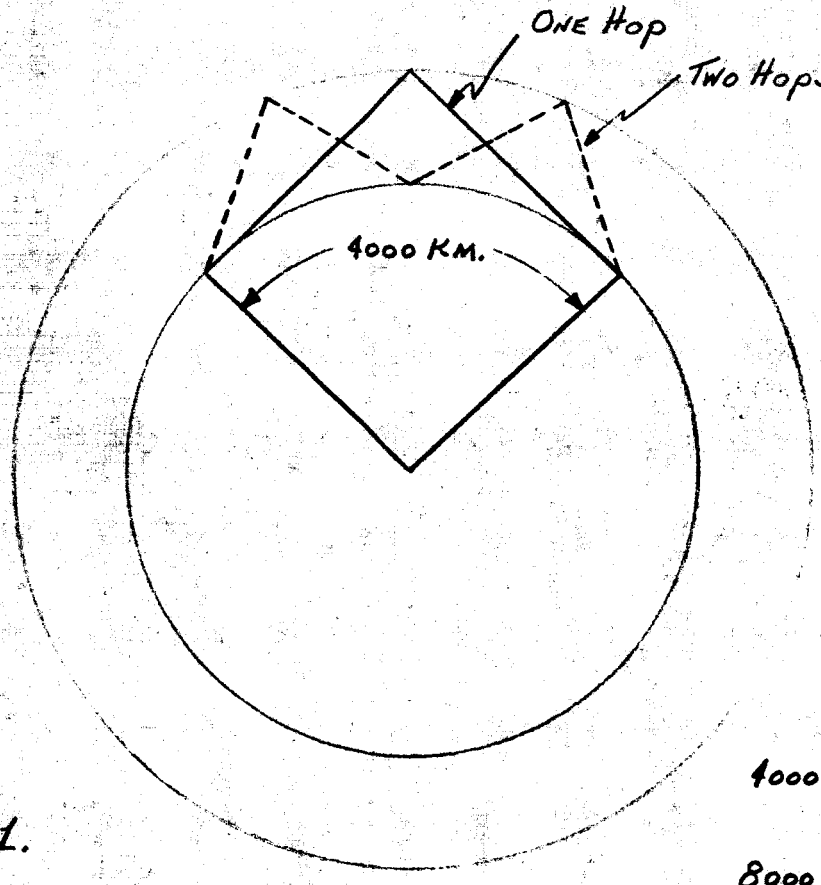

FIGURE 1.

4000 KM. = MAXIMUM ONE-HOP RANGE

8000 KM. = MAXIMUM TWO-HOP RANGE

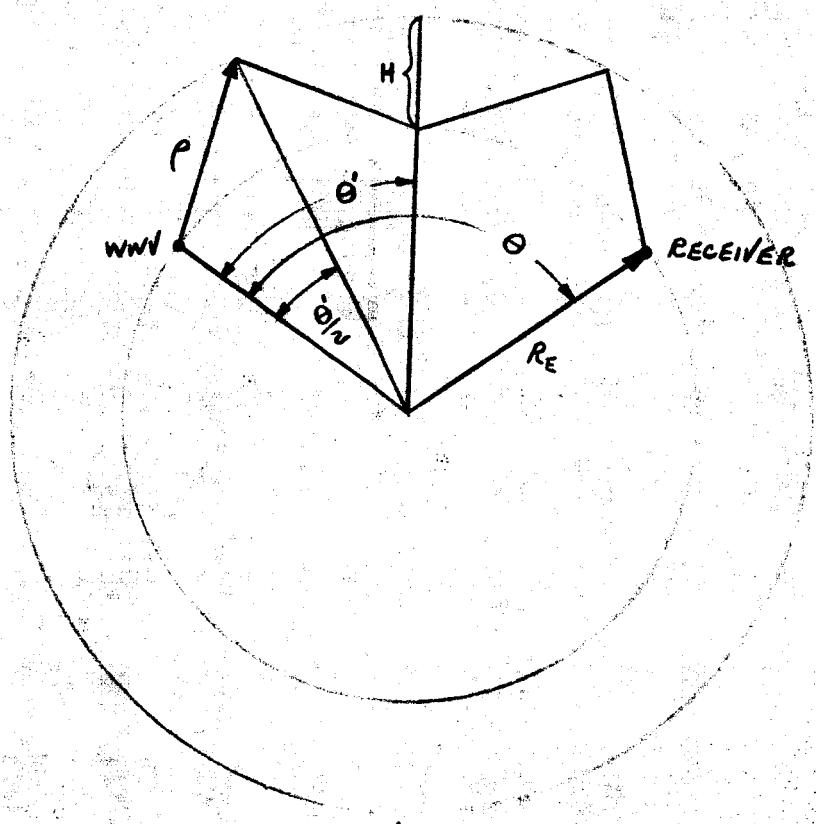

FIGURE 2.

Then

$$\rho = \sqrt{R_E^2 + (R_E+H)^2 - 2(R_E+H)R_E \cos\frac{\theta'}{2}}$$

$$\rho = 2\sqrt{(R_E^2 + R_E H)\sin^2\frac{\theta'}{4} + \left(\frac{H}{2}\right)^2}$$

Now, by definition, the total path length is $\rho_T = 2m\rho$ the angle $\theta' = \theta/m$, and the propagation time, $t = \rho_T/c$, c being the velocity of light in the propagating medium. Thus

$$t = \rho_T/c = 2m\rho/c = \frac{4m}{c}\sqrt{(R_E^2 + R_E H)\sin^2\frac{\theta}{4m} + \left(\frac{H}{2}\right)^2}$$

4.2 Error Analysis

4.2.1 Velocity of Light

Estimating the error in using this equation can be based on standard differential techniques.

First, assume that c, the velocity of propagation in the medium, differes from the free space velocity. Then,

$$\frac{dt}{dc} = \frac{-\rho_T}{c^2} = -\frac{t}{c}$$

$$dt = -t\frac{dc}{c}$$

Assuming that t is at its maximum, i.e., $t \approx 65$ milliseconds and that c is in error by 1×10^{-4}, $dt = 65 \times 10^{-4}$ milliseconds, a negligible amount.

4.2.2 H, height of reflecting layer

$$\frac{dt}{dH} = \frac{8m^2}{c^2 t}\left(R_E \sin^2\frac{\theta}{4m} + \frac{H}{2}\right)$$

Example 1

Let $n = 1$, $C = 298{,}000$ KM/SEC., $R_E = 6370$ KM., $H = 350$ KM.,

$\theta = 6.1$ degrees, t = 3.6 milliseconds (equivalent to WWV to Rosman, N.C. path). Then,

$$\frac{dt}{dH} = 4.4 \times 10^{-6} \text{ SEC./KM.}$$

For a critical height differential of 100 KM between an assumed value (in this example 350 KM) and the true value, the resulting error in time is

$$\Delta t = (4.4)(10^{-6})(100) = 0.44 \text{ MILLISECONDS}$$

Example 2

Let $n = 5$, $C = 298{,}000$ KM./SEC., $R_E = 6370$ KM., $H = 350$ KM., $\theta = 151.6$

$t = 59.1$ milliseconds (equivalent to WWV to Woomera, Australia)

Then,

$$\frac{dt}{dH} = 11 \times 10^{-6} \text{ SEC./KM.}$$

In this case, the timing error for an error of 100 KM in H is 1.1 milliseconds.

For both examples, the error is seen to be significant.

4.2.3 Summary of Error Analysis

A 18229 pkw

The magnitudes of the numbers which arise from errors in H might indicate a problem area. However, NASA's experience has been that a millisecond accuracy can be achieved. The explanation for this apparent discrepancy between theory and observation is to be found in the mechanization of the time-keeping apparatus at the ground sites.

Each station has a highly stable, atomic oscillator-controlled clock which is synchronized to WWV. The long term stability of these clocks act as a filter on the high frequency (periods of one day or less) components of time shift due to the ionospheric height change. Thus, the net effect is the same as if the ionospheric height was averaged over the day. Thus, choosing the value of H = 350 KM and assuming it to be a constant is probably very reasonable.

4.3 Calculation of Great Circle Arc

The calculation of the great circle arc between two stations follows the usual laws of solid geometry. Define + North Latitude, − South; all longitude are + east from Greenwich, 0 to 2π.

1. For two stations A and B, compute the angle between the North pole and the station

   $a = 90 - \text{Lat (A)}$

   $b = 90 - \text{Lat (B)}$

2. Compute the polar angle between A and B,

   $P = \text{Long (B)} - \text{Long (A)}$

3. Solve for p, the Great Circle Arc,

   $$\rho = \cos^{-1}[\cos a \cos b - \sin a \sin b \cos P$$

   where $0 \leq \rho \leq \pi$.

0-08-10

CA Same

N64-18230

5.0 TIME ADJUSTMENT AND AMBIGUITY RESOLUTION OF MINIVAR INPUT DATA

C. A. LASPINA

8 Nov, 1963

P61-64 ref (See N64-18226 10-01) OTS; etc.

[2]

Tracking data from both the Minitrack and Range and Range Rate (RARR) systems include errors in the time ascribed to the various quantities measured by these systems approximately equal to the propagation time of the signals from the vehicles to the ground station. In addition, the RARR measures range with an ambiguity of approximately 11,000, 2750, or 550 miles depending on the lowest range tone used. Both the time adjustment and the ambiguity resolution require a knowledge of the approximate range to the vehicle and hence both corrections will be made as part of the MINIVAR program using a nominal range computed from the most recent estimates of the state variables.

These errors and proposed corrections are described below.

5.1 MINITRACK System

The time ascribed to the direction cosines measured by the Minitrack system are in error by the propagation time from the vehicle to the station. This error will be corrected by using a nominal range computed by integrating the equations of motion with the most recent estimate of the state variables as the initial conditions. One value of nominal range will be used to correct all data within a five second interval. Using this single nominal range for five seconds of data causes a timing error of less than 0.3 milliseconds, which is negligible.

5.2 Range and Range Rate System

The RARR system data block includes 10 measured quantities and a reference time, T_s, plus various data quality indicators and four control digits. Each of the measured quantities requires a time adjustment for the effects of propagation in order to effect the correct correspondence between the measurement and its associated time. The errors in angle, range and range rate measured by the RARR system and the proposed adjustments are described below.

5.3 Angles

The antenna pointing angles recorded in a data block are measured at the reference time, T_s. However these angles

describe the position of the vehicle not at time, T_s, but at a time earlier than T_s by an interval equal to the propagation time from the vehicle to the station. However, since the angle data is relatively inaccurate it has been decided that, at least for Phase I, the reference time, T_s, will be used for angle data.

5.4 Range Data

Unlike angle data, range data from the RARR system is very accurate and must be correctly time-labeled to fully reflect the available instrumentation accuracy. In addition, the RARR system uses a periodic modulation to measure range and hence is subject to range ambiguities; these ambiguities must be resolved not only to yield the correct range but also to accurately time label the range reading.

The range ambiguity can be resolved by integrating the equations of motion to determine a nominal range, R_I. This same nominal range could be used to resolve the ambiguities in at least a minute of tracking data but the time corrections computed using this nominal range would be in error by an excessive amount. Computing a new nominal range for every five seconds of tracking data reduces this error to a tolerable value. The unambiguous range, R_a, is dependent on the lowest range time, f_L, used and is given by

$$R_a = \frac{c}{2f_L} \tag{1}$$

The data block includes a control digit, C1, which specifies the lowest range tone used to measure the range:

c1	f_L, cps
1, 2, 3	8
4, 5, 6	32
7, 8, 9	160

The correct (unambiguous) round trip propagation time, T_{RT}, including the effect of transponder delay, T_T, is given by

$$T_{RT} = T_P + \left[\frac{R_I}{R_a}\right] T_a - T_T \tag{2}$$

where T_p is the measured time interval between corresponding zero crossings of the transmitted and received signal (R in the data block) and T_a is the period of the lowest range tone:

$$T_a = \frac{1}{f_L} \tag{3}$$

The brackets, $[\ ]$, in Eq. 2 mean the integer portion of the quotient R_I/R_a. The true range, R_c, is then given by

$$R_c = \frac{c}{2} T_{RT} \tag{4}$$

In terms of the round trip time, the time of the range measurement, T_{RM}, is

$$T_{RM} = T_S + T_P - \frac{T_{RT}}{2} \tag{5}$$

Using Eq. 2 this becomes

$$T_{RM} = T_S + \frac{T_P}{2} - \frac{1}{2} \left[\frac{R_I}{R_a}\right] T_a \tag{6}$$

In order to insure that small errors in R_I do not cause the wrong number of periods of the lowest range tone to be added to the indicated range a reasonableness check will be made:

$$R_I - \frac{1}{2} \left(\frac{c}{2} T_a\right) < T_{RT} \cdot \frac{c}{2} < R_I + \frac{1}{2} \left(\frac{c}{2} T_a\right) \tag{7}$$

If this inequality is not satisfied an appropriate change in the integer $[R_I/R_a]$ will be made.

5.5 Range Rate Data

The range rate data requires only time adjusting. However since the range rate data is actually a measure of the change in range at two times, the actual time of the measurement for an accelerating vehicle is unknown. However a reasonably close time can be obtained. Furthermore, while errors in range timing can be significant because of the high velocities involved, errors in the time ascribed to the range rate measurement will be negligible for all but the lowest satellites near zenith and then only when the lowest data recording rate is used. The time of the range rate measurement, T_{DM}, is taken to be

$$T_{DM} = T_S + \frac{T_D}{2} - \frac{T_{RT}}{2} \tag{8}$$

where T_D is the time required to count N cycles of bias plus doppler frequency ($\dot{R}$ in the data block). The counter setting, N, depends on the band being used and the data recording rate. This information is carried by the control digits C2 and C3; the counter setting, N, is given in the following table.

C2	C3	
	0.1.2	3
0 or 4	229263	14328
1 or 5	131007	8187
2 or 6	65503	4093
3 or 7	32751	2046

The range rate, $\dot{R}_T$, is given by

$$\dot{R}_T = \frac{c}{2f_u}\left(K - \frac{N}{T_O}\right) \qquad (9)$$

where f_u is the up-link frequency and K is the bias frequency. The up-link frequency and the bias frequency are determined from C_3 and are given in the following table:

C_3	f_u	K	
0	2270.1328 MC	500 KC	S-band
1	2270.9328 MC	500 KC	S-band
2	2271.9328 MC	500 KC	S-band
3	148.260 MC	30 KC	VHF

The velocity of propagation, C, has not as yet been selected and can be an input to the program

0-20-10

Some CA

N64-18231

A STUDY OF IBM 7094 FORTRAN IV SUBROUTINES

D. EPSTEIN

This document describes the results of an investigation to determine the accuracy of the single and double precision numerical subroutines which are standard for the IBM 7094 version of FORTRAN IV. The purpose of the investigation is to estimate the level of confidence to be placed in the subroutines and to find the RMS error and maximum error for error analysis purposes. An incidental purpose was to provide experience in using the subroutines.

6.1 Method

Regardless of which numerical subroutine, F(x), is under investigation, the problem is the same: to compare the value given by the subroutines to the exact value of the function at some argument. It was decided to simplify the post-run analysis by inputting the exact value of the function and letting the computer evaluate the error. The program deck used in this analysis together with a program description and listing will be delivered to GSFC.

6.2 Source of Tables

For the square root function the exact values were obtained by hand calculation rounded to 17 significant figures for input to the computer. For sine and cosine, a 30 place table published at 1° intervals was utilized after rounding to 17 places. For the exponential (e^{x}), an 18 place table was used rounded to 17 places prior to input. For the natural logarithm, tables to 16 decimal places were the best obtainable so that the inputted tables (between $e^{-1} < y < e$) are probably limiting the accuracy. For arctangent, the best tables available were 12 places which was not sufficiently accurate for use so that, instead of arctan x, arctan [(sin x /cos x)] was evaluated since the exact answer ($x \bmod \pi$) was accurately known (π was obtained to 20 places from Burington). Thus, the errors in the sine and cosine subroutines are confounded with the arctan subroutine errors.

6.3 Definitions

It is convenient to use $\underline{S}$ to denote 1 in the last place for single precision evaluation and $\underline{D}$ to denote 1 in the last place for double precision evaluation.

To be rigorous, let $F(4) = M \cdot 2^{b}$ where $0.5 \leq M < 1$

We will call b the "scale of F" and 2^{b} the "unity". Also, $S = 2^{b-27}$ and $D = 2^{b-54}$ are the exact definitions of S and D.

6.4 Error

The error is defined as the computed value minus the exact value. Therefore, the error is positive if F(x), the value yielded by the subroutine, is larger than the exact value.

For double precision computation there are errors other than the one made in the subroutine calculation which are introduced into the program resulting in a somewhat larger total error than should occur. For single precision computations, these extra errors in F(x) are 8 orders of magnitude below the error in the subroutine and are thus entirely negligible.

6.4.1 Arguments

In most cases, the arguments were exactly expressible in binary notation so that there is no error due to computing the argument. For sine and cosine, though, $1^{\circ} = \pi/180$ is transcendental and cannot be exactly expressed in binary notation so that there is an unavoidable error in F(x) due to rounding off x.

6.4.2 Exact Function

In most cases, the exact values are known to sufficient places so that the error in expressing them in decimal is negligible, the exception being log x for $e^{-1} < x < e$. However, the number, on being inputted, is transformed to binary and a certain error is made in doing so. This error is not known and cannot be eliminated from the total error.

6.5 Subroutines Tested

The double precision subroutines used in the tests were

DATAN 2, DCOS, DLOG, DSIN, DSQRT, DEXP

while the single precision subroutines used were

ATAN 2, COS, ALOG, SIN, SQRT, EXP

6.5.1 Square Root

6.5.1.1 Single Precision

The arguments are expressable exactly in binary notation so that there is no input error.

The IBM writeup indicates that an iterated Newton-Raphson method is used. It is a characteristic of this method that the error is always positive. A characteristic negative error is caused by a truncation on the final division in the subroutine.

The runs showed that the error was not continuous but, rather, random both in sign and magnitude. Of the 97 cases run, 60% gave negative errors and 40% gave positive errors indicating that the iteration error is well balanced with the truncation error. The maximum error was 1.0S (1 in the last place) which was perfectly satisfactory and the RMS error was .411S which was also satisfactory. For a unity of $1.0 = 2^0$, $.745 \times 10^{-8}$ was the maximum error and the RMS was $.306 \times 10^{-8}$ (the subroutine specification was was $1. \times 10^{-8}$).

6.5.1.2 Double Precision

The same cases were run using the double precision routine so there was no input error.

The error was almost always negative (95 out of 97 times) which indicates that roundoff was not a problem nor was the number of Newton-Raphson iterations. The largest error in magnitude was 3D which includes all the errors discussed in Section 6.4.2 as well as the error in the subroutine itself. It is believed that the error which was random in magnitude, was about equally caused by the various effects. The RMS value of the error was found to be 1.13D which for a unity of 1.0 gave $.626 \times 10^{-16}$ as RMS and 1.88×10^{-16} as maximum. The subroutine write-up lists $1. \times 10^{-17} < 2^{-56}$ which is probably a misprint.

6.5.2 Sine and Cosine

Since the same routine is used for computing the sine and cosine, it is convenient to discuss them together. Two types of tests were made: one in the region 0 to 90° at 1° intervals to determine accuracy and another between $\pm 13\pi$ to test the reduction to the interval $\pm \frac{\pi}{2}$. The reduction was found satisfactory within the above range for both the single and double precision.

Since the argument must be in radian measure and the only tables of the right accuracy were for degree measure, the arguments were multiples of $\frac{\pi}{180}$. Thus there was an input error (see Section 6.4.1) for both the single and double precision cases of at most one bit.

6.5.2.1 Single Precision

The data were divided into 12 groups (6 for sine, 6 for cosine) each group covering 15°. For each group, the RMS error was calculated and the statistical input error removed from the output error. The resultant RMS error for the sine subroutine itself was 1.10S. For the cosine, the subroutine error was found to be 1.16S. The subroutine error for either sine or cosine can be taken as 1.13S or $.842 \times 10^{-8}$ (both are RMS values). The subroutine write-up gives 1.0×10^{-8} as the maximum error which is in good agreement with the empirically determined values above.

The error in sine was always negative and in cosine almost always positive but both were random in magnitude.

6.5.2.2 Double Precision

Here, in addition to the subroutine error, there are argument errors (see Section 6.4.1) and errors in inputting the exact function (see Section 6.4.2). We assume that the former is at most one bit (at the argument scale factor) and the latter one bit at the output scale factor. Both are taken to be uniformly distributed.

As in Section 6.5.2.1, the data were divided into 6 groups of 15 points and statistical corrections made for the argument error and the exact function input error. For the sine, the resultant RMS error was found to be 2.075×10^{-16} and for the cosine 1.570×10^{-16}. Thus, for either sine or cosine, the RMS subroutine error may be taken as 1.840×10^{-16} or 3.32D. The write-up for the subroutine lists $.7 \times 10^{-16}$ as the maximum error and is about 2:1 lower than the empirically derived value.

The error for sine was always negative whereas for cosine it was of random sign. The magnitude of the error was random.

6.5.3 Logarithm

Two types of runs were made: one to determine the accuracy of the logarithm function and the second to ensure that the computation is adequate over the required range.

On the basis of about 60 runs of each logarithm subroutine (both single and double precision versions), the subroutines were spot-checked over the range of arguments 1×10^{-4} through 2.1×10^{4} and the errors were found to be reasonable for the precision involved.

There are three types of logarithms in current use differing in the base: binary (base 2), natural (base e = 2.718) and Briggs (base 10). The same FORTRAN subroutine is capable of computing any of the three, the difference being in an output transformation. Since the difference between the subroutines is so minor, only one was tested, that one being the natural logarithm since tables of high accuracy are available.

The arguments used for the 40 runs checking accuracy were between e^{-1} and e^{+1} and were arranged so that there was no argument error made (as discussed in Section 6.4.1). The same 40 arguments were used for the single and double precision cases.

6.5.3.1 Single Precision

For this case, the RMS error found was $.461 \times 10^{-8}$ as the error in the subroutine itself which corresponds to about .619S which may be used for error analysis purposes. The subroutine write-up lists 3×10^{-8} as the maximum error which is in agreement with the empirically derived error of 1.35×10^{-8} (maximum).

The errors were random in magnitude but mainly positive.

6.5.3.2 Double Precision

For this case the exact values were only known to 16 decimal places, that being the most accurate table available, so that an error of $\pm .5 \times 10^{-16}$ is the maximum error in the exact value. There is also an error of at most 1.0 D made inputting the exact value.

When the errors were added in an RMS sense and corrected statistically for the assumed uniformly distributed errors mentioned above, the RMS error was found to be 1.37 D which, for a unity of 1.0, is $.760 \times 10^{-16}$ and is close to $.7 \times 10^{-16}$ which the subroutine write-up gives as the maximum error. For error analysis purposes, 1.37 D may be used as the RMS error.

6.5.4 Exponential

As in the case of logarithm, there are three exponential functions in wide use: 2^x, 10^x and e^x. The FORTRAN subroutine is capable of finding any one of the exponentials, the only difference being an input transformation. For this reason only one of the exponential functions was checked out, namely e^x, for which accurate tables are available.

Two types of runs were made: one set from which the accuracy of the subroutine can be determined and the second to determine that the subroutine works for the range of argument over which we expect to use it.

To test the routine over a large range, about 40 runs each were made of the single and double precision routines covering the range $1.9 \times 10^{-12} \leq y \leq 3.3 \times 10^{6}$, about 2 or 3 runs per decade of e^x. The resulting runs showed that e^x was being computed correctly by the single and double precision subroutines over the range $-27. \leq y \leq 15.$ which corresponds to the range of e^x given above.

For accuracy determination, 25 runs were planned covering the range $-.75 \leq y \leq .75$, corresponding to $.5 \leq e^y \leq 2.0$. The arguments for all runs were chosen so that no argument error was made. The 40 runs designed for testing the range of e^x were, later, also used for evaluating the accuracy.

6.5.4.1 Single Precision

The 25 runs were divided into two groups of 12 runs, one group having a unity of 1. and the other of 2. The RMS error of each group was found, $.882 \times 10^{-8} = 1.184S$ for the first group and $.941 \times 10^{-8} = .631S$ for the second. Thus, the assumption of the same relative error for the two groups was doubtful. Instead, a tentative assumption was made that the subroutine method yields a different relative error for negative x than for positive x. The runs: $-27. \leq y \leq -1.0$ and the runs: $1. \leq y \leq 15.$ were used and the RMS of the relative error was found to be 1.256×10^{-8} for negative y and

$.644 \times 10^{-8}$ for positive γ, corresponding to errors of about 1.10S and .565S, respectively. These results agree well with the values obtained from the $-0.75 \leq \gamma \leq .75$ range.

It is felt that $(1.26 \times 10^{-8})e^{\gamma}$ or 1.18S should be used as the RMS error for negative γ and that $(.644 \times 10^{-8})e^{\gamma}$ or .631S should be used for positive γ. It was noted that all runs with positive γ had negative errors and all with negative γ had positive errors.

6.5.4.2 Double Precision

Although there is no argument error or error in knowing the exact value, as error in inputting the exact value (at most 1.0 D) is made and was removed from the data statistically.

The resulting RMS error was found to be .763D for negative exponents and 2.565D for positive exponents from 25 runs in the $-.75 \leq \gamma \leq .75$ range. There is evidence, however, that for large negative exponents, the relative accuracy deteriorates by 10:1 as determined from the 27 runs in the $-27 \leq \gamma \leq -1$ range. Empirically, it was found that, for negative γ $(.763 + .32|\gamma|)$D or $(.59 + .25|\gamma|)10^{-16}e^{\gamma}$ is a better approximation for the RMS error in e^{γ} for negative γ and 2.57D (or $1.99 \times 10^{-16}e^{\gamma}$) is a good value of the RMS error in e^{γ} for positive exponents.

A possible explanation for the $.32|\gamma|$D term in the error is an error of .5 bit maximum in $|\gamma|$ (the result of an input multiplication in the subroutine by $\log_2 e$). Why there is no evidence of this error for positive or for the single precision cases is not known.

6.5.5 Arctangent

Since accurate tables of the arctangent are not available, the function that was actually used for the test was arctan $(\sin\gamma / \cos\gamma)$. Therefore errors in the sine and cosine subroutines were unavoidably confounded with those in the arctangent subroutine. The result of this is that we can not separate the RMS error due to the arctan subroutine alone but can only find a total RMS error, including these and other errors as well. For single precision, this total RMS error was found to be 1.38×10^{-8} radians and for double precision, 4.16×10^{-16} radians.

It was also found that 3rd and 4th quadrant angles are computed as negative by the subroutine so that the output quadranting is $-\pi < \arctan\gamma \leq \pi$.

6.5.6 Double Precision Input-Output Errors

As a by-product of the above investigations an approximation was obtained for the total error obtained by use of the standard FORTRAN IV library subroutines for inputting and outputting double precision numbers.

A total of 60 numbers of 17 decimal digits each were inputted into the machine and then, in the course of the program, converted and printed out in decimal. All of the numbers were between .5 and 1.0 in magnitude. The RMS error was $.395 \times 10^{-16} = .712D$. Assuming equal errors in the input and output subroutines, we get .51D (RMS) in each. Assuming that output is good to .5D (max) or .289D (RMS) then the input error would be .651D (RMS). The maximum error found was $1.0 \times 10^{-16} = 1.80D$.

0-29-10

Same CA

N64-18232

7.0 SIMULATION OF ATMOSPHERIC DRAG

D. EPSTEIN

2 P 72-87 refs (See N64-18226 10-01) OTS: JPL

7.1 Introduction

To accurately simulate the trajectory of an artificial satellite or space probe, the deceleration from atmospheric drag must be considered. In addition to the Earth, there is evidence that Mars, Venus and Jupiter have sufficiently dense atmospheres to affect the motion of a space vehicle.

This paper discusses some problems involved in simulating planetary atmospheres themselves, and the results of making certain simplifying assumptions. The object of this report is to come up with a recommendation for a method of simulating atmospheric drag representing a complexity commensurate with the state of the art.

It should be noted that the mission of the vehicle has to be considered. There are three missions in which atmospheric drag could play an important part. The first mission is a low eccentricity orbit about the Earth or another planet. The second mission is a planetary re-entry and the third is a fly-by orbit of the space vehicle. The three cases will be referred to as the "orbiting", "reentry" and "fly-by" cases.

7.2 Discussion

7.2.1 Deceleration

7.2.1.1 Continuum Flow

The usual formula (assuming continuous air) for the magnitude of the acceleration from drag is

$$a_D = \frac{1}{2m}\left\{\rho V_a^2 C_D S\right\} \qquad (1)$$

where

ρ is the density of the atmosphere at the vehicle
V_a is the magnitude of the velocity of the vehicle with respect to the atmosphere
C_D is the drag coefficient of the vehicle
S is the effective surface area presented by the vehicle
m is the mass of the vehicle

The quantity a_D represents an acceleration and depending on the choice of units for the variables will have units in ft/sec^2, in cm/sec^2, or "g's", and will require conversion to the cononical units used in computation.

7.2.1.2 Free Molecular Flow

As the atmosphere becomes more and more diffuse, the mean free path (average distance between impacts of air molecules) increases until it exceeds the diameter of the vehicle. Figure 1 shows mean-free-path as a function of altitude as obtained from U.S. Standard Atmosphere. When the mean free path becomes this large, the collisions become two-body collisions and the continuity of the air mass is no longer applicable. The assumption of a diffuse atmosphere, where all collisions are two-body and the mean-free-path exceeds the dimension of the vehicle passing through, is called free molecular flow.

Ketchum has derived, using the Maxwell-Blotzman Distribution Law, the following formula for drag deceleration:

$$a_D = \frac{\pi}{8m}\left\{(1+2R/\lambda)\rho V_a \bar{c} S\right\} \qquad (2)$$

where

R is the radius of the vehicle
λ is the mean free path
$\bar{c}$ is the average velocity of particles in the medium

Ketchum is uncertain about the correctness of the $(1+2R/\lambda)$ term being in the equation (2) or whether a more correct equation is

$$a_D = \frac{\pi}{8m}\left\{\rho V_a \bar{c} S\right\} \qquad (3)$$

From figure (1), it will be seen that λ varies very rapidly with altitude so that the change from $2R = \lambda$ (where the transition from continuum flow occurs) to $2R = 0.1\lambda$ (where the correction becomes negligible) takes a short time.

7.2.1.3 Drag Direction

By definition, the drag force acts opposite to the direction of the vehicle velocity with respect to the air. Section 7.2.4 describes the calculation of the V_a vector in inertial coordinates. By normalizing this vector, the direction in which the drag force acts may be computed.

7.2.2 Mass of Vehicle

For utmost generality, vehicle mass should be considered as variable with time. In the orbiting case or the fly-by case, a step change in mass representing the separation of a landing craft could be imagined. A long-term steady-state mass flow rate would probably be small.

For the reentry case, if the reentry vehicle is of the heat-sink type, the mass would be constant. For an ablative nose cone, the mass flow rate is a function of the drag. For ballistic missile applications, this mass change is usually ignored. In any event, such changes in mass represent a small error in the location of the impact point.

7.2.3 Surface Area

The effective surface area is not simply the cross-sectional area of the vehicle. The vehicle, in passing through the air, produces a shock wave which skirts the missile and makes the effective cross sectional area the area at a point somewhat close to the nose. Since the shock wave changes with air speed, so does the effective cross-sectional area. In practice, S is made constant and any variation with speed is included in the coefficient of drag.

The above discussion assumes that the angle of attack of the vehicle is zero, i.e., that the velocity (relative to the air mass) is in line with the vehicle longitudinal axis.

7.2.4 Air Speed

Since the velocity of the vehicle is computationally available in an inertial coordinate system, the velocity of the air mass in the same coordinate system is subtracted to give the velocity with respect to the moving air mass; the magnitude of this velocity is the air speed. A good first approximation to the velocity of the air mass is given by assuming the air mass to be rigidly attached to the rotating planet.

A better approximation could be obtained by adding the wind velocity. The purely local effects have to be neglected but the long term horizontal effects are known as a function of position on the Earth's surface and altitude. To take them into account, we would have to include direction (independent of altitude but dependent on latitude and longitude), magnitude (strongly dependent on altitude, less strongly on latitude and least on longitude). The error made by neglecting Earth winds is about 1500 feet at impact for a typical

ICBM mission. Note that winds are of importance only in the lower atmosphere, mainly for the reentry case.

7.2.5 Drag Coefficient

The drag coefficient (C_D) is sometimes considered to be constant but a much more accurate representation is to consider it to be a function of Mach number.

7.2.5.1 Speed of Sound

The Mach number is defined as air speed (see section 7.2.4) divided by speed of sound. The speed of sound is a function of altitude but can be easily computed from a stored table by a table look-up procedure using linear interpolation between tabular values. A different table is used for each planet. The Mach number is then computed by dividing into the air speed as previously computed.

As altitude increases, the atmosphere becomes rarified to the point that speed of sound loses its physical significance.

7.2.5.2 Accuracy of Drag Coefficient

One of the major sources of inaccuracy in the simulation of drag is in the knowledge of the drag coefficient. The data are obtained from wind tunnel measurements and tabulated to about 1 part in 30. At best, then, the error is $\leq$ 1.7% from truncation. The total error is believed to be more in the order of $\leq$ 3% even at the tabulated points.

7.2.5.3 Calculation of Drag Coefficient

In practice, C_D is tabulated for about 25 different Mach numbers which are denser below Mach 2 than above and very dense in the region around Mach 1. For intermediate values of M, linear interpolation is used.

7.3 Atmospheric Models

7.3.1 Jupiter

At the present time the concentration is on determining the composition of Jupiter's atmosphere. It is considered premature to even begin to consider denisty versus altitude at the present time.

7.3.2 Mars

The density versus altitude for Mars is fairly well agreed-on to an altitude of about 30 km. Up to 80 km of altitude, Schilling gives a value for density with a maximum uncertainty

of about 8:1 and a one-sigma uncertainty of about 3:1. The model of Schilling is easily approximated by an exponential interpolation: the logarithm of density is stored in a table versus altitude, linearly interpolated between tabulated values, and then exponentiated. With a 7-value table of density and altitude, a maximum error of 1.4% can be obtained for the Schilling Model II Mars atmosphere.

7.3.3 Venus

Because the surface of Venus is always obscured from view, there is little agreement about the atmospheric model or composition within the cloud level (at about 30 km in altitude). At the point where the star Regulus was occulted in 1959 (100 km in altitude) fairly definite data exist.

Of the three theories of the model of the atmosphere (greenhouse, aeolosphere and ionosphere) no one theory explains all of the available information about Venus. At the present time, there is no generally acceptable density versus altitude curve for Venus.

7.3.4 Earth

The knowledge of the Earth's atmosphere is not complete, but the known effects are far more complete than for any of the planets and represent an adequate model of the Earth's atmosphere even at altitudes of 2000 km (about 6.6 million feet). It is convenient to separate the atmosphere into two parts, the lower atmosphere and upper atmosphere with a separation at about 120 km (400,000 ft.). Drag in the lower atmosphere is large and a vehicle entering it will usually be slowed down sufficiently to be captured by the Earth. Thus, the lower atmosphere is primarily of use in the re-entry case. The upper atmosphere is characterized by lower drag which would be significant mainly over long time arcs which is characterized by an orbiting mission. In case of re-entry or fly-by, the upper atmosphere could probably be neglected. It is convenient to consider the two atmospheres separately.

7.3.4.1 Lower Atmosphere

An average model has been well established for the lower atmosphere. There are five sources for these data: U. S. Standard Atmosphere 1962; COSPAR International Reference Atmosphere 1959; ARDC Model Atmosphere 1956. Table 1 shows the density deviation (in percent) of each of the others from the U. S. Standard as a function of altitude. It will be seen that, except for Tropical Tables, there is good agreement between the various tables at low altitudes. Note that the Standard and International agree all the way to 120 km (400,000 feet).

There are seasonal variations in the lower atmosphere and diurnal variations as well as latitude variations but these are not sufficiently well documented. The only effect of omitting them is that the impact point of the reentering body would be slightly different. It was estimated in 1958 that the 1 sigma variation for a heat-sink type nose cone used in the ICBM application is about 0.5 nm.

Speed of sound can likewise be obtained from the five sources given above but only in the range 0 to 90 km. However, for the U. S. Standard and the COSPAR International, values up to 120 km. can be computed from absolute temperature and mean molecular weight which are tabulated there.

7.3.4.2 Upper Atmosphere

7.3.4.2.1 Eleven Year Cycle

An eleven year cycle in solar flux (corresponding to the sunspot period of the Sun) has been found to lead to an upper atmosphere model with diurnal variations and with variations due to solar flux (see Harris and Priester). R. Bryant (of GSFC) has used density from this model to predict the orbit of the Echo Satellite over an extensive period of time with excellent results.

7.3.4.2.2 Simulation of Density by Use of the Harris-Priester Model

Roemer assumed the exosphere to start at 600 km and performed a Fourier analysis below that altitude and assumed isothermal conditions above. The resulting numerical approximation was good to $\pm 2\%$. The resulting program (written by R. Devaney of GSFC) occupies 1530 words on the IBM 7094. Approximately 1710 words of storage are needed for constants. Harris indicated that the start of the exosphere could be reduced to 400 km which would reduce the constants storage to 1450 words but leave the program size unchanged at 1530 for a total of 2980 words.

In an attempt to shorten computation and reduce storage without causing a significant deterioration in accuracy, a simple table look-up procedure was investigated. The result is a table comprising 1074 words of storage. Density is stored at each combination of 16 values of altitude, 13 values of local time and 5 values of solar flux (the values of altitude, time, and solar flux are also stored, adding 34 values). For a maximum error of 2.7%, linear exponential interpolation (in 3 dimensions) is satisfactory. This maximum error can only be obtained if, simultaneously, solar flux is high, local time is at 14 hours and altitude is half-way between two tabulated values. The

average error would probably be below 1%. The program size was estimated from the equations as 645 for a total of 1900, after adding 10% of the total for contingency.

7.3.4.2.3 Latitude Variation

There is evidence that there is no variation of the model with latitude. It has been suggested that the use of zenith angle instead of local time as one of the parameters might give more intuitively satisfying results. "Zenith angle" is the angle subtended on the celestial sphere between the vehicle position and the Sun's position while the "local solar time" is the difference in the right ascensions of the vehicle and the Sun.

The intuitive difficulty in using local time is that at the North or South Pole, there is no midnight and no noon, local time being constant. The zenith angle, for a vehicle 30° above the ecliptic is 30° at noon (at minimum) and then increases again. To yield a cyclic function we would have to arbitrarily have zenith negative before noon, going to -30° at noon, and + 30° instantaneously after noon. This discontinuity would not be satisfactory.

7.3.4.2.4 Other Variations

There is evidence of solar cycle variations (and hence atmospheric variations) having 27 days, 6 months and 1 year cycles. No theoretical model exists for these effects and whether they have corresponding diurnal variations, as the 11 year cycle has is not known. The 27-day variation is not expected to be completed until mid-1964, the others after that.

7.3.5 Altitude

Harris has suggested that the geocentric altitude above the oblate earth should be used for the Harris-Priester Model. For the lower atmosphere, the same definition of altitude should be used.

For other planets, geocentric altitude above an ellipsoidal or spherical planet could be used.

7.3.6 Medium Velocity

The average velocity of particles in the medium ($\bar{c}$) is of importance only when the altitude is high enough so that free molecular flow is valid. As was indicated in a previous section, free molecular flow can be obtained only for the Earth since, for other planets, the atmospheres are not known to a

high enough altitude. For the Earth, from Figure 1, we see that free molecular flow occurs in the upper atmosphere for usual vehicle dimensions. From equations I. 3.4-(1) and I. 2.6-(1) of U. S. Standard Atmosphere $\bar{C}$ is found to be proportional to $\sqrt{\frac{T}{M}}$:

$$\bar{C} \propto \sqrt{\frac{T}{M}} \tag{4}$$

where T is absolute temperature
M is mean molecular weight

from which the medium velocity can be computed with values of T and M from the Harris-Priester Model. The variation in with local time and solar flux was -22% for altitudes below 500 km and ±14% for altitudes above 500 km. Therefore, were we to approximate $\bar{C}$ by a function of altitude only, we would be causing an error in drag of ±22% which is not tolerable.

Thus, drag is linearly proportional to both density and medium velocity, both of which are functions of the same three parameters (altitude, local time, and solar flux). It is natural then, for altitudes where free molecular flow pertains, to store the product of density and medium velocity (as a function of the three parameters) instead of both density and medium velocity separately.

7.4 Difficulties and Possible Solutions

7.4.1 Density Discontinuity Between Lower and Upper Atmospheres

The density at 120 km is fixed independently of solar flux and time of day in the Harris-Priester Model and is 34% higher than the U. S. Standard Atmosphere. No other model for the lower atmosphere gives a value close to it so that there is a discontinuity in density between the Harris-Priester Model and all of the models of the lower atmosphere.

7.4.2 Drag Discontinuity Between Free Molecular and Continuum Flow

Since the formulas for drag are different in the region of free molecular flow and in the region of continuum flow, even if they were to agree at one altitude (for a given V_a and $\bar{C}$) permitting a continuous transition from one formula to the other, there would, for a different V_a (or $\bar{C}$) no longer be continuity at the junction of the regions.

A possible solution is to introduce a transition region in which we take a weighted average between the drag values computed by the two methods and gradually slide the weight from unity for free-molecular and zero for continuum to unity for continuum and zero for free molecular. A complication occurs in

the transition region, since a ρ table is needed for continuum flow drag and a $\rho \cdot \bar{c}$ table for free molecular drag.

Although an altitude between 120 km and 130 km would be a theoretically desirable one (see figure 1) to transfer from free molecular to continuum flow, the table duplication would be trivial below 120 km. If we arbitrarily choose 100 km to 120 km as the transition region, we gain one other advantage: we can bridge the discontinuity between the lower and upper atmospheres by using for the $\rho \cdot \bar{c}$ table values continuous with the Harris-Priester Model.

7.4.3 Accuracy

From previous discussions, the computation of drag is probably accurate to $\lesssim$5% in the Earth's lower atmosphere and is less accurate in the upper atmosphere. For Mars, the knowledge of drag is probably not as accurate as $\lesssim$10% and for Venus considerably worse. Therefore, calculation of drag and the parameters composing it can always be computed in single precision without degrading the precision of computation.

7.5 Recommendations for Simulation

The statements made below are recommendations for computation method and represent, in most cases, a compromise between state-of-the-art and ease of computation.

7.5.1 Logic of the Drag Computation

On the basis of a control card option, programs and tables will be included for computing drag over any combination of the following:

a) lower atmosphere Earth
b) upper atmosphere Earth
c) Mars
d) Venus
e) Jupiter

and appropriate gates will be set.

Depending on which reference system the vehicle is in and the settings of the gates, a distance test will be made. The distance to the center of the reference body is computed and compared with center distances corresponding to altitudes of 200 km, 1100 km, 80 km, 180 km, 0 km.

If all tests fail, drag is computed as zero and exit. If any test passes, drag will be computed: first compute the geocentric altitude; then, for the Earth, geocentric latitude is computed together with the radius based on an oblate spherical earth. If in any other reference system, compute geocentric altitude using a constant radius for each planet.

7.5.2 Choice of Drag Equation

If option b) is chosen, and if the altitude exceeds 100 km when the vehicle is in Earth reference, equation (3) (rather than (2)) will be used.

If option b) is not chosen, or if the vehicle is in other than Earth reference, or if option a) was among those chosen and altitude is less than 120 km, use equation (1). Note that between 100 and 120 km when options a) and b) are both chosen, then both computations are made together with the transition function.

Only those quantities which are required for the equation being used (either (1) or (3)) are computed.

7.5.3 Air Velocity

The velocity with respect to the air mass ($\vec{V}_a$) is computed from the inertial velocity by subtracting out the velocity of the air mass with respect to the planet and the velocity of the planet with respect to the coordinate system. The latter comes from the ephemeris tape, the former is calculated. To calculate it, an assumption is made that the air mass is rigidly attached to the planet and rotating with the planet. It is recommended that winds be neglected.

The magnitude of $\vec{V}_a$ is the air speed and is used in the calculation of Mach number (for the lower atmosphere). The direction of the drag vector is computed by assuming it to be aligned with $-\vec{V}_a$.

7.5.4 Lower Atmosphere Tables

The independent variable used in the lower atmosphere tables is altitude; density and speed of sound are computed from altitude.

Three tables are stored for the Earth's lower atmosphere: altitude, log density, speed of sound (about 50 values per table). For a given value of altitude, a table look-up is performed by linear interpolation in the log density and speed of sound tables. Density is then computed by exponentiating log density.

Three tables are stored for the Mars atmosphere (about 15 values per table). Density and speed of sound are again found by linear exponential and linear interpolation against altitude.

For the Venus atmosphere, three tables are stored (about 15 values each) as above and, similarly, density and speed of sound are found by interpolation.

Space will be supplied for later inclusion of a Jupiter atmosphere.

For the Earth, it is recommended that the U. S. Standard Atmosphere be used as the basis of the three tables. For Mars, it is recommended that the Schilling "Mean" Model II atmosphere be used (see page 9 of the reference report) until a better table is available. No recommendation is made as to where to obtain a speed of sound table for Mars or any of the tables for Venus.

7.5.5 Upper Atmosphere

The use of the Harris-Priester model is recommended for the upper atmosphere. The independent variables are three in number: solar flux(s), local solar time (t_L) and altitude (h). The local solar time is computed from the difference between the right ascensions of the Sun and the vehicle. The solar flux is computed as an "inputted" function of time-since-a-base-date (also "inputted"). Altitude has already been discussed.

At 100 km and 120 km, log ($\rho \cdot \bar{c}$) is stored for use in the transition period.

An altitude table is stored (16 values), a solar flux table (5 values) and a time table (13 values). Then log of ($\rho \cdot \bar{c}$) is stored in a three dimensional array for each tabulated point, simultaneous linear interpolation in 3 dimensions is used to yield log ($\rho \cdot \bar{c}$). Exponentiation yields $\rho \cdot \bar{c}$.

In order to form the 3 dimensional table of stored values, ρ and $\bar{c}$ are both needed. In the referenced document by Harris and Priester, ρ is established but $\bar{c}$ is not. It is recommended that equation (4) (see section 7.3.6) be used to compute $\bar{c}$.

7.5.6 Coefficient of Drag

Mach number is computed from air speed and speed of sound as in section 7.5.3 and 7.5.4 respectively for any planet.

Mach number (M) is used as the independent variable and the coefficient of drag (C_D) computed from it. Two tables are stored M and C_D (each of 25 or 35 values) and linear interpolation is used to find the C_D corresponding to a given M, which may lie between tabular values.

Each combination of 2 tables represents one particular space vehicle. In order to avoid the inconvenience of inserting these tables as input, 4 sets of tables will be available on the program tape and one set will be chosen by an input card option. The tables are independent of planet.

7.5.7 Surface Area

Two values of effective surface area are inputted: one for use in equation (3) for free molecular flow and one for use in equation (1) for continuum flow.

7.5.8 Mass

Mass rates are not considered to be a part of the atmospheric models. Schedules for changes in mass will be incorporated into another routine of the Orbit Determination Program.

7.6 References

1. Ketchum, Harold B.; Advances in Astronautical Sciences; Vol. 1,; pp 31-41; Plenum Press; 1957.

2. U. S. Standard Atmosphere, 1962; U. S. Government Printing Office; 1962.

3. Schilling, G. F.; Limiting Model Atmospheres of Mars; reorder number 62-239, The Rand Corporation, Santa Monica, Calif.; 1962.

4. Kellogg, W. W. and Sagan, C.; The Atmospheres of Mars and Venus; Publication 944 of National Society of Sciences - National Research Council, Washington, D.C.; 1961.

5. CIRA, 1961 (COSPAR International Reference Atmosphere 1961); North-Holland Publishing Company; Amsterdam; 1961.

6. Harris, I. and Priester, W.; Theoretical Models for the Solar Cycle Variation of the Upper Atmosphere; NASA TN D-1444 Goddard Space Flight Center; 1962.

7. Roemer, M.; Fourier-Analysis of Atmospheric Densities Given by the Harris-Priester Models; Bonn University Observatory.

8. Harris, I. and Priester, W.; Relation Between Theoretical and Observational Models of the Upper Atmosphere; X-640-63-145; Goddard Space Flight Center; 1963.

Altitude		US STANDARD DENSITY	PER CENT DEVIATION FROM STANDARD			
km	ft	slugs/ft^3	ARDC 1956	ARDC 1959	CIRA 1961	TROPICAL 1962
0	0	2.38^{-3}	0	0	.55	-4.77
3.0	10,000	1.76^{-3}	0	0	-.91	-5.32
5.5	18,000	1.36^{-3}	.04	0	1.85	-1.67
10.1	33,000	7.97^{-4}	.05	0	1.68	1.92
14.6	48,000	4.00^{-4}	.09	0	2.36	15.5
20.4	67,000	1.61^{-4}	3.28	.16	.48	6.80
29.0	95,000	4.20^{-5}	.59	-2.36	.10	.46
33.5	110,000	2.07^{-5}	-3.13	-3.13	.68	2.53
48.8	160,000	2.32^{-6}	4.77	4.77	.77	8.93
67.1	220,000	2.50^{-7}	15.0	15.5	1.30	8.10
91.4	300,000	4.62^{-9}	31.2	-10.8	.11	--
121.9	400,000	3.62^{-11}	81.5	-35.0	1.17	--

TABLE 1 - Percentage Density Deviations at Various Altitudes - U. S. Standard Atmosphere 1962 taken as reference values

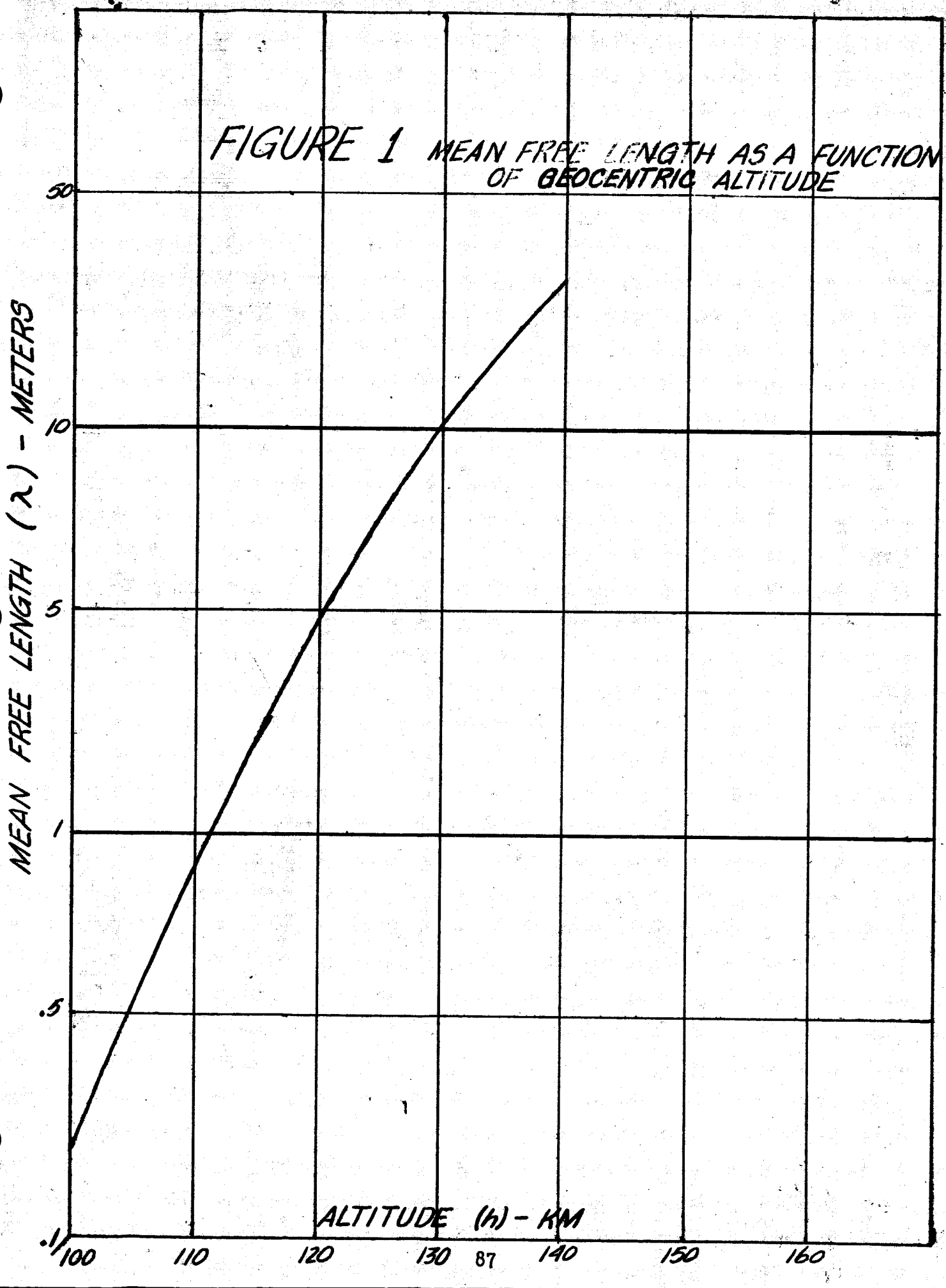
FIGURE 1 MEAN FREE LENGTH AS A FUNCTION OF GEOCENTRIC ALTITUDE
MEAN FREE LENGTH (λ) - METERS
50
10
5
1
.5
.1
ALTITUDE (h) - KM
100
110
120
130
140
150
160

0-20-10

Same CA

N64-18233

8.0 [MATRIX MANIPULATIONS]

[2]

J. A. Winokur

P 88-98 refs (See N64-18226 10-01) OTS: etc.

The matrix operations of addition, multiplication, subtraction, transposition and inversion are carried out in the MINIVAR Program. Since a precision of 1 ± 10^{9} is desired throughout the program, those operations which are susceptible to loss of precision must be examined.

8.1 Analysis of Matrix Operations

It is clear that no precision is lost in transposition. Loss of precision in matrix multiplication occurs for the same reason as in subtraction; that is, it occurs if numbers of nearly equal magnitude are subtracted during the course of the computation of the matrix product. The only remedy for loss of precision in matrix addition, subtraction or multiplication is to perform these operations in double precision, since it is impossible to know in advance exactly where in the computations a bad situation will arise. It is understood that those situations which can be foreseen in advance, such as the computation of $\bar{R}/r^3 - \bar{R}_o/r_o^3$ have already been remedied by expansion in binomial series or some equivalent action. The cases which are under consideration here are due to the more or less accidental groupings of numbers during the course of the computations.

The matrix inversion operation is one which does lend itself to remedial procedures which may be tried before resorting to increased precision in the input quantities.

At present, matrix inversion in the Orbit Determination Program is being managed by a standard SHARE routine which uses a Gauss-Jordon pivotal condensation technique in single precision.

The only matrix which must be inverted in the program is the covariance matrix of the observational errors, denoted by Y. It is highly probable that this will never exceed 4×4 in dimensions; even though the total number of possible observables is much higher than 4, not more than four will ever be used at any one time.

Considering the relatively small size of the Y matrix, there is no reason to believe that the present share routine will not be sufficiently precise for this application, if done in double precision. However, it would be desirable to incorporate in the program a check in the inversion process, with an option for increasing its precision if necessary. The following paragraphs describe the recommended check and the optional iterative process.

8.2 Precision Check on Matrix Inversion

Let Y be the matrix whose inverse is desired, and let Y^{-1} be its exact inverse. If an approximation to Y^{-1}, say S_o is obtained by any means,

the accuracy of the approximation can be judged by back multiplication with Y,

$$B_o Y = I + \epsilon C$$

where ϵC represents the error in the computation, and ϵ is determined by requiring the largest non-zero element of C to have unit magnitude.

8.3 Matrix Inversion Iterative Procedure

Supposing ϵ to be sufficiently small, expand the exact matrix inverse in a power series as follows

$$Y^{-1} = B_o + \epsilon Y_1^{-1} + \epsilon^2 Y_2^{-1} + \dots .$$

choosing as a first approximation the matrix B_o obtained by some as yet unspecified method. Since Y^{-1} is the exact inverse of Y, multiplication of the right hand side of the above equation by Y must yield the identity:

$$\left(B_o + \epsilon Y_1^{-1} + \epsilon^2 Y_2^{-1} + \dots\right) Y = I$$

and since $B_o Y = I + \epsilon C$,

$$\left(\epsilon Y_1^{-1} + \epsilon^2 Y_2^{-1} + \dots\right) Y = -\epsilon C$$

or, dividing by ϵ ,

$$\left(Y_1^{-1} + \epsilon Y_2^{-1} + \dots\right) Y = -C$$

Now, if the above equation is post-multiplied by Y^{-1} in its expanded form, the result is

$$Y_1^{-1} + \epsilon Y_2^{-1} + \dots = -C\left[B_o + \epsilon Y_1^{-1} + \epsilon^2 Y_2^{-1} + \dots\right]$$

Equating equal powers of ϵ gives the following successive approximations to Y^{-1}:

$$Y_o^{-1} = B_o$$

$$Y_1^{-1} = -C Y_o^{-1}$$

$$\vdots \qquad \vdots$$

$$Y_k^{-1} = -C Y_{k-1}^{-1}$$

$$\vdots \qquad \vdots$$

This formulation can be put into a more compact form by letting $B_k = \epsilon^k y_k^{-1}$. When this substitution is made, the expansion for the true inverse is

$$y^{-1} = B_0 + B_1 + B_2 + \dots + B_k + \dots \quad (1)$$

and the iterative procedure for obtaining the B's is

$$\left.\begin{aligned} B_1 &= -C B_0 \\ B_2 &= -C B_1 \\ &\vdots \\ B_k &= -C B_{k-1} \end{aligned}\right\} \quad (2)$$

where B_0 is the initial guess and where now

$$B_0 y - I = C \quad (3)$$

Equations (1), (2), and (3) constitute the precision check (Eq. (3)) and iterative process (Eq. (2)) which are suggested for use in the MINIVAR program.

It must be realized, of course, that sooner or later in the iterative process the accumulating round-off error will begin to wipe out the additional precision which has been gained. When this point is reached the iteration should be stopped.

8.4 Choice of Matrices Used for Test of Iterative Procedure

In order to test the efficiency of the proposed iterative procedure, a set of matrices with a reputation for difficult inversion was chosen (Ref. 2). This set is known as the class of Hilbert matrices H_n and the members of this set are defined by

$$H_n = \left\{ \frac{1}{i+j-1} \right\}, \qquad i, j = 1, 2, \dots, n.$$

The difficulty of inversion arises from the fact that the matrices approach singularity as n increases.

However, it is possible to obtain analytic expressions for the elements of the inverse matrix, so that an accurate estimate of the error for any given approximation may be made. The inverse matrix, defined by T_n, is

$$T_N = H_n^{-1} = \left\{ (-1)^{i+j} \frac{(n+i-1)!\,(n+j-1)!}{(i+j-1)\left[(i-1)!\,(j-1)!\right]^2 (n-i)!\,(n-j)!} \right\}$$

8.5 Details of the Test of the Iterative Procedure

The iteration algorithm described by Equation (2) was applied to the Hilbert matrices of order $n = 4,5,6,7$ and 8, even though it is not expected that anything of higher order than 4 will be encountered.

H_N and T_N were first computed in single precision from their analytical forms. A first approximation to the inverse of H_N, (denoted by B_0 in Eq. (3)) was then computed in single precision by means of the present share routine. The residual matrix C of Eq. (3) was then computed

$$C = B_0 H_N - I$$

and the accuracy of B_0 was judged by computing the sum of the squared elements of C. If $\sum c_{ij}^2 \leq n^2 \times 10^{-16}$, the accuracy was judged sufficient and no further action was taken. If $\sum c_{ij}^2 > n^2 \times 10^{-16}$, the iterative procedure of Eq. (2) was initiated for a total of six cycles. If at the end of six cycles of iteration the error test was still not met, H_N, T_N and B_0 were recomputed in double precision and the iteration was repeated, using as a test $\sum c_{ij}^2 \leq n^2 \times 10^{-18}$.

8.6 Results of the Test

The results of the comparison between the SHARE routine inverse and the iterated inverse are shown in graphic form in Figures 1 through 6.

Each of Figures 1 through 5 provides $\sum c_{ij}^2$, defined as $\|C\|$ and also $|c_{ij}|_{max}$ as a function of the number of iterations completed in single precision. The zero order iteration in each case is the share routine inverse. The acceptable level of accuracy for single precision in terms of $\|C\|$ is given in the upper right corner. Note that in no case does the single precision share routine meet the requirements, and that iteration does not satisfy them either, although there is significant improvement. The case of $n = 8$ is quite clearly outside of the "small error" range assumed in the development of the iteration equations.

Figure 6 provides $\|C\|$ and $|c_{ij}|_{max}$ for the double precision calculation, in the case of $n = 8$. The corresponding curves for $n = 4,5,6$ and 7 were omitted because in each case the precision requirement was met either by the share routine inverse ($n = 4,5,6$) or by the first iteration on the latter ($n = 7$). It is clear that the required level of precision is not met even by the double precision iteration, although there is a factor of nine improvement.

In almost every case, the reduction of error is greatest in the first iteration and the error either increases or remains constant with succeeding iterations. This implies that the number of iterations attempted in the program could be limited to one or two without penalty.

The test used in these comparisons involves the sum of the squared of the error matrix C, and as a consequence does not limit the magnitude of the individual elements of C as much as is desirable. This is illustrated in the figures by the fact that the largest magnitude entries of the error matrix exceed the desired level of error (1 part in 10^9) even in the double precision computations. A finer test is therefore needed.

8.7 Conclusions

The present SHARE routine is inadequate in single precision and iteration does not provide acceptable accuracy.

The share routine is probably adequate in double precision for most of the matrix inversions which will be done. However, the iteration routine provides a large factor of improvement in critical cases, and should therefore be included as an option.

The precision test on the elements of the error matrix should be $|C_{ij}| < 10^{-9}$, instead of the coarser test $\|C\| \leq m^2 \times 10^{-18}$ used in this comparison. This new criterion being incorporated into the test program.

8.8 References

1. Lanczos, C – "Applied Analysis", Prentice-Hall, 1956.

2. Taussky, O. et al – "Contributions to the Solutions of Linear Equations and the Determination of Eigenvalues", NBS Appl-Math Series 39, Sept., 1954.

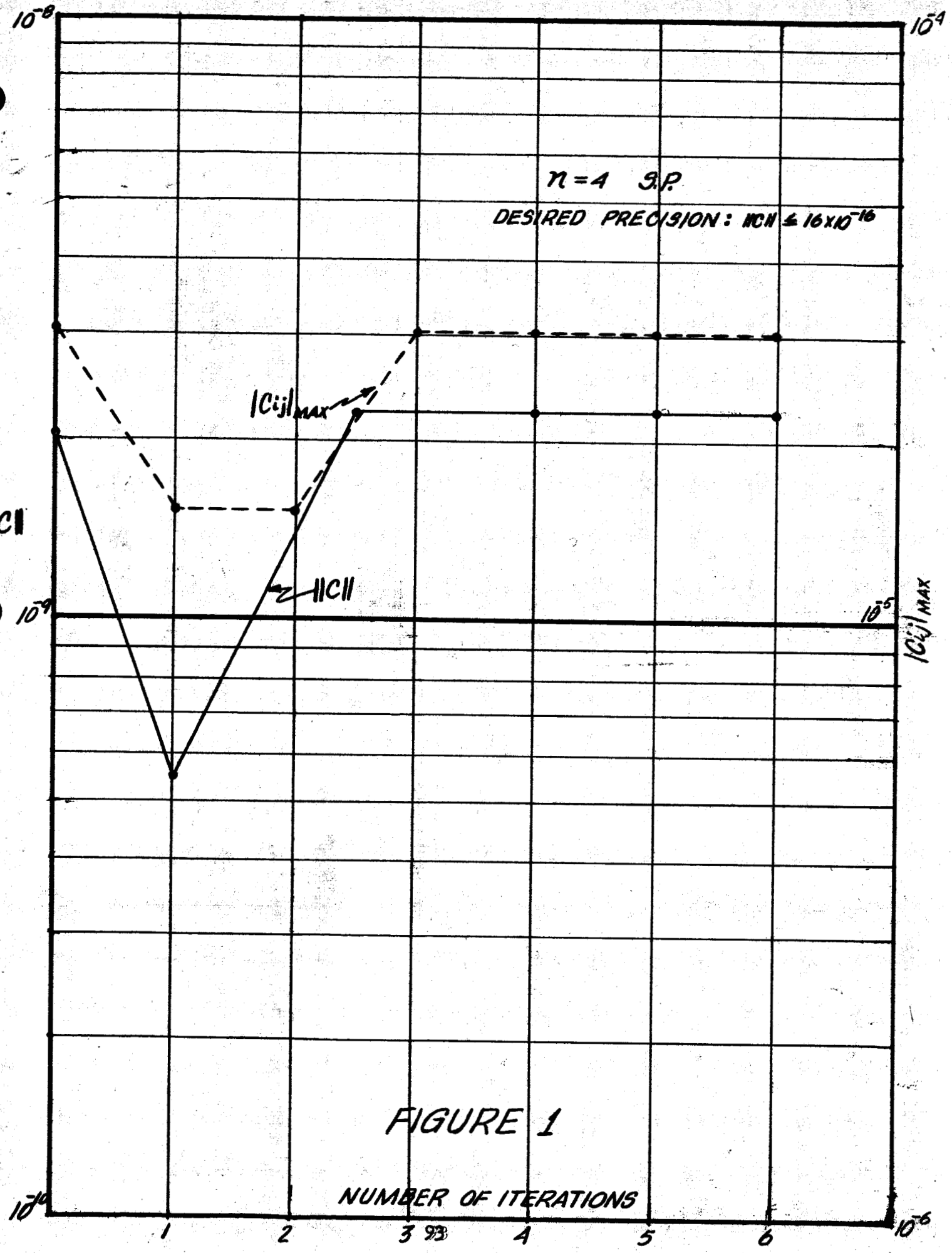
10^{-8}
10^{-4}
$n = 4$ S.P.
DESIRED PRECISION: $\|C\| \leq 16 \times 10^{-16}$
$|C_{ij}|_{max}$
$\|C\|$
$\|C\|$
10^{-9}
10^{-5}
$|C_{ij}|_{MAX}$
10^{-10}
NUMBER OF ITERATIONS
1
2
3
4
5
6
10^{-6}

FIGURE 1

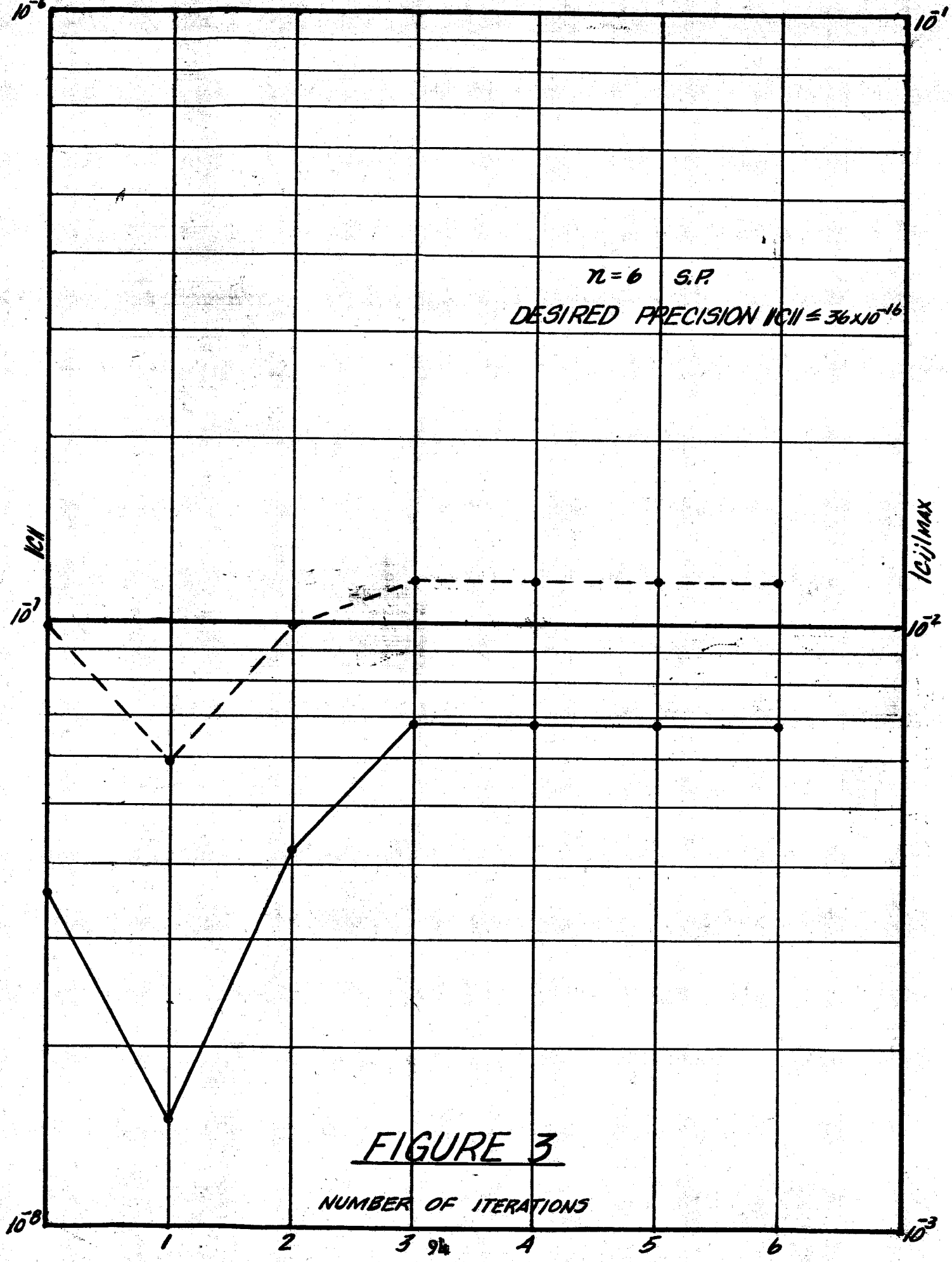
10^{-6}
10^{-1}
$n = 6$ S.P.
DESIRED PRECISION $\|C\| \leq 36 \times 10^{-16}$
$\|C\|$
$\|c_{ij}\|_{MAX}$
10^{-7}
10^{-2}
10^{-8}
10^{-3}
1
2
3
4
5
6
NUMBER OF ITERATIONS

FIGURE 3

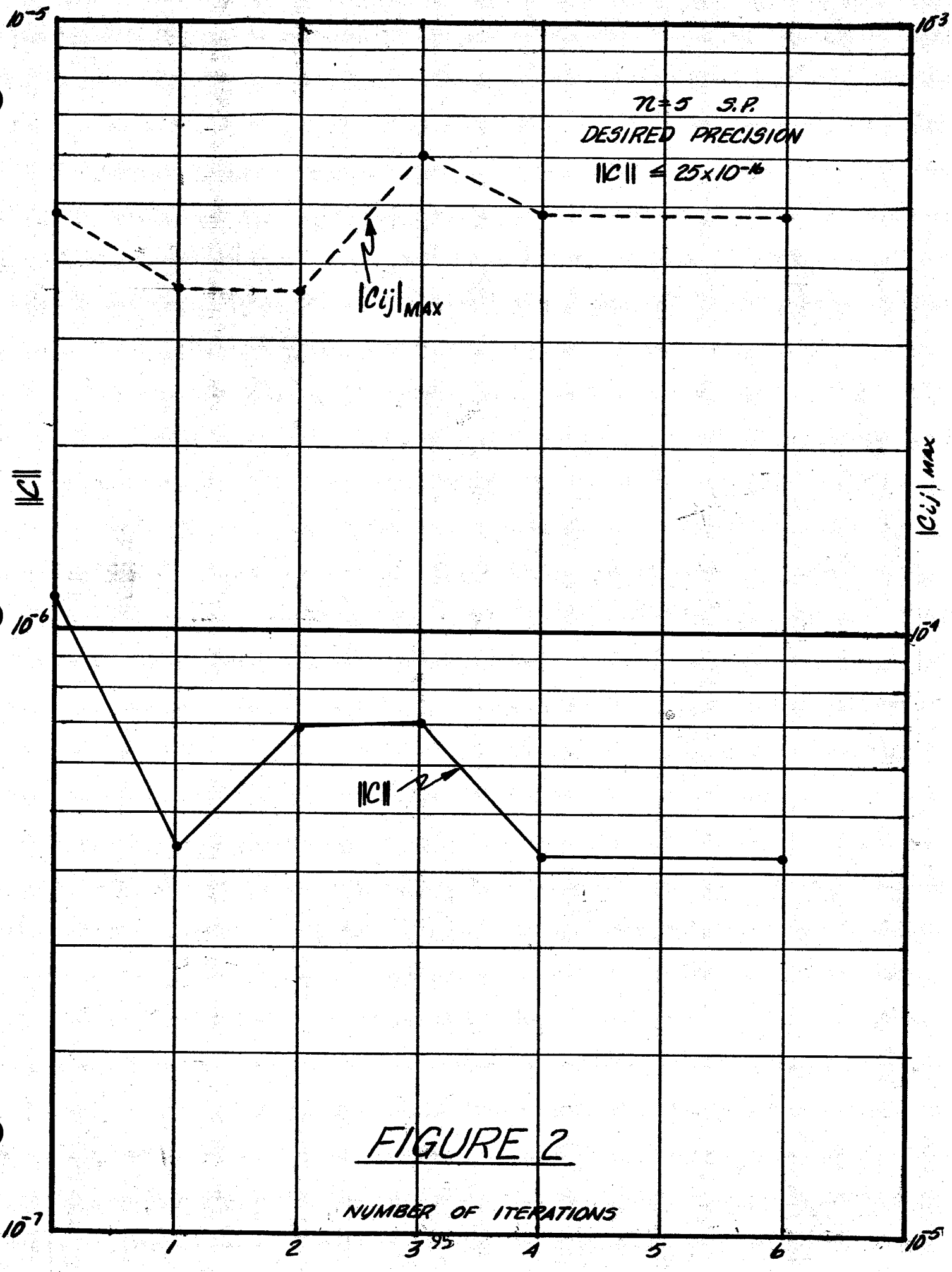
10^{-5}
10^{3}
n = 5 S.P.
DESIRED PRECISION
$\|C\| \leq 25 \times 10^{-16}$
$|C_{ij}|_{MAX}$
$\|C\|$
$|C_{ij}|_{MAX}$
10^{-6}
10^{-1}
$\|C\|$
10^{-7}
10^{-5}
1
2
3
4
5
6
NUMBER OF ITERATIONS

FIGURE 2

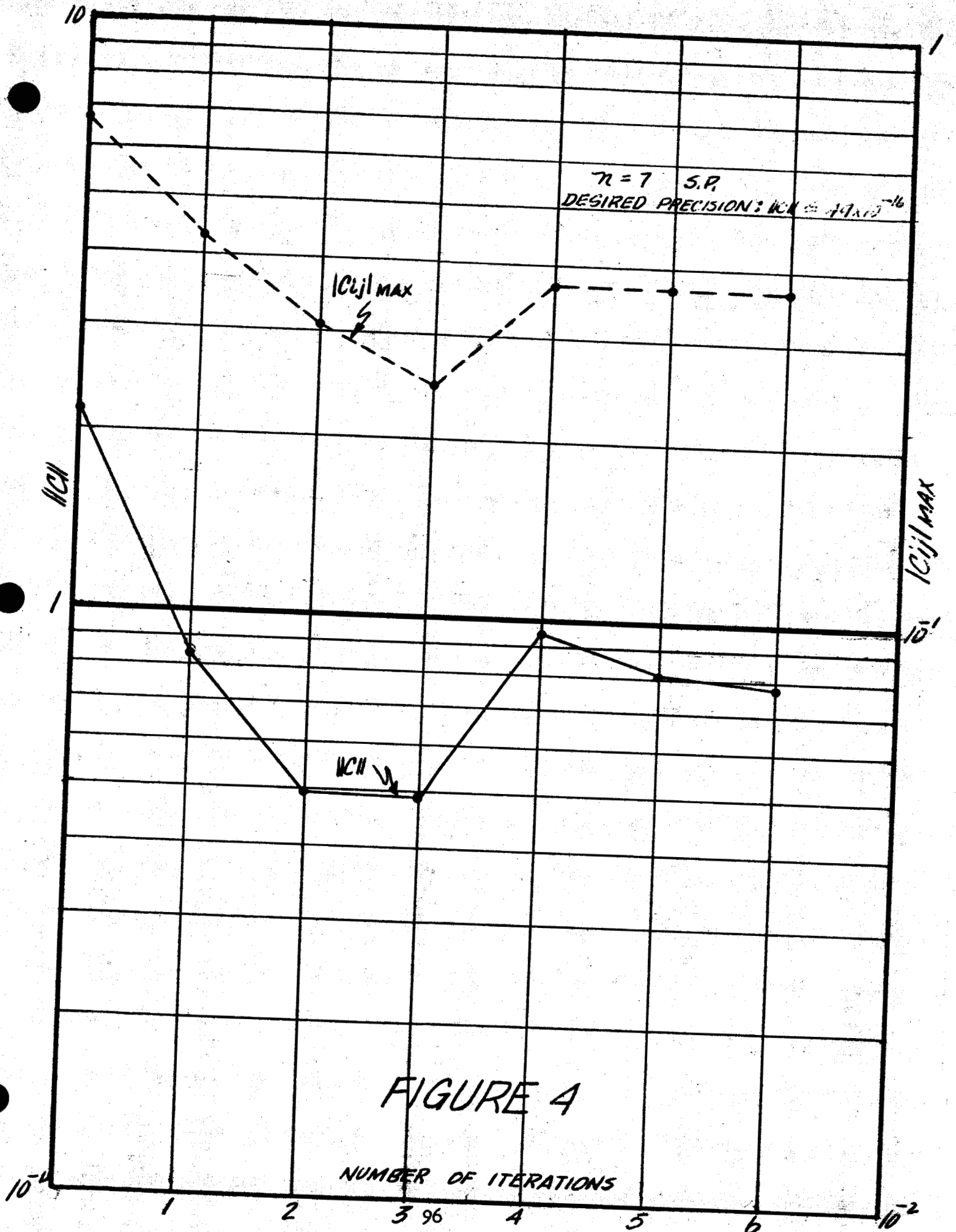
10
1
n = 7 S.P.
DESIRED PRECISION: ||C|| = 4 x 10^-16
|Cij| MAX
||C||
1
10^-1
|Cij| MAX
||C||
10^-4
1
2
3
96
4
5
6
10^-2
NUMBER OF ITERATIONS

FIGURE 4

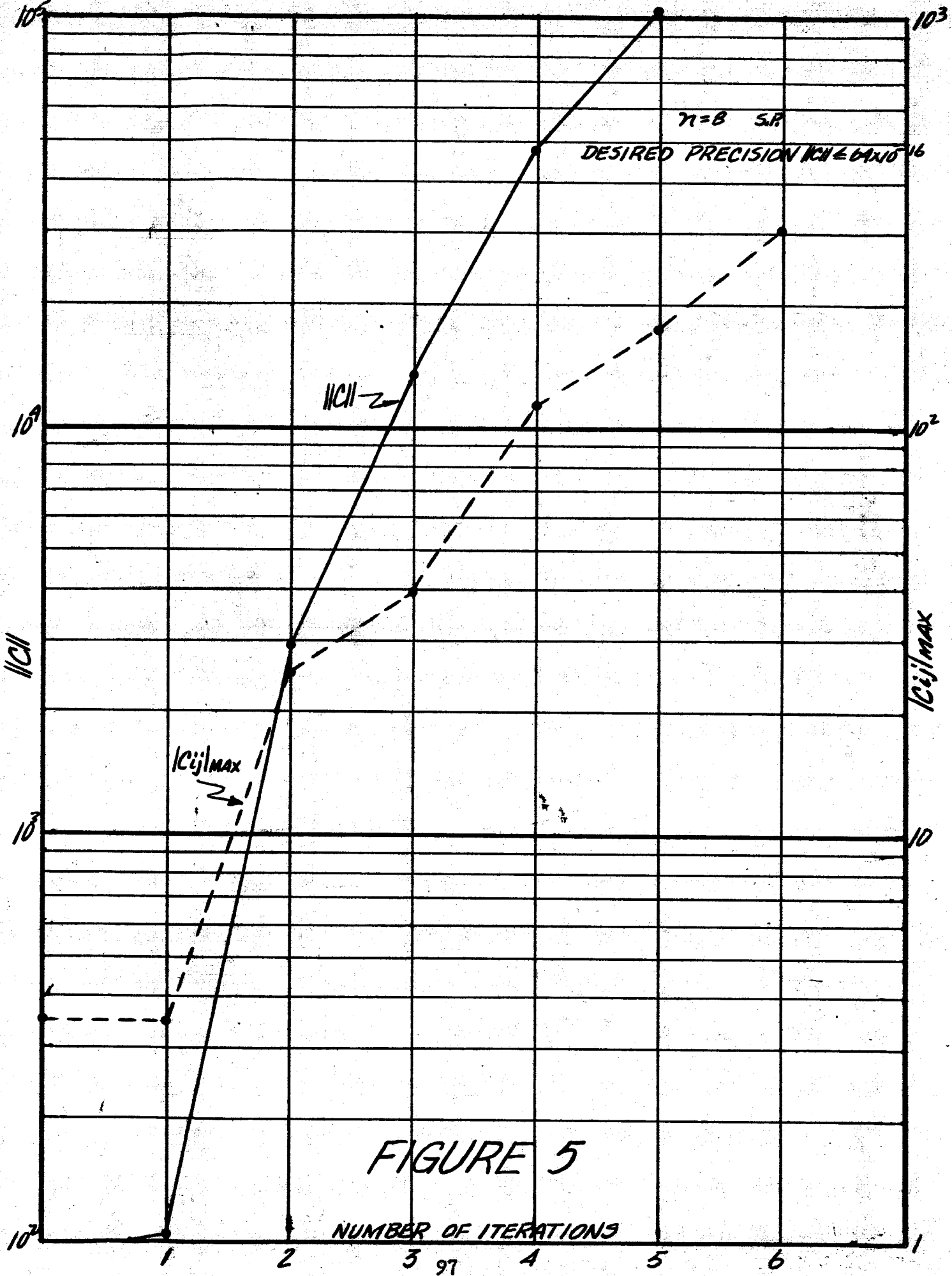
10^5
10^4
10^3
10^2
10^1
10^3
10^2
10
1
n=8 S.P.
DESIRED PRECISION ||C|| ≤ 64x10^-16
||C||
|Cij|max
||C||
|Cij|max
1
2
3
4
5
6
NUMBER OF ITERATIONS

FIGURE 5

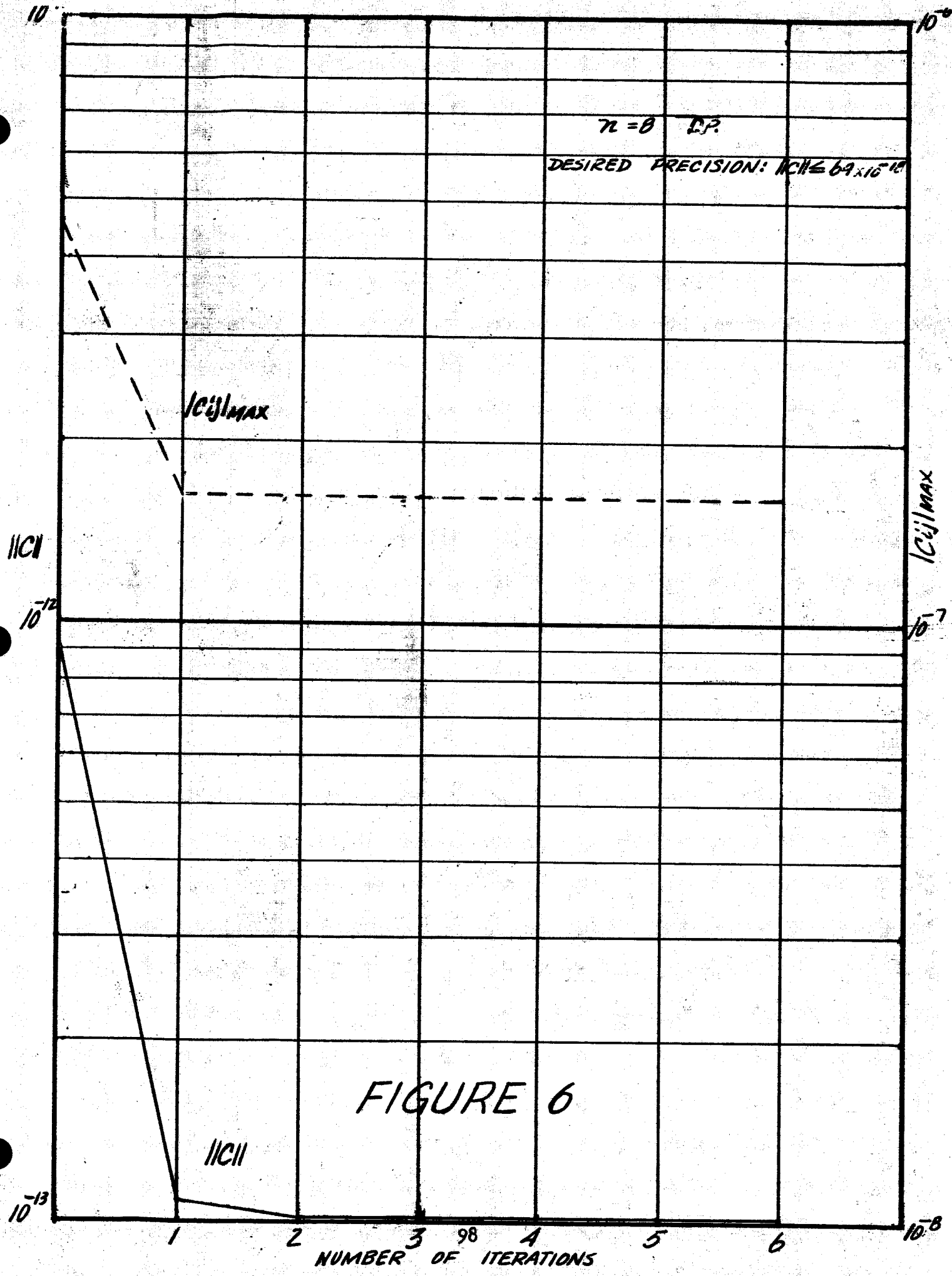
10
10^{-6}
n = 8 D.P.
DESIRED PRECISION: ||C|| ≤ 64 x 10^{-15}
$|C_{ij}|_{MAX}$
||C||
10^{-12}
10^{-7}
$|C_{ij}|_{MAX}$
10^{-13}
10^{-8}
1
2
3
4
5
6
NUMBER OF ITERATIONS

FIGURE 6

0-20-10

Some CA

N64-18234

9.0 DERIVATIVES IN TERMS OF CENTRAL DIFFERENCES

E. E. GRINOCH

p99-102 ref (See N64-18226 10-01) OTS: etc.

An elegant and powerful method for obtaining formulae for differentiation in terms of functional values, at equally spaced points of the independent variable, is by means of finite difference operators. In particular, formulae are considered here in terms of the central difference operator.

9.1. Symbols and Definitions:

Define: $x_{i+1} - x_i = h$, $i = 0, 1, 2, \ldots$

The central difference symbol δ, when prefixing a functional symbol, say f, represents an operator. Specifically, it operates as follows:

$$\delta f(x_{i+\frac{1}{2}}) = f(x_{i+1}) - f(x_i) = f_{i+1} - f_i$$

or, similarly; $\delta f_i = f_{i+\frac{1}{2}} - f_{i-\frac{1}{2}}$ (1)

where the subscript $i \pm \frac{1}{2}$ refers to the midpoint between x_i and $x_i \pm 1$.

y_{-2}	f_{-2}		$\delta^2 f_{-2}$		$\delta^4 f_{-2}$	$\delta^6 f_{-2}$
		$\delta f_{-3/2}$		$\delta^3 f_{-3/2}$	$\delta^5 f_{-3/2}$	
y_{-1}	f_{-1}		$\delta^2 f_{-1}$		$\delta^4 f_{-1}$	$\delta^6 f_{-1}$
		$\delta f_{-1/2}$		$\delta^3 f_{-1/2}$	$\delta^5 f_{-1/2}$	
y_0	f_0		$\delta^2 f_0$		$\delta^4 f_0$	$\delta^6 f_0$
		$\delta f_{1/2}$		$\delta^3 f_{1/2}$	$\delta^5 f_{1/2}$	
y_1	f_1		$\delta^2 f_1$		$\delta^4 f_1$	$\delta^6 f_1$
		$\delta f_{3/2}$		$\delta^3 f_{3/2}$	$\delta^5 f_{3/2}$	
y_2	f_2		$\delta^2 f_2$		$\delta^4 f_2$	$\delta^6 f_2$

TABLE OF CENTRAL DIFFERENCES

The central differences table given above shows that only even order differences have integral suffixes.

To express differences in terms of the function values from which they are derived, take in succession:

$$\delta f_{1/2} = f_1 - f_0$$

$$\delta^2 f_0 = \delta f_{1/2} - \delta f_{-1/2} = f_1 - 2f_0 + f_{-1}$$

$$\delta^3 f_{1/2} = \delta^2 f_1 - \delta^2 f_0 = f_2 - 3f_1 + 3f_0 - f_{-1}$$

and in general:

$$\delta^m f_i = \sum_{k=0}^{m} (-1)^k \frac{m!}{k!(m-k)!} f_{i+\frac{m}{2}-k}$$

It is convenient to introduce a few more operators.

The operator E is defined by

$$Ef(x) = f(x + h) \qquad (2)$$

or, in general,

$$Ef_i = f_{i+1}$$

That is, E is a "forward shift operator", as it advances the argument from one value to the next in a table of finite differences. In a similar fashion E^{-1} is defined as a backward shift operator, i.e.,

$$E^{-1} f_i = f_{i-1}$$

Now, if a table is the only source of information about a function, we may assume the function represented by the table as being differentiable as many times required, but must keep in mind that functions defined by analytical formulae are adequately represented by tables only in ranges away from singularities and discontinuities.

This assumption implies, therefore, that the function under consideration can be expanded in a Taylor series over the range, say $[\tilde{x}, \tilde{\tilde{x}}]$. That is:

$$f(x_o \pm nh) = f_{\pm n} = f_o \pm nhDf_o + \frac{1}{2!}(nh)^2 D^2 f_o \pm \frac{1}{3!}(nh)^3 D^3 f_o + \ldots . \qquad (3)$$

where $D^k = \frac{d^k}{dx^k}$, $k = 1, 2, \ldots .$

Of course if the series is cut off after m terms, the remainder is of the order of $(nh)^m$.

From $e^u = \sum_{k=0}^{\infty} \frac{1}{k!} u^k$, comparison with (1) shows that formally the Taylor expansion can be written:

$$f(x_o + nh) = \sum_{k=0}^{\infty} \frac{1}{k!} (nh)^k D^k f_o = e^{nhD} f_o.$$

In particular, for n=1:

$$f(x_o + h) = e^{hD} f_o = f_1 \tag{4}$$

from which

$$E = e^{hD}$$

and

$$e^{\frac{1}{2}hD} f_o = f(x_o + \tfrac{1}{2}h).$$

Define $E^{\frac{1}{2}} f(x_o) = f(x_o + \frac{1}{2}h)$, which is consistent with the previous definition (2) of E.

We can establish a relation between the central operator δ and E as follows:

$$\delta f_i = f_{i+\frac{1}{2}} - f_{i-\frac{1}{2}} = (E^{\frac{1}{2}} - E^{-\frac{1}{2}}) f_i$$

so that formally:

$$\delta = E^{\frac{1}{2}} - E^{-\frac{1}{2}} \tag{5}$$

and

$$\delta^2 = E^{\frac{1}{4}} - 2 + E^{-\frac{1}{4}}$$

The "averaging operator" μ will also be used. It is defined by:

$$\mu f_i = \tfrac{1}{2}(f_{i+\frac{1}{2}} + f_{i-\frac{1}{2}}) = \tfrac{1}{2}(E^{\frac{1}{2}} f_i + E^{-\frac{1}{2}} f_i)$$

so that formally

$$\mu = \tfrac{1}{2}(E^{\frac{1}{2}} + E^{-\frac{1}{2}}) \tag{6}$$

and

$$\mu^2 = 1 + \tfrac{1}{4}\delta^2$$

Now if (4) is substituted in (5) and (6),

$$\delta = 2 \sinh \tfrac{1}{2} hD \tag{7}$$

$$\mu = \cosh \tfrac{1}{2} hD$$

Of course, use of the above relations imply use of the Taylor expansion in

the form

$$e^{\xi D} f(x) = f(x+\xi)$$

and in practice only a few terms of the series can be retained, thus introducing a truncation error.

With these operators and relationships among operators, formulae for numerical differentiation are readily obtained. Indeed, from (7),

$$hD = 2 \sinh^{-1} \tfrac{1}{2}\delta \tag{8}$$

$$= \left[\frac{\sinh^{-1} \frac{1}{2}\delta}{\frac{1}{2}\delta}\right]\delta \tag{8a}$$

$$= \mu^{-1}\left[\frac{\sinh^{-1} \frac{1}{2}\delta}{\frac{1}{2}\delta}\right]\mu\delta \tag{8b}$$

which gives the derivative D in terms of central differences.

Expressions (8a) and (8b) have been introduced for practical reasons. Since the function is usually available for integral values of the subscript an expansion is sought which gives hD in terms of tabular values.

The form of (8b) gives hD in terms of μ, δ and μ^{-1}. Now, if for μ^{-1} we write:

$$\mu^{-1} = (1 + \tfrac{1}{4}\delta^2)^{-\frac{1}{2}}$$

$$= 1 - \tfrac{1}{2}(\tfrac{1}{4}\delta^2) + \frac{1.3}{2.4}(\tfrac{1}{4}\delta^2)^2 - \frac{1.3.5}{2.4.6}(\tfrac{1}{4}\delta^2)^3 + \frac{1.3.5.7}{2.4.6.8}(\tfrac{1}{4}\delta^2)^4 + O(h^{10})$$

and if for $\dfrac{\sinh^{-1} \frac{1}{2}\delta}{\frac{1}{2}\delta}$ we write:

$$\frac{\sinh^{-1} \frac{1}{2}\delta}{\frac{1}{2}\delta} = 1 - \frac{1}{24}\delta^2 + \frac{3}{640}\delta^4 - \frac{5}{7168}\delta^6 + \frac{35}{294912}\delta^8 + O(h^{10})$$

and substitute both expansions in (8b) we obtain:

$$hD = 1 - \frac{1}{6}\delta^2 + \frac{1}{30}\delta^4 - \frac{1}{140}\delta^6 + \frac{1}{630}\delta^8 + O(h^{10}) \tag{9}$$

or

$$D = \frac{1}{2h}\left[f_1 - f_{-1} - \frac{1}{6}(\delta^2 f_1 - \delta^2 f_{-1}) + \frac{1}{30}(\delta^4 f_1 - \delta^4 f_{-1}) - \frac{1}{140}(\delta^6 f_1 - \delta^6 f_{-1})\right] \tag{10}$$

which is an expression for D which only involves even order differences, as required.

0-29-10

Same as A.

N64-18235

~~10.0~~ THE RECTIFICATION PROCESS

N. F. TODA abs its Minimum --- 8 Nov. 1963
P103-107 only (See N64-18226 10-01) OTS: etc.

2 This analysis of the rectification process is concerned with the preservation of accuracy in the computation of the osculating orbit.

The position and velocity at time t may be computed from

$$\left.\begin{aligned} \bar{R}(t) &= f\,\bar{R}_0 + g\,\dot{\bar{R}}_0 \\ \dot{\bar{R}}(t) &= \dot{f}\,\bar{R}_0 + \dot{g}\,\dot{\bar{R}}_0 \end{aligned}\right\} \qquad (1)$$

where $\bar{R}_0$ and $\dot{\bar{R}}_0$ are the position and velocity vectors, respectively, at epoch, t_0. The functions f, g, $\dot{f}$ and $\dot{g}$ are implicit functions of time. In two of the formulations under consideration they are explicit functions of either range angle, Θ (differential true anomaly, $v - v_0$) or Herrick's Variable, $\hat{\chi}$. The first formulation is valid for elliptic, parabolic and hyperbolic orbits while the formulation in terms of Herrick's variable is valid for all conic sections including the rectilinear cases.

10.1 Herrick's Variable

The position $\bar{R}_0$ and velocity $\dot{\bar{R}}_0$ vectors at epoch, t_0, are assumed to be known in a non-rotating Cartesian coordinate system. The following quantities are then computed

$$r_0 = \sqrt{\bar{R}_0 \cdot \bar{R}_0} \qquad (2)$$

$$\dot{s}_0^2 = \dot{\bar{R}}_0 \cdot \dot{\bar{R}}_0 \qquad (3)$$

$$D_0 = \frac{\bar{R}_0 \cdot \dot{\bar{R}}_0}{\sqrt{\mu}} \qquad (4)$$

$$C_0 = \frac{r_0 \dot{s}_0^2}{\mu} - 1 \qquad (5)$$

$$\frac{1}{a} = \frac{2}{r_0} - \frac{\dot{s}_0^2}{\mu} \qquad (6)$$

$$\hat{n} = \sqrt{\mu} \qquad (7)$$

The computation then requires the calculation of $\hat{X}$ when time t is specified. The process continues with the calculation of

$$\hat{M} = \hat{n}\,(t - t_0) \tag{8}$$

Next solve the transcendental equation

$$\hat{M} = r_0 \hat{X} + D_0 \hat{C} + C_0 \hat{U} \tag{9}$$

for $\hat{X}$ where

$$\hat{U} = \hat{X}^3 \left[\frac{1}{3!} - \frac{\hat{X}^2}{5!a} + \frac{\hat{X}^4}{7!a^2} - \frac{\hat{X}^6}{9!a^3} + \cdots \right] \tag{10}$$

$$\hat{C} = \hat{X}^2 \left[\frac{1}{2!} - \frac{\hat{X}^2}{4!a} + \frac{\hat{X}^4}{6!a^2} - \frac{\hat{X}^6}{8!a^3} + \cdots \right] \tag{11}$$

The Newton-Raphesen technique may be employed for the solution of the transcendental equation (9). The study will determine a first approximation to the solution of (9) that is suitable for the iterative process. After obtaining an accurate value of $\hat{X}$ the calculation continues with

$$f = 1 - \frac{\hat{C}}{r_0} \tag{12}$$

$$g = \frac{\hat{M} - \hat{U}}{\sqrt{\mu}} \tag{13}$$

$$\hat{S} = \hat{X} - \frac{\hat{U}}{a} \tag{14}$$

$$r = r_0 + D_0 \hat{S} + C_0 \hat{C} \tag{15}$$

$$\dot{f} = \frac{-\sqrt{\mu}\,\hat{S}}{r r_0} \tag{16}$$

$$\dot{g} = 1 - \frac{\hat{C}}{r} \tag{17}$$

These values are then substituted into (1) to determine the value of $\bar{R}(t)$ and $\dot{\bar{R}}(t)$.

The functions $\hat{U}$ and $\hat{C}$ (Eqs. (10) & (11)) are infinite series expansions. Since the argument $\hat{x}^2/a$ could in certain situations become large, a great many terms would have to be employed to limit the truncation error at the expense of accumulated round off error. Herrick foresaw the possibility that this difficulty might arise and provided a shifting epoch concept to cope with this problem.

In order to calculate $\bar{R}$ and $\dot{\bar{R}}$, at time tj where $t_j - t_o$ is large, select an intermediate time t_i such that $t_j > t_i > t_o$. Let

$$\left.\begin{aligned} \hat{M}_i &= \hat{n}(t_i - t_o) \\ \hat{M}_{ij} &= \hat{n}(t_j - t_i) \end{aligned}\right\} \tag{18}$$

Similarly one may obtain

$$\hat{x}_j = \hat{x}_i + \hat{x}_{ij} \tag{19}$$

$$\hat{s}_j = \hat{s}_i + \hat{s}_{ij} - \frac{1}{a}\left(\hat{s}_i \hat{c}_{ij} + c_i \hat{s}_{ij}\right) \tag{20}$$

$$\hat{c}_j = \hat{c}_i + \hat{c}_{ij} - \frac{1}{a}\hat{c}_i \hat{c}_{ij} + \hat{s}_i \hat{s}_{ij} \tag{21}$$

$$\hat{U}_j = \hat{U}_i + \hat{U}_{ij} - \left(\hat{s}_i \hat{c}_{ij} + \hat{c}_i \hat{s}_{ij}\right) \tag{22}$$

These formulae may be used when one wants to retain the vectors $\bar{R}_o$ and $\dot{\bar{R}}_o$; however in generating an ephemeris one would shift the epoch by employing

$$\left.\begin{aligned} \bar{R}_i &= f_i \bar{R}_o + g_i \dot{\bar{R}}_o \\ \dot{\bar{R}}_i &= \dot{f}_i \bar{R}_o + \dot{g}_i \dot{\bar{R}}_o \end{aligned}\right\} \tag{23}$$

then

$$\left.\begin{aligned} \bar{R}_j &= f_{ij} \bar{R}_i + g_{ij} \dot{\bar{R}}_i \\ \dot{\bar{R}}_j &= \dot{f}_{ij} \bar{R}_i + \dot{g}_{ij} \dot{\bar{R}}_i \end{aligned}\right\} \tag{24}$$

By suitably choosing $t_j - t_i$ the argument $\hat{X}_{ij}^2/a$ may be kept small.

In addition to the above techniques for insuring the accuracy of the computation a continued fraction expansion of $\hat{U}$ and $\hat{c}$ will be tested in hopes of enlarging the practical interval of convergence.

10.2 Range Angle Formulation

The computation of $\bar{R}$ and $\dot{\bar{R}}$ in terms of the range angle θ is outlined below

$$r_0 = \sqrt{\bar{R}_0 \cdot \bar{R}_0} \tag{25}$$

$$\bar{C} = \bar{R}_0 \times \dot{\bar{R}}_0 \; ; \quad C = |\bar{C}| \tag{26}$$

$$m_0 = \frac{\bar{R}_0 \cdot \dot{\bar{R}}_0}{C} \tag{27}$$

The equation

$$t - t_0 = \frac{1}{C} \int_0^{\theta} \frac{d\phi}{U^2(\phi)} \tag{28}$$

where

$$U(\theta) = \frac{1}{r(\theta)} = \frac{\mu}{C^2} + \left(\frac{1}{r_0} - \frac{\mu}{C^2} \right) \cos\theta - \frac{m_0}{r_0} \sin\theta \tag{29}$$

may be iterated by the Newton-Raphson technique to determine θ when t is given. It can be shown that

$$f = \frac{1}{r_0 U(\theta)} \left\{ \cos\theta - m_0 \sin\theta \right\} \tag{30}$$

$$g = \frac{r_0 \sin\theta}{C\, U(\theta)} \tag{31}$$

$$\dot{f} = \frac{\mu}{r_0 C} \left\{ m_0 (1 - \cos\theta) - \sin\theta \right\} \tag{32}$$

$$\dot{g} = 1 - \frac{\mu r_0}{C^2} (1 - \cos\theta) \tag{33}$$

Finally as before

$$\left.\begin{aligned} \bar{R}(t) &= f\,\bar{R}_o + g\,\dot{\bar{R}}_o \\ \dot{\bar{R}}(t) &= \dot{f}\,\bar{R}_o + \dot{g}\,\dot{\bar{R}}_o \end{aligned}\right\} \qquad (34)$$

The integral in equation (28) may be evaluated in closed form. However the closed form depends on whether the conic is an ellipse, parabola or hyperbola. These formulae will be subject to large errors in the near-parabolic case.

One possible method of eliminating the difficulty in the near-parabolic case is to evaluate the integral numerically. Several techniques for evaluating definite integrals such as the trapezoidal rule with and without end correction, Simpson's Rule with and without end correction will be tested. These methods will also be employed with and without interval control. If at last one of these methods gives good results, then an integration of the Chevyshev polynomial approximation will be tested in an effort to increase the efficiency of the program.

An in-house program is already available for computing the elements of the state transition matrix in terms of the range angle θ which is valid for elliptic, parabolic and hyperbolic orbits. The precision of the computation of these elements depends on the precision of the evaluation of two definite integrals similiar to that in equation (28).

0-20-10

Same as

N64-18236

~~11.0~~ INCORPORATION OF BIAS ERRORS INTO THE ESTIMATIONS PROCEDURE

J. A. Winokur chapter Minimum -- 8 Nov. 1963

P 108-116 ref (See N64-18226 10-01) OTS: etc.

In some trajectory computations an estimate of bias errors will be desirable as an output of the program in addition to the position and velocity coordinate estimates which are presently provided.

The following sections provide a list of the bias errors which will be made available as options in the XR, and show how they can be incorporated into the estimation procedure. The partial derivatives which are required to fill out the various matrices are not explicitly derived in this report.

11.1 Bias Error Types

The bias errors to be considered are of 19 different types, e.g., unknown errors in latitude of a given tracking station, or errors in the knowledge of the second harmonic of the earth's gravitational potential. This does not limit the total number of bias errors to 19, however, since there may be several of a given type -- for example, ten latitude errors to be determined for ten different tracking sites.

Type 1 LATITUDE ERROR . . . . . $\Delta\psi_7 - \Delta\psi_{44}$

Type 2 LONGITUDE ERROR. . . . . $\Delta\psi_{45} - \Delta\psi_{82}$

Type 3 HEIGHT ERROR . . . . . $\Delta\psi_{83} - \Delta\psi_{120}$

These indices allow any or all of 38 separate stations to be located. The indices will be subdivided as follows:

7-14, 45-52, 83-90	lat., long., height errors respectively for 8 R-R tracking systems
15-26, 53-64, 91-102	lat., long., height errors respectively for 12 MINITRACK stations
27-36, 65-74, 103-112	lat., long., height errors respectively for 10 DSIF stations
37-44, 75-82, 113-120	lat., long., height errors respectively for 8 MERCURY stations

Type 4 ERROR IN THE KNOWLEDGE OF VELOCITY OF LIGHT. . . $\Delta\psi_{121}$

Type 5 ERROR IN KNOWLEDGE OF GRAVITATIONAL CONSTANT TIMES MASS OF THE EARTH . . . . . $\Delta\psi_{122}$

Type 6-13 ERRORS IN KNOWLEDGE OF HARMONIC COEFFICIENTS OF EARTH. . . . . $\Delta\psi_{123} - \Delta\psi_{130}$

In other words, the earth's gravitational potential will be considered as described by the eight harmonics $\psi_{123} = J_2$ through $\psi_{130} = J_9$, with errors $\Delta\psi_{123}, \ldots, \Delta\psi_{130}$.

Type 14 ERROR IN KNOWLEDGE OF THE ASTRONOMICAL UNIT . . . $\Delta\psi_{131}$

Types 15-19 ERRORS IN KNOWLEDGE OF ATMOSPHERIC PARAMETERS FOR ELECTROMAGNETIC PROPAGATION PATH COMP . . . . $\Delta\psi_{132}$

No allowance has been made for estimating bias errors in the computation of the drag forces due to the atmosphere and to the solar flux because the fundamental parameters in this computation are not constants, but are derived from tables of experimental data, and thus do not lend themselves to a bias estimate.

In the case of atmospheric computations for the electromagnetic path correction, a cruder model of the atmosphere can be used, which is expressed analytically in terms of the five "constants" No, H, ρ_0, Hm and Ho. Consequently, a bias estimate on these "constants" is possible, at least over a short period of time during which they actually do remain constant.

11.2 Incorporation of Bias Errors in the State Vector and the Variational Parameter Vector

At present the state vector consists of the six quantities which correspond to the "best" estimates of position and velocity corrections. This set of quantities are to be expanded to include any or all of the components $\Delta\psi_7, \ldots, \Delta\psi_{132}$. In all probability, only a few of these will ever be used on any particular trajectory run; for example, the state vector may be

$$\Delta\psi = \begin{Bmatrix} \Delta\psi_1 \\ \vdots \\ \Delta\psi_6 \\ \hline \Delta\psi_{10} \\ \Delta\psi_{15} \\ \Delta\psi_{31} \end{Bmatrix}, \text{ or in general, } \Delta\psi = \begin{Bmatrix} \Delta\psi_1 \\ \vdots \\ \Delta\psi_6 \\ \hline \Delta\psi_{p_1} \\ \vdots \\ \Delta\psi_{p_r} \end{Bmatrix}$$

where P_1, P_2 ... P_r are chosen from the list of numbers 7-132. Note that the vector has dimensions (r + 6) x 1.

Since the variational parameters rather than the state variables themselves are being used for internal computations, the $\Delta\alpha$ vector must also be modified. It will be expanded to the same dimension as that to which $\Delta\psi$ has been augmented. The proper choice of augmented S^{-1}, S and Ψ matrices (to be discussed in the following sections) makes it possible to define the new $\Delta\alpha$ vector as

$$\Delta\alpha = \begin{Bmatrix} \Delta\alpha_1 \\ \vdots \\ \Delta\alpha_6 \\ \hline \Delta\psi_{P_1} \\ \vdots \\ \Delta\psi_{P_r} \end{Bmatrix}$$

where $\Delta\alpha_1, \ldots, \Delta\alpha_6$ are the old variational parameter increments and $\Delta\psi_{P_1}, \ldots, \Delta\psi_{P_r}$ are the r bias errors.

11.3 Review of Minimum Variance Equations and Summary of Matrices to be Expanded

In order to see clearly which matrices must be modified, it is helpful to write down the minimum variance equations which must be handled.

1) $\Delta\psi = K\Delta\gamma$

2) $K = Q(t_k^-)N^T Y^{-1}$

3) $Y = NQ(t_k^-)N^T + \bar{\epsilon}^2$

4) $Q(t_k^-) = \Psi Q(t_{k-1}^+)\Psi^T$

5) $Q(t_k^+) = Q(t_k^-) - KN^T Q(t_k^-)$

The number of observables in the $\Delta\gamma$ vector is not affected by any change in the state vector, so that the changes must be reflected in the K matrix, which is determined by Q, N, and Y.

But Q is updated by means of Ψ from its value at t_o, which is

6) $Q(t_o) = S^{-1}(t_o)P(t_o)\left(S^T(t_o)\right)^{-1} = S^{-1}(t_o)P(t_o)\left(S^{-1}(t_o)\right)^T$

where P(to) is the covariance matrix of the state vector $\Delta\chi$, and S^{-1} and S relate the state vector to the variational parameter vector as follows

$$\Delta\psi = \frac{\partial\psi}{\partial\alpha}\Delta\alpha = S\Delta\alpha$$

$$\Delta\alpha = \frac{\partial\alpha}{\partial\psi}\Delta\psi = S^{-1}\Delta\psi$$

Thus, if the new form of S and S^{-1} and that of Ψ are known, Q is determined from the input matrix P(to) by items 6) and 3).

Similarly Y is determined by 4) if Q is known and if N is known. The $\bar{\epsilon}^2$ matrix is the covariance matrix of the instrument errors and is not affected by any change in the state vector.

But N describes the relation between the observables and the variational parameters:

$$\Delta\gamma = N\Delta\alpha = \frac{\partial\gamma}{\partial\alpha}\Delta\alpha = \frac{\partial\gamma}{\partial\psi}\frac{\partial\psi}{\partial\alpha}\Delta\alpha$$

$$\Delta\gamma = MS\Delta\alpha = N\Delta\alpha$$

$$N = MS$$

One additional matrix, $M = \frac{\partial\gamma}{\partial\psi}$, must be modified, therefore, when $\Delta\alpha$ is modified. Note that all the quantities in 1) - 5) are now determined.

In summary, the matrices which must be augmented when $\Delta\psi$ and $\Delta\alpha$ are expanded are

7) $S(t) = \frac{\partial\psi}{\partial\alpha}$

8) $S^{-1}(t) = \frac{\partial\alpha}{\partial\psi}$

9) $P(t_o) = E\left(\Delta\psi(t_o), \Delta\psi^T(t_o)\right)$

10) $\Psi(t, t_o) = \frac{\partial\alpha(t)}{\partial\alpha(t_o)}$

11) $M(t) = \frac{\partial\gamma}{\partial\psi}$

11.4 Augmentation of S(t) and $S^{-1}(t)$

According to the definition of S, and the expanded vectors $\Delta\psi$ and $\Delta\alpha$,

$$\begin{Bmatrix} \Delta\psi_1 \\ \vdots \\ \Delta\psi_6 \\ \hline \Delta\psi_{P_1} \\ \vdots \\ \Delta\psi_{P_r} \end{Bmatrix} = \left\{\begin{array}{c|c} S_1 \; (6\times 6) & S_2 \; (6\times r) \\ \hline S_3 \; (r\times 6) & S_4 \; (r\times r) \end{array}\right\} \begin{Bmatrix} \Delta\alpha_1 \\ \vdots \\ \Delta\alpha_6 \\ \hline \Delta\psi_{P_1} \\ \vdots \\ \Delta\psi_{P_r} \end{Bmatrix}$$

It is clear that the 6 x 6 matrix S_1 which relates the old $\Delta\psi$ to the old $\Delta\alpha$ must be the old S(t) matrix.

Since the position and velocity coordinates at time t cannot change if there should be a change in the bias errors at time t, $S_2 = 0$.

The bias errors at time t, on the other hand, do not depend on the variational parameters $\Delta\alpha_1, \ldots \Delta\alpha_6$, so that $S_3 = 0$, and since the same bias errors appear in both $\Delta\psi$ and the $\Delta\alpha$ vector, $S_4 = I$.

Similar reasoning for $S^{-1}(t)$ results in conclusions which are summarized graphically below.

$$S(t) = \left|\begin{array}{c|c} S(t) \; (6\times 6) & 0 \; (6\times r) \\ \hline 0 \; (r\times 6) & I \; (r\times r) \end{array}\right|$$

$$S^{-1}(t) = \left|\begin{array}{c|c} S^{-1}(t) \; (6\times 6) & 0 \; (6\times r) \\ \hline 0 \; (r\times 6) & I \; (r\times r) \end{array}\right|$$

11.5 Computation of Q(to) and Expansion of P(to)

$$Q(t_o) = S^{-1}(t_o)\, P(t_o) \left(S^{T}(t_o)\right)^{-1}$$

$$= S^{-1}(t_o)\, P(t_o) \left(S^{-1}(t_o)\right)^{T}$$

The matrix P(to) must be provided as an input.

$$P(t_o) = E\left(\Delta\psi(t_o), \Delta\psi^{T}(t_o)\right) = \left|\begin{array}{ccc|ccc} E\Delta\psi_1^2 & \cdots & E\Delta\psi_1\Delta\psi_6 & \cdots & E\Delta\psi_1\Delta\psi_{P_r} \\ \vdots & P(t_o) & \vdots & & \vdots \\ & & E\Delta\psi_6^2 & & \\ \hline \vdots & & \vdots & & \vdots \\ E\Delta\psi_{P_r}\Delta\psi_1 & \cdots & & \cdots & E\Delta\psi_{P_r}^2 \end{array}\right|$$

It is reasonable to assume that the bias errors are uncorrelated with each other or with the errors in the initial estimates of position and velocity, in which case the upper right-and lower left-corner entries are all zero.

This assumption makes it necessary to supply only the r additional terms along the main diagonal, plus the original 6 x 6 P(to) matrix indicated above.

11.6 Augmentation of $\Psi(t, t_o)$.

The definition of $\Psi(t, to)$ is in terms of the new and old value of the variational parameter vector

$$\Delta\alpha(t) = \frac{\partial\alpha(t)}{\partial\alpha(t_o)}\,\Delta\alpha(t_o) = \Psi(t, t_o)\,\Delta\alpha(t_o)$$

In order to see what must be done to the Ψ matrix it is helpful to exhibit this relation graphically as follows.

$$\begin{Bmatrix} \Delta\alpha_1(t) \\ \vdots \\ \Delta\alpha_6(t) \\ \hline \Delta\psi_{p_1}(t) \\ \vdots \\ \Delta\psi_{p_r}(t) \end{Bmatrix} = \left[\begin{array}{c|c} \Psi_1 = \Psi \quad (6\times 6) & \Psi_2 = \dfrac{\partial\alpha_i(t)}{\partial\alpha_j(t_0)} \quad (6\times r) \\ & i = 1,\ldots,6 \\ & j = p_1,\ldots,p_r \\ \hline \Psi_3 = 0 \quad (r\times 6) & \Psi_4 = I \quad (r\times r) \end{array}\right] \begin{Bmatrix} \Delta\alpha_1(t_0) \\ \vdots \\ \Delta\alpha_6(t_0) \\ \hline \Delta\psi_{p_1}(t_0) \\ \vdots \\ \Delta\psi_{p_r}(t_0) \end{Bmatrix}$$

It is clear that Ψ_1 must be the original variational parameter transition matrix, i.e., $\Psi_1 = \Psi$.

The S(t) and $S^{-1}(t)$ matrices represented point transformations at a given time t, and therefore changes in the bias errors produced no changes in the six original variational parameters. However, Ψ_2 above relates changes in the bias errors at time t_0 to changes in the six original variational parameters <u>at time t</u>, and this means that Ψ_2 is not identically zero.

To see how the elements of Ψ_2 are obtained, imagine that the variational parameters are simply the ordinary state variables, position and velocity, so that

$$\Psi_2 = \frac{\partial\psi_i(t)}{\partial\psi_j(t_0)}, \quad i = 1,\ldots,6; \quad j = p_1,\ldots,p_r.$$

Now, one column of Ψ_2 might be $\partial\psi_i/\partial\mu$, where μ is the earth's gravitational constant ($\mu = \psi_{122}$ in the nomenclature of 11.1.). Remembering that ψ_i, $(i = 1,\ldots,6)$ is obtained from Encke integration of the motion equations, i.e.

$$\dot{\psi}_i = F_i(\psi_j, \psi_{iTB}, \mu) \qquad \begin{matrix} i = 1,\ldots,6 \\ j = 1,\ldots,6 \end{matrix}$$

the following set of differential equations in $\frac{\partial\psi_i}{\partial\mu}$ results:

$$\frac{d}{dt}\left(\frac{\partial\psi_i}{\partial\mu}\right) = \sum_{j=1}^{6} \frac{\partial F}{\partial\psi_j}\frac{\partial\psi_j}{\partial\mu} + \sum_{j=1}^{6} \frac{\partial F_i}{\partial\psi_{jTB}}\frac{\partial\psi_{jTB}}{\partial\mu} + \frac{\partial F_i}{\partial\mu}, \quad i = 1,\ldots,6.$$

In the above equations, $\psi_{j,TB}$ stands for the jth component of the vector which is the solution to the two body problem. This set must now be solved for $\partial\psi_i/\partial\alpha_j$. Note that since F is a known function, the coefficients of $\partial\psi_i/\partial\alpha_j$ on the right side are known also.

Returning to the more general problem of obtaining the matrix $\Psi_2 = \frac{\partial\alpha_i(t)}{\partial\alpha_j(t_0)}$, $i = 1, \ldots, 6$; $j = p_1, \ldots, p_r$, when the α_i's are the variational parameters, note that,

$$\Psi_2 = \frac{\partial\alpha_i(t)}{\partial\alpha_j(t_0)} = \frac{\partial\alpha_i(t)}{\partial\psi_i(t)} \frac{\partial\psi_i(t)}{\partial\alpha_j(t_0)},$$

since the α_j's are the same as the corresponding components of the expanded state vector (see 11.2). Graphically, Ψ_2 may be displayed as follows:

$$\Psi_2 = \left\{ \begin{array}{c} \frac{\partial\alpha_i(t)}{\partial\psi_i(t)} \\ (6\times 6) \end{array} \right\} \left\{ \begin{array}{c} \frac{\partial\psi_i(t)}{\partial\psi_j(t_0)} \\ (6\times r) \end{array} \right\}$$

On comparison with the augmented $S^{-1}(t)$ of 11.4, it is clear that the first 6 x 6 matrix above is the same as that of $S^{-1}(t)$; it is the original (6 x 6) S^{-1} which is presently in the program.

The second of the two matrices which constitute Ψ consists of partials such as the one mentioned earlier in this section. The remainder of these partials have not yet been evaluated.

To complete the augmentation of Ψ, the two submatrices Ψ_3 and Ψ_4 are required. Ψ_3 is the zero matrix, because the bias errors do not depend on the variational parameters. Ψ_4 is the r x r identity, since the bias errors are constant in time.

11.7 Augmentation of M(t)

By definition, $M(t) = \partial\gamma(t)/\partial\psi$ is the matrix of partials of the observables with respect to the state variables. If the number of observables is m, and the order of the state vector is 6 + r, then M must be an (m)x (6 + r) matrix. Graphically,

$$\begin{Bmatrix} \Delta\gamma_1 \\ \vdots \\ \Delta\gamma_m \end{Bmatrix} = \left[\begin{array}{c|c} M_1(t) & M_2(t) \\ (m \times 6) & (m \times r) \end{array}\right] \left\{\begin{array}{c} \Delta\psi_1 \\ \vdots \\ \Delta\psi_6 \\ \hline \Delta\psi_{P_1} \\ \vdots \\ \Delta\psi_{P_r} \end{array}\right\}$$

The first m x 6 submatrix must be the old M(t), since it describes the relationship between the observables, which have not changed in number, and the old state variables.

The second m x r submatrix, M_2, describes the variation of the observables with the bias errors. It consists of partials which have not yet been explicitly evaluated.

An example of the type of partial involved in M_2 is illustrated by the case in which range to the vehicle from a radar station is one of the observables, and the location of the radar is in error by an unknown bias. Letting γ be the observable range,

$$\gamma = \sqrt{(x - x_s)^2 + (y - y_s)^2 + (z - z_s)^2}$$

where (x, y, z) are the inertial coordinates of the ship and (x_s, y_s, z_s) those of the station.

Then $\partial\gamma/\partial x_s, \partial\gamma/\partial y_s, \partial\gamma/\partial z_s$ represent the sensitivity of the observation to errors in the station position errors, where

$$\frac{\partial\gamma}{\partial x_s} = -\frac{(x - x_s)}{\gamma}$$

$$\frac{\partial\gamma}{\partial y_s} = -\frac{(y - y_s)}{\gamma}$$

$$\frac{\partial\gamma}{\partial z_s} = -\frac{(z - z_s)}{\gamma}$$

These partials then appear in the appropriate column of the M_2 sub-matrix.

0-20-10

Same CA

N64-18237

PRECISION OF THE OPTIMUM FILTER K

C. I. Smith

12.1 Introduction

In MINIVAR, the state transition matrix is used only to transform the covariance matrix of the state variables from one data point to the next. Consequently, the transition matrix precision affects the precision of the following arrays:

1. the transformed covariance matrix;
2. the optimum filter K;
3. the updated covariance matrix obtained from 1. by the inclusion of data.

It is of particular interest in this study to evaluate the effect of the elements of Φ, the state transition matrix, on the elements of K. The importance of this investigation has been pointed out by D. Proctor; since the updated state vector is given by

$$\Delta\chi = K(y_c - y_o) = K\Delta y \tag{1}$$

where $\Delta\chi$ = state variable;

K = optimum filter;

y_c = calculated observation;

y_o = observation;

and since y_c is computed to high precision, it is reasonable to expect K to be calculated to the same precision as Δy. A program is described in this memorandum which calculates the sensitivity coefficients $\partial k_{ij}/\partial \phi_{rsm}$. This program will be employed in a computer study to determine to what precision the ϕ_{rsm} must be calculated so that the k_{ij} are sufficiently precise. These results will then be used in Task 2, Phase II of the Orbit Determination Program to decide the validity of two-body partial derivatives in computing the state transition matrix.

12.2 Calculation of

The optimum filter K is obtained from

$$K = P(t)M^T\left[MP(t)M^T + \bar{\epsilon}^2\right]^{-1} \tag{2}$$

where $P(t)$ = covariance matrix of the state variables at time t;

M = observation matrix relating the state variables and the observations;

$\bar{\epsilon}^2$ = matrix of observational errors.

The array $P(t)$ is given by

$$P(t) = \Phi(t,t_o)P(t_o)\ \Phi^T(t,t_o) \tag{3}$$

where $\Phi(t,t_o)$ = state transition matrix relating state variables at time t_o to state variables at time t;

$P(t_o)$ = covariance matrix of state variables at time t_o.

Letting $P(t_o) = P_o$ and substituting (3) into (2),

$$K = \Phi P_o \Phi^T M^T \left[M \Phi P_o \Phi^T M^T + \bar{\epsilon}^2\right]^{-1} \tag{4}$$

Postmultiplying (4):

$$K\left[M \Phi P_o \Phi^T M^T + \bar{\epsilon}^2\right] = \Phi P_o \Phi^T M^T \tag{5}$$

Then,

$$\frac{\partial K}{\partial \phi_{lm}} = (I-KM)\left\{\frac{\partial \Phi}{\partial \phi_{lm}} P_o \Phi^T + \Phi P_o \frac{\partial \Phi^T}{\partial \phi_{lm}}\right\} M^T \left[M \Phi P_o \Phi^T M^T + \bar{\epsilon}^2\right]^{-1} \tag{6}$$

or,

$$\frac{\partial K}{\partial \phi_{lm}} = (I-KM)\frac{\partial (\Phi P_o \Phi^T)}{\partial \phi_{lm}} \left(\Phi P_o \Phi^T\right)^{-1} K \tag{7}$$

Assuming that there are, in general, six state variables, and letting n be the number of observables at a data point, the matrices in (7) have the following orders:

K: 6Xn

M: nX6

P_o: 6X6

Φ: 6X6

$(I-KM)$: 6X6

It is the purpose of this program to evaluate $\partial k_{ij}/\partial \phi_{\ell m}$. Since the $\phi_{\ell m}$ are 36 in number, and since n may be as large as 4, the maximum number of partials is (36)X(6)X(4) = 864. The minimum number of partials occurs when n = 1: (36) X (6) X (1) = 216.

12.3 Evaluation of $\partial(\Phi P_o \Phi^T)/\partial \phi_{\ell m}$.

Partial derivatives of the matrix $\Phi P_o \Phi^T$ are composed of partials of the elements of Φ itself. Since we are here concerned with the evaluation of these partials at the time K is computed, we are interested in the change in the elements of $\Phi(t_r)$ arising from a change in $\phi_{\ell m}(t_r)$. It is evident, then, that

$$\left.\frac{\partial \phi_{ij}}{\partial \phi_{\ell m}}\right]_{t=t_r} = \delta_{i\ell}\,\delta_{jm} \tag{8}$$

In other words, the partial of an element with respect to itself is unity; the partial of an element with respect to any other element is zero. Rewriting Eq. (7),

$$\frac{\partial K}{\partial \phi_{\ell m}} = (I-KM)\left\{\frac{\partial \Phi}{\partial \phi_{\ell m}} P_o \Phi^T + \Phi P_o \frac{\partial \Phi^T}{\partial \phi_{\ell m}}\right\}(\Phi P_o \Phi^T)^{-1} K \tag{9}$$

To analyze the computation, let

$$(I-KM) = A\text{: } 6X6$$

$$P_o \Phi^T = Q\text{: } 6X6$$

$$\Phi P_o = R\text{: } 6X6$$

$$(\Phi P_o \Phi^T)K = B\text{: } 6Xn$$

Eq. (9) then becomes

$$\frac{\partial K}{\partial \phi_{\ell m}} = A\frac{\partial \Phi}{\partial \phi_{\ell m}} QB + AR\frac{\partial \Phi^T}{\partial \phi_{\ell m}} B \tag{10}$$

Again, let

$$QB = S\text{: } 6Xn$$

$$AR = T\text{: } 6X6$$

so that

$$\frac{\partial K}{\partial \phi_{\ell m}} = A\frac{\partial \Phi}{\partial \phi_{\ell m}} S + T\frac{\partial \Phi^T}{\partial \phi_{\ell m}} B \tag{11}$$

The matrix $\partial K/\partial \phi_{lm}$ is 6Xn. Considering the right side of (11), we will compute each term factor by factor. From the first term, the product $A\,\partial\Phi/\partial\phi_{lm}$ is a 6X6 matrix of the form

$$\begin{Bmatrix} a_{11} & a_{12} & a_{13} & a_{14} & a_{15} & a_{16} \\ a_{21} & \cdot & \cdot & \cdot & \cdot & \cdot \\ a_{31} & \cdot & \cdot & \cdot & \cdot & \cdot \\ a_{41} & \cdot & \cdot & \cdot & \cdot & \cdot \\ a_{51} & \cdot & \cdot & \cdot & \cdot & \cdot \\ a_{61} & \cdot & \cdot & \cdot & \cdot & \cdot \end{Bmatrix} \begin{Bmatrix} 0 & 0 & 0 & 0 & 0 & 0 \\ 0 & \cdot & \cdot & \cdot & \cdot & \cdot \\ 0 & \cdot & \cdot & 1 & \cdot & \cdot \\ 0 & \cdot & \cdot & \cdot & \cdot & \cdot \\ 0 & \cdot & \cdot & \cdot & \cdot & \cdot \\ 0 & \cdot & \cdot & \cdot & \cdot & \cdot \end{Bmatrix}$$

$$= \begin{Bmatrix} 0 & 0 & 0 & a_{1l} & 0 & 0 \\ 0 & \cdot & \cdot & a_{2l} & \cdot & \cdot \\ 0 & \cdot & \cdot & a_{3l} & \cdot & \cdot \\ 0 & \cdot & \cdot & a_{4l} & \cdot & \cdot \\ 0 & \cdot & \cdot & a_{5l} & \cdot & \cdot \\ 0 & \cdot & \cdot & a_{6l} & \cdot & \cdot \end{Bmatrix} = A \frac{\partial \Phi}{\partial \phi_{lm}} \qquad (12)$$

so that the product has non-zero elements a_{il} only in the m^{th} column. Postmultiplying (12) by S:

$$A \frac{\partial \Phi}{\partial \phi_{lm}} S = \begin{Bmatrix} a_{1l}\rho_{m1} & a_{1l}\rho_{m2} & \cdot & \cdot & a_{1l}\rho_{mn} \\ a_{2l}\rho_{m1} & a_{2l}\rho_{m2} & \cdot & \cdot & a_{2l}\rho_{mn} \\ \cdot & \cdot & \cdot & \cdot & \cdot \\ \cdot & \cdot & \cdot & \cdot & \cdot \\ a_{6l}\rho_{m1} & a_{6l}\rho_{m2} & \cdot & \cdot & a_{6l}\rho_{mn} \end{Bmatrix} \qquad (13)$$

Consequently, the typical term of (13) is $C_{ij} = a_{il}\rho_{mj}$ where $C = A \frac{\partial \Phi}{\partial \phi_{lm}} S$.

Turning now to the second term of (11), the product has the form

$$\begin{Bmatrix} t_{11} & t_{12} & t_{13} & t_{14} & t_{15} & t_{16} \\ t_{21} & \cdot & \cdot & \cdot & \cdot & \cdot \\ t_{31} & \cdot & \cdot & \cdot & \cdot & \cdot \\ t_{41} & \cdot & \cdot & \cdot & \cdot & \cdot \\ t_{51} & \cdot & \cdot & \cdot & \cdot & \cdot \\ t_{61} & \cdot & \cdot & \cdot & \cdot & \cdot \end{Bmatrix} \begin{Bmatrix} 0 & 0 & 0 & 0 & 0 & 0 \\ 0 & \cdot & \cdot & \cdot & \cdot & \cdot \\ 0 & \cdot & \cdot & \cdot & \cdot & \cdot \\ 0 & \cdot & 1 & \cdot & \cdot & \cdot \\ 0 & \cdot & \cdot & \cdot & \cdot & \cdot \\ 0 & \cdot & \cdot & \cdot & \cdot & \cdot \end{Bmatrix}$$

$$\begin{Bmatrix} 0 & 0 & t_{1m} & 0 & 0 & 0 \\ 0 & \cdot & t_{2m} & \cdot & \cdot & \cdot \\ 0 & \cdot & t_{3m} & \cdot & \cdot & \cdot \\ 0 & \cdot & t_{4m} & \cdot & \cdot & \cdot \\ 0 & \cdot & t_{5m} & \cdot & \cdot & \cdot \\ 0 & \cdot & t_{6m} & \cdot & \cdot & \cdot \end{Bmatrix} = T \frac{\partial \Phi^T}{\partial \phi_{lm}} \qquad (14)$$

so that the product has now-zero elements t_{im} only in the l^{th} column. Postmultiplying (14) by B:

$$\frac{T \partial \Phi^T}{\partial \phi_{lm}} B = \begin{Bmatrix} t_{1m} b_{l1} & t_{1m} b_{l2} & \cdot & \cdot & t_{1m} b_{lm} \\ t_{2m} b_{l1} & t_{2m} b_{l2} & \cdot & \cdot & t_{2m} b_{lm} \\ \cdot & \cdot & \cdot & \cdot & \cdot \\ \cdot & \cdot & \cdot & \cdot & \cdot \\ t_{6m} b_{l1} & t_{6m} b_{l2} & \cdot & \cdot & t_{6m} b_{lm} \end{Bmatrix} \qquad (15)$$

The typical term of (15) is $d_{ij} = t_{im} b_{lj}$ where $D = T \frac{\partial \Phi^T}{\partial \phi_{lm}} B$.

Combining (13) and (15),

$$\frac{\partial K}{\partial \phi_{lm}} = C + D = G \qquad (16)$$

so that

$$\frac{\partial k_{ij}}{\partial \phi_{lm}} = g_{ij} = a_{il} \rho_{mj} + t_{im} b_{lj} \qquad (17)$$

12.4 Programming Procedures

In order to compute Eq. (17), a program must be available to provide the elements of the following matrices: K, M, P_o, and Φ. Having these matrices available, the following operations are performed:

1. Form the product KM: (6X6)
2. Take the difference A = (I-KM): (6X6)
3. Form the product $Q = P_o \Phi^T$: (6X6)
4. Form the product $R = \Phi P_o$: (6X6)
5. Form the product $\Phi P_o \Phi^T = \Phi Q$: (6X6)
6. Take the inverse $(\Phi P_o \Phi^T)^{-1}$: (6X6)
7. Form the product $B = (\Phi P_o \Phi^T)^{-1} K$: (6Xn)
8. Form the product S = QB: (6Xn)
9. Form the product T = AR: (6X6)
10. From the elements of A & S, construct C such that $c_{ij} = a_{il} \rho_{mj}$ for specified l & m.
11. From the elements of B & T, construct D such that $d_{ij} = t_{im} b_{lj}$ for specified l & m.
12. From the elements of C & D, construct G such that $g_{ij} = c_{ij} + d_{ij}$.

As noted previously, there are 864 g_{ij}'s if n = 4, & 216 g_{ij}'s if n = 1. The subscripts l & m range from 1 to 6 in all combinations.

12.5 Application to Variational Parameters

In order to evaluate the precision of the variational parameters used in the MINIVAR Program, recourse may be had to two procedures:

1. Analytically convert the variational parameters to elements of the state transition matrix and proceed as described above;

2. Develop corresponding equations for the parameters and investigate the effect of the variational elements on L.

For the second alternative, one may take advantage of the symmetry existing between the formulations for K & L:

$$\Delta\alpha = L\,\Delta\gamma \tag{18}$$

$$L = \Omega Q_0 \Omega^T N^T \left[N \Omega Q_0 \Omega^T N^T + \bar{E}^2 \right]^{-1} \tag{19}$$

Consequently, the matrix of partials becomes

$$\frac{\partial L}{\partial \omega_{lm}} = (I - LN) \frac{\partial (\Omega Q_0 \Omega^T)}{\partial \omega_{lm}} \left(\Omega Q_0 \Omega^T \right)^{-1} \tag{20}$$

0-20-10

Same SA

~~13.0.~~ EXECUTIVE ROUTINE

C. Milner Limited Minimum --- 8 Nov. 1963

(2) P124-125 ref (See N64-18226 10-01) OTS date

Implementation of the Executive Routine (XR) on the 7094 under IBFTC system is hampered by certain system restrictions. Among these restrictions are:

1. SYSIN1 cannot be rewound or written on during execution.

2. Files cannot be written or read in mixed mode. This restriction prevents the generation of a mixed mode file of BCD control cards and binary text.

3. Handling of a mixed mode file utilizing IOCS MAP subroutines requires standard look-ahead characters for successful processing.

13.1 Alternate Executive Routine

13.1.1 Utilization of History Tape

The BCD program decks and compiled binary versions will be maintained on a history tape. The executive routine will be in three parts as follows:

Part 1 controls reading-in of control cards, additions, and deletion for the run. This part reads in control cards for future processing, updates the programs to be compiled onto SYSIN1 and loads onto SYSIN1 parts 2 and 3 of the XR. Control is then transferred back to IBJOB and compilation of source programs proceeds.

Part 2 executes after compilation of changes is complete. The compiled binary output on SYSPP1 and altered source programs are updated onto the history tape. Part 3 of the XR is now executed.

Part 3 reads run parameters and assembles the object programs required on the SYSIN1. IBJOB loads and executes the program.

The history tape procedure will require MAP subroutines utilizing IOCS to form the mixed-mode tape SYSIN1 and to convert the binary tape SYSPP1 to mixed BCD-binary form with correct look-ahead characters. All manipulations of SYSIN1 will be controlled by IOCS MAPS subroutines.

13.1.2 Library Tape Procedure.

This procedure will require definition of SYSLB2 tape to contain library routines exclusively. All routines to be utilized in the program will be maintained on SYSLB2 via the Librarian function included in IBSYS.

13.1.2.1 Library Tape Procedure 1.

This procedure will require all programs to be updated into SYSLB2 to be on SYSIN1 in binary compiled form. The library tape SYSLB2 is updated via the librarian routine in IBSYS utilizing replace, insert and delete control cards.

Execution of the program is governed by control cards on SYSIN1 as a separate run. $OEDIT options utilizing alternate drive feature will be used.

No MAP-coded routines are required but the user must specify via correct control cards the routines to be loaded at object time.

13.1.2.2 Library Tape Procedure 2.

The XR routine in this implementation will accept source programs and control cards for object time execution and generate the required binary images on SYSIN1 after IBFTC compiles them.

This procedure would require IOCS MAP subroutines to write SYSPP1 onto SYSIN1 in proper format for the librarian.

The alternatives presented thus far are based on a limited knowledge of the IBSYS-IBJOB monitor system. Information is being sought concerning IBSYS system usage and system modifications affecting implementing of these schemes.

0-22-11

Same CA

N64-18239

~~14.0~~ (THE OBLATENESS COEFFICIENTS)

D. W. PROCTOR Smithsonian Minimum --- 8 Nov. 1963

P 126-130 refs (See N64-18226 10-01) offsite

The following notes relate to the assignment of values to the second, third, and fourth harmonics of the earth's potential. It is hoped that these notes will provide the basis for a more accurate orbit determination program.

14.1 Comparison of Kaula's Representation and Minivar

The recommended notation of the earth potential, as given by Kaula (Ref. 1) is

$$U = \frac{\mu}{r}\left[1 + \sum_{n=1}^{\infty}\sum_{m=0}^{n}\left(\frac{R}{r}\right)^n P_n^m(\sin\beta)\left(C_{n,m}\cos m\lambda + S_{n,m}\sin m\lambda\right)\right]$$

where

μ = GM

r = distance from the earth center

R is the mean equatorial earth radius

$P_n^m(\sin\beta)$ is the Legendre Polynominal with argument $(\sin\beta)$

β is the latitude

λ is the longitude

n, m are the zonal and sectoral harmonic under consideration

Since here we are only concerned with zonal harmonics and the oblate component of the potential, the above expression can be reduced by letting $m = 0$, using only the harmonic terms, and letting the distance units be in earth radii:

$$U_{ob} = \frac{\mu}{r}\left[\sum_{n=1}^{\infty}\left(\frac{1}{r}\right)^n P_n^0(\sin\beta)\, C_{n,0}\right]$$

Further, Kaula recommends that when $n = 0$, let $C_{n,m} = -J_n$.

Thus

$$U_{ob} = -\frac{\mu}{r}\left[\frac{J_1}{r} P_1^0(\sin\beta) + \frac{J_2}{r^2} P_2^0(\sin\beta) + \frac{J_3}{r^3} P_3^0(\sin\beta) + \frac{J_4}{r^4} P_4^0(\sin\beta) + \dots\right]$$

$$= -\frac{\mu}{r}\left[\frac{J_1}{r}\cos\beta + \frac{J_2}{r^2}\left(\frac{3}{2}\sin^2\beta - \frac{1}{2}\right) + \frac{J_3}{r^3}\left(\frac{5}{2}\sin^2\beta - \frac{3}{2}\sin\beta\right) + \frac{J_4}{r^4}\left(\frac{35}{8}\sin^4\beta - \frac{15}{4}\sin^2\beta + \frac{3}{8}\right) + \dots\right]$$

But J_1 is zero, and $\sin\beta = z/r$,

so that

$$U_{ob} = -\frac{\mu}{r}\left[\frac{J_2}{r^2}\left(\frac{3}{2}\left(\frac{z}{r}\right)^2 - \frac{1}{2}\right) + \frac{J_3}{r^3}\left(\frac{5}{2}\left(\frac{z}{r}\right)^3 - \frac{3}{2}\left(\frac{z}{r}\right)\right) + \frac{J_4}{r^4}\left(\frac{35}{8}\left(\frac{z}{r}\right)^4 - \frac{15}{4}\left(\frac{z}{r}\right)^2 + \frac{3}{8}\right) + \dots\right]$$

This notation agrees with that given by the MINIVAR manual (ref 2) page XII-27, except that MINIVAR uses the Jno notation, rather than the Jn notation. However, the two are equivalent.

Since Kaula's representative equation for the potential is in full agreement with that given in the MINIVAR manual and program, the coefficients should also agree. A comparison of Kaula's values of J_2, J_3, and J_4 with that of MINIVAR

(Ref 2, page XII-27) shows exact agreements except for the sign of J_4 term.

14.2 Comparison with J.P.L.

The program of J.P.L. (ref. 2), uses the symbols J, H, and D for the second, third and fourth harmonics, respectively. The oblate potential is given by

$$U = \frac{\mu}{R}\left[\frac{Ja^2}{3R^2}\left(1-3\sin^2\phi\right) + \frac{Ha^3}{5R^3}\left(3-5\sin^2\phi\right)\sin\phi + \frac{Da^4}{35R^4}\left(3-30\sin^2\phi+35\sin^4\phi\right)+\ldots\right]$$

By properly manipulating the J.P.L. equation, and letting $a=1$, $\sin\phi = z/r$, $R=r$,

$$U = -\frac{\mu}{r}\left[\frac{2J}{3r^2}\left(\frac{3}{2}\left(\frac{z}{r}\right)^2-\frac{1}{2}\right) + \frac{2H}{5r^3}\left(\frac{5}{2}\left(\frac{z}{r}\right)^2-\frac{3}{2}\right)\left(\frac{z}{r}\right) + \frac{(-8D)}{35r^4}\left(\frac{3}{8}-\frac{15}{4}\left(\frac{z}{r}\right)^2+\frac{35}{8}\left(\frac{z}{r}\right)^4\right)+\ldots\right]$$

Equating MINIVAR & Kaula's representation of the potential with J.P.L.'s,

$$J_{20} = \frac{2}{3}J$$

$$J_{30} = \frac{2}{5}H$$

$$J_{40} = -\frac{8}{35}D$$

These equalities agree with standard procedures. The values for J, H, and D used by J.P.L. are

$$J = +1.62345 \times 10^{-3}$$

$$H = -.575 \times 10^{-5}$$

$$D = +.7875 \times 10^{-5}$$

Therefore, using J.P.L.'s notation and finding the equivalent values of J_{20}, J_{30} and J_{40}:

$$J_{20} = +1.08230 \times 10^{-3}$$

$$J_{30} = -.230 \times 10^{-5}$$

$$J_{40} = -1.800 \times 10^{-6}$$

These numbers agree precisely with the values of J_2, J_3 and J_4 given by Kaula (Ref. 1, pps 2 and 4):

$$J_2 = +1082.30 \times 10^{-6}$$

$$J_3 = -2.3 \times 10^{-6}$$

$$J_4 = -1.8 \times 10^{-6}$$

Thus, it would appear that the J.P.L. program and MINIVAR agree in definitions of the constants, agree precisely in magnitude, but disagree in that the sign of J40, given on page XII-27 of the MINIVAR Manual, should be negative rather than positive to be consistent with J.P.L. This also agrees with the comparison with Kaula, given in the preceding section.

Thus, the printed value of CONKR from MINIVAR would be $+.1343886 \times 10^{-3}$, rather than the negative of this value, since CONKR = $-\frac{15}{4} J_{40}$ (Ref 2 p.XII-28).

14.3 Comparison with ITEM

According to the ITEM Manual and the program listing, the ITEM input quantities are

Second Harmonic = μJ = $19.9 \times 1623 \times 10^{-6} = .03229$

Third Harmonic = μJ_{30} = $19.9 \times -2.30 \times 10^{-6} = -.4577 \times 10^{-4}$

Fourth Harmonic = $-\frac{1}{2}\mu K = \frac{19.9}{2} \times 6.75 \times 10^{-6} = -.6665 \times 10^{-4}$

Numerical values of J, J_{30} have been selected here and K derived from Kaula and others. The quantities in the right hand side of the equalities are roughly in agreement in magnitude and exactly in sign with the print-outs from the ITEM program.

14.4 Conclusions

1. The second harmonic term is correct in both ITEM and MINIVAR and agrees with standard practice.

2. The third harmonic term is correct in both programs; the difference in print-out being explained by ITEM's use of $A_{30} = \mu J_{30}$ (see ITEM program listing) and MINIVAR's (CONAR) which is $-\mu J_{30}$ (see pages XII-28 of the MINIVAR manual).

3. The fourth harmonic term is correct in ITEM, but has the wrong sign in MINIVAR. That is, J_{40} on page XII-27 of the MINIVAR manual should read -1.8×10^{-6}, thereby agreeing with the ITEM program and the work of Kaula and others.

Ref 1: "A Review of Geodetic Parameters", W. M. Kaula, NASA TN D-1847, Goddard Space Flight Center, 1963.

Ref 2: "Program Manual for Minimum Variance Precision Tracking and Orbit Prediction Program", D. S. Woolston and John Mohan, Goddard Space Flight Center, X-640-63-144, July 2, 1963.

Ref 3: "Space Trajectories Program for the IBM 7090 Computer", D. B. Holdridge, J.P.L. TR No. 32-223, March 2, 1962.

0-08-10

Same as

N64-18240

15.0. PROPAGATION CORRECTION

A. CRISTINA

15.1. Introduction

The bending of radio waves passing through the troposphere and ionosphere limits the inherent precision of modern electronic tracking systems. Some form of refraction correction is therefore necessary to achieve the maximum accuracy of our satellite tracking systems.

Correction of the troposphere error can be approached from two points of view. The first, the analytical method, involves assuming a simple expotential decay of the index of refraction with altitude. The resulting tropospheric errors for range and elevation are soluable in closed form as a function of the elevation angle.

The second method is numerical in form. For this method, it is not necessary to assume an exponentially decaying troposphere; any model will suffice. The error is determined by numerically integrating over the total propagation path with the index of refraction at each integration point being determined by the assumed model.

Because of the complex nature of the ionosphere, it is very difficult to find a simple model upon which analytic solutions to the ionospheric errors can be based. Therefore, a numerical approach seems to be more likely for an ionospheric analysis.

A further refinement to this program may be that the refraction correction will be made dependent on the predicted elevation angle rather than the measured elevation angle, and, since the predicted angle is subject to an error, a test is made on the variance of this predicted angle. If this variance is above a present limit, the computer will make one iteration to include the data point to get a better estimate of the elevation angle before making the final correction.

The refraction correction is then based upon this new elevation angle and it is the results of this second iteration which will be processed by the minimum variance system.

15.2. Method of Attack

The method that will be used is one derived by S. Weisbrod as detailed in Reference 1. The method is particularly simple and can be applied to both tropospheric and ionospheric bending. There are no limitations on the shape of the profile or angle of elevation. The only assumptions are that the index of refraction gradient is only in the vertical plane, that the index of refraction profile can be approximated by a number of linear segments and that the thickness of these steps is small compared to earth's radius. These assumptions are readily justifiable in all practical cases. In addition to refractive bending, the problem of signal retardation, resulting in range error, is considered. Also, the effect of refractive bending on range rate measurements is included.

15.3. Index of Refraction Models Used

15.3.1. General

Since it would be an overwhelming task to analyze completely atmospheric propagational effects under all parametric conditions, atmospheric models representative of average conditions are employed to simplify the computational problem.

In the models that are used, the following assumptions are made: 1) The troposphere extends to approximately 40 km with refractivity decreasing with height; 2) The region between the end of the troposphere and the beginning of the ionosphere is assumed to have zero refractivity; 3) The ionosphere lies between h and 2000 km; 4) Beyond 2000 km the refractivity is zero.

With few exceptions, the formulai used to compute range and elevation errors are the same for both the troposphere and ionosphere. The refractivity, however, is computed differently.

This approach results in answers which are as accurate as the models assumed. Since profiles of refractive index in the atmosphere (especially for the ionosphere) are not precisely known under all conditions a more exact solution seems unwarranted at this time.

15.3.2. Tropospheric Model

In this analysis, the tropospheric model will be assumed as an exponential, with the ground index of refraction and the scale height as parameters.

The equation for this model is

$$N = N_o e^{-h/H} \qquad (1)$$

where N_o = 313 (refractivity at sea level)
H = 7 km (height scale factor)
h = height above the earth
N = (n-1) x 10^6, where n is the index of refraction

15.3.3. Ionospheric Model

15.3.3.1. Ionospheric Parameters

In the ionosphere, the index of refraction is dependent on more parameters than those considered in the troposphere. As a minimum, the index of refraction in the ionosphere is dependent upon the height of the base of the ionosphere layer, the height of the maximum electronic density of the F2 layer, and the maximum electronic density of the F2 layer. In addition, the index of refraction in the ionosphere is also dependent upon diurnal, solar activity, seasonal, geographical, and daily variations as well as other miscellaneous sporatic variations. Also, unlike the troposphere, the refraction errors in the ionosphere are frequency dependent.

15.3.3.2. Electron Density Profile

In the ionosphere, the relationship between the index of refraction, the radii frequency and the electron density in the ionosphere is the following:

$$\eta = \left[1 - \frac{\rho_e e^2}{\epsilon_0 m \omega^2} \right]^{1/2} \qquad (2)$$

where ρ_e = electrons per cubic meter
e = electronic charge (1.60×10^{-19}
m = electronic mass (9.08×10^{-31} kilogram
ω = 2π times the frequency
ϵ_0 = permittivity of free space (8.854×10^{-12}

Using the first two terms of the binomial expansion and substituting the above constants, the formula for index of refraction reduces to

$$\eta \simeq 1 - \frac{40.3}{f^2} \rho_e \qquad (3)$$

This formula holds for frequencies above the critical frequency, fc, which is given by the following relationship

$$f_c = 8.97 \rho_0^{1/2} \times 10^{-6} \quad \text{megacycles per second} \qquad (4)$$

Defining the refractivity by the following relation:

$$N = (n-1)10^6 \qquad (5)$$

equation (3) can be written as follows

$$N = -4.03 \left(\frac{\rho_e}{f^2} \right) \times 10^{-5} \qquad (6)$$

The model selected for electron density versus height in the ionosphere consists of a parabolic variation below the height of maximum electron density matched to a hyperbolic secant profile above the maximum. The relationships are as follows:

$$\begin{aligned} \rho_e &= \rho_0 [1 - (1-\sigma)^2] \qquad 0 \le \sigma \le 1 \\ &= \rho_0 \operatorname{sech} \frac{\pi}{4} (\sigma - 1) \qquad \sigma \ge 1 \end{aligned} \qquad (7)$$

where ρ_e = electron density per cubic meter
ρ_0 = maximum density
$\sigma = \frac{h - h_0}{h_m - h_0}$
h = height above the ground
h_0 = height of the base of the layer
h_m = height of the maximum electron density

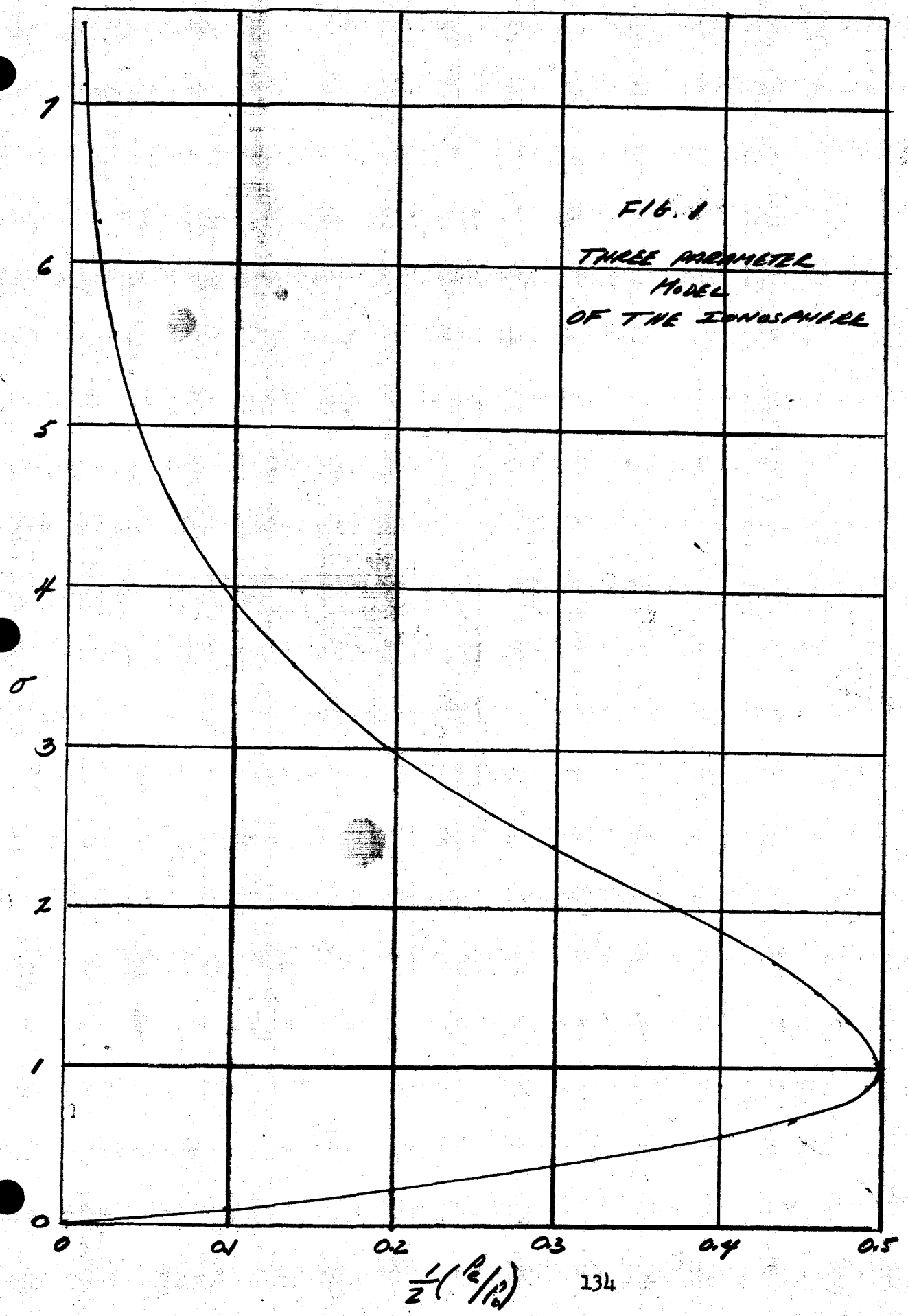

FIG. 1
THREE PARAMETER
MODEL
OF THE IONOSPHERE

This model has the following desirable characteristics.

1. The model has three degrees of freedom (h_o, h_m, and ρ_o) which can be obtained from ionogram data. These parameters uniquely specify the entire distribution.

2. The distribution is parabolic below the maximum density, nearly parabolic immediately above the maximum, and exponential at great heights.

3. The electron content of the distribution above the maximum is three times that below it.

4. The entire electron density profile and its derivatives are continuous everywhere.

Figure 1 is a plot of the ionosphere model normalized with respect to σ and 1/2 (ρ/ρ_o). The h_o, h_m, and B parameter refer to the F layer. Using this model, the refractive effects of the D and E layer are not singled out, because they are quite small in comparison with those due to the F layer and are approximately accounted for by allowing the electron density at the bottom edge of the F layer to be zero.

15.4. Development of the Method

15.4.1. Computation of Ray Bending

Referring to Fig. 2, consider a ray entering at angle β an infinitesimal layer of thickness $d\rho$. Since the curvature of the ray is equal to the component of the refractive gradient normal to the ray, divided by the index of refraction, it follows that:

$$\frac{1}{K} = \frac{1}{n}\frac{dn}{d\rho}\cos\beta \tag{8}$$

where K is the radius of curvature.

The length of the ray path in the layer is

$$K\,d\gamma = \cos\beta\, d\rho \tag{9}$$

which, combined with (8), gives

$$d\gamma = \frac{1}{n}\frac{dn}{d\rho}\cot\beta\, d\rho \tag{10}$$

Since $d\gamma$'s of all elementary layers are directly additive, as shown in Fig. 2, by considering $d\gamma'$ due to bending between points Q and R, it follows that the contribution to the total bending γ, due to a layer bounded by the heights ρ_j and ρ_k is

$$\gamma_{jk} = \int_{\rho_j}^{\rho_k} \frac{1}{n}\frac{dn}{d\rho}\cot\beta\, d\rho \tag{11}$$

If the ray departs from the earth's surface with the elevation angle of θ_0 Snell's Law for spherical stratification states:

$$n_0 a \cos\theta_0 = n\rho\cos\beta = \text{constant} \qquad (12)$$

where

n_0 = surface index of refraction,
a = Earth's radius
ρ = $a + h$
h = height above earth,
n = index of refraction at the specified height.

From (12) we get

$$\cos\beta = (n_0 a/n\rho)\cos\theta_0 = (n_j\rho_j/n\rho)\cos\beta_j \qquad (13)$$

$$\sin\beta = (n_0 a/n\rho)[(n\rho/n_0 a)^2 - \cos^2\theta_0]^{1/2}$$

$$= (n_j\rho_j/n\rho)[(n\rho/n_j\rho_j)^2 - \cos^2\beta_j]^{1/2} \qquad (14)$$

$$\cot\beta = [(n\rho/n_0 a)^2 - \cos^2\theta_0]^{-1/2}\cos\theta_0$$

$$= [(n\rho/n_j\rho_j)^2 - \cos^2\beta_j]^{-1/2}\cos\beta_j \qquad (15)$$

where n, p and β are the values of these parameters at some height h.

Eq. (15) can be substituted in (11) to give the general equation for refractive bending

$$\gamma_{jk} = \int_{\rho_j}^{\rho_k} \frac{1}{n}\frac{dn}{d\rho}\frac{\cos\theta_0}{[(n\rho/n_0 a)^2 - \cos^2\beta_j]^{1/2}}\,d\rho$$

$$= \int_{\rho_j}^{\rho_k} \frac{1}{n}\frac{dn}{d\rho}\frac{\cos\beta_j}{[(n\rho/n_j\rho_j)^2 - \cos^2\beta_j]^{1/2}}\,d\rho \qquad (16)$$

We now assume that a) $dn/dp = -k$ = constant, b) $\rho_k - \rho_j \ll \rho_j$ and c) index of refraction n is very nearly equal to unity. On the basis of these assumptions we can write:

$$k = \frac{(N_j - N_k)\times 10^{-6}}{\rho_k - \rho_j} = \frac{(N_j - N)\times 10^{-6}}{\rho - \rho_j} \qquad (17)$$

where

$$N = (n-1)10^6$$

$$(n\rho/n_j\rho_j)^2 = \{[1 - (N_j - N)10^{-6}][1 + (\rho - \rho_j)/\rho_j]\}^2$$

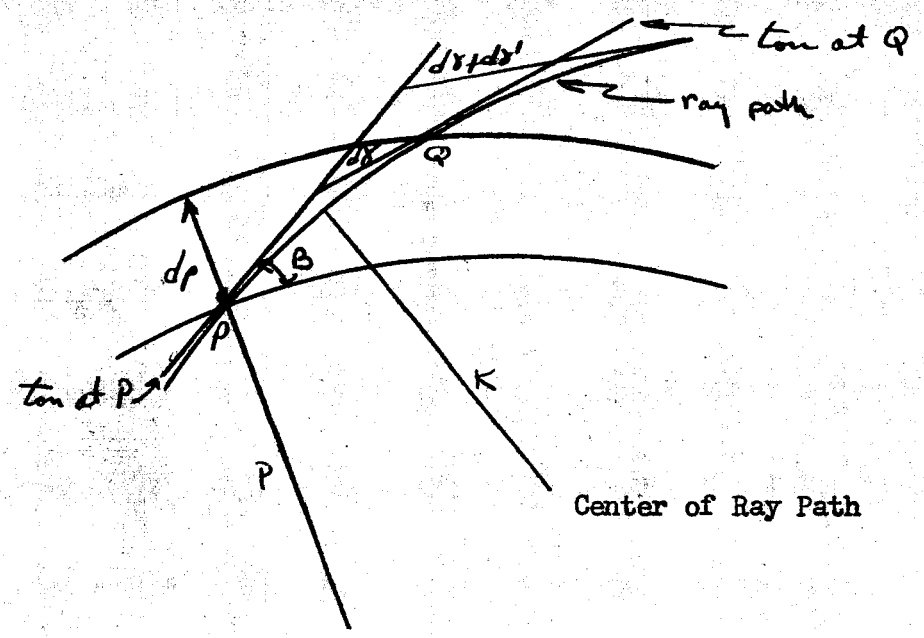

Fig. 2 Geometry of Bending Through an Infinitesimal Layer

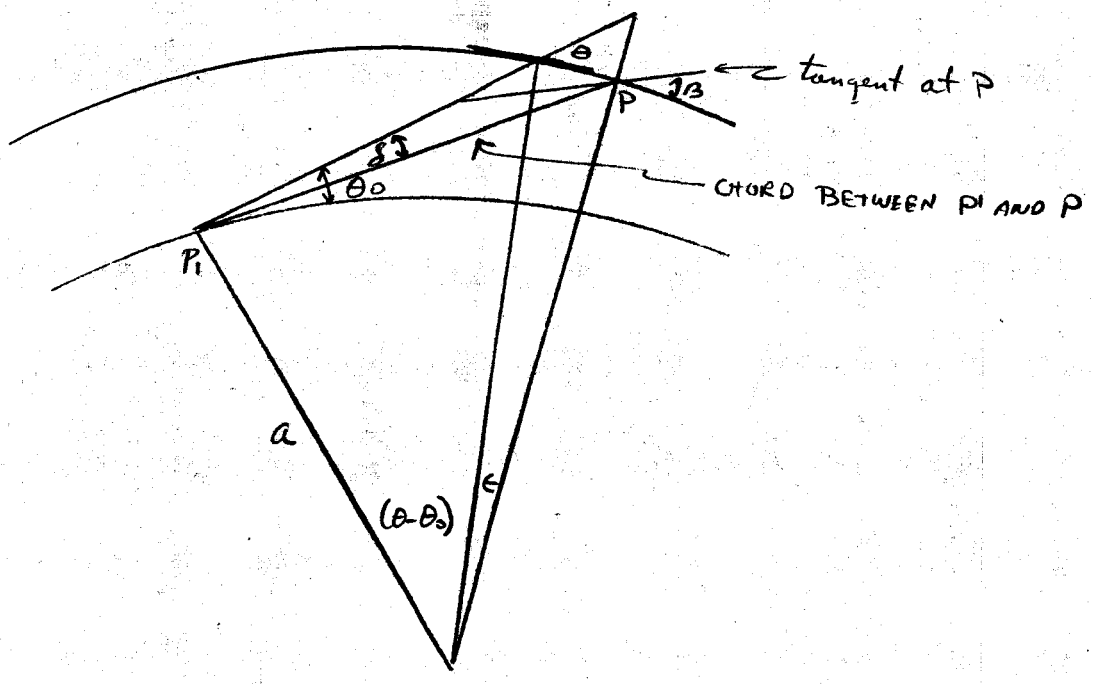

Fig. 3 Geometry of Bending Through a Refrnetive Layer -

$$(n\rho/n_j\rho_j)^2 \cong 1 + 2(\rho-\rho_j)(1-k\rho_j)/\rho_j \qquad (18)$$

and, substituting in (16) we get

$$\gamma_{jk} = k\cos B_j \int_{\rho_j}^{\rho_k} \left[\sin^2 B_j + 2(\rho-\rho_j)(1-k\rho_j)/\rho_j\right]^{-1/2} d\rho$$

$$= \frac{k\rho_j \cos B_j}{1-k\rho_j}\left\{\left[\sin^2 B_j + 2(\rho_k-\rho_j)(1-k\rho_j)/\rho_j\right]^{1/2} - \sin B_j\right\} \qquad (19)$$

From (15), (16), and (18)

$$\sin B_k = (n_j\rho_j/n_k\rho_k)\left[(n_k\rho_k/n_j\rho_j)^2 - \cos^2 B_j\right]^{1/2} \qquad (20)$$

$$= \frac{\cos B_k}{\cos B_j}\left[\sin^2 B_j + 2(\rho_k-\rho_j)(1-k\rho_j)/\rho_j\right]^{1/2}$$

Combining with (19)

$$\gamma_{jk} = \frac{k\rho_j \cos^2 B_j}{1-k\rho_j}(\tan B_k - \tan B_j) \qquad (21)$$

From (15), (17), and (18)

$$\frac{k\rho_j}{1-k\rho_j} = \frac{2(N_j-N_k)10^{-6}\sec^2 B_j}{\sec^2 B_k - \sec^2 B_j}$$

$$= \frac{2(N_j-N_k)10^{-6}\sec^2 B_j}{\tan^2 B_k - \tan^2 B_j} \qquad (22)$$

which, substituted in (21), gives the desired expression for

$$\gamma_{jk} = \frac{(N_j-N_k)10^{-6}}{\frac{1}{2}(\tan B_j + \tan B_k)}$$

$$= \frac{N_j-N_k}{500(\tan B_j + \tan B_k)} \text{ milliradions} \qquad (23)$$

where N is expressed in N units $(n - 1) \times 10^6$.

Total bending through the atmosphere is simply the sum of individual contributions.

$$\gamma(mr) = \sum_{i=1}^{m_h} \frac{(N_{i-1} - N_i)}{500(\tan B_{i-1} + \tan B_i)} \tag{24}$$

It is frequently convenient to measure the refractive error in terms of the angle subtended from the earth's center. This quantity, denoted by ϵ, can be readily obtained from Fig. 3.

$$\epsilon = \gamma - (\theta - B) \tag{25}$$

The quantity $(\theta - B)$ may be conveniently found in the following manner. From Snell's law we have

$$n_0 \cos\theta = n \cos B$$

or

$$\cos B = \cos[\theta - (\theta - B)]$$
$$= [1 + (N_0 - N)10^{-6}] \cos\theta \tag{26a}$$

$$\cos\theta = \cos[B + (\theta - B)]$$
$$= [1 - (N_0 - N)10^{-6}] \cos B \tag{26b}$$

Expansion of (26) and the application of small angle approximations results in

$$(\theta - B) = \{1 - [1 - 2(N_0 - N)10^{-6}\cot^2\theta]^{1/2}\}\tan\theta \tag{27a}$$
$$= \{[1 + 2(N_0 - N)10^{-6}\cot^2 B]^{1/2} - 1\}\tan B \tag{27b}$$

At heights above the troposphere for rays departing tangentially, or for angles of elevation greater than 100 milliradians at any height, θ and B are very nearly equal and (27) reduces to:

$$(\theta - B) \cong (N_0 - N)10^{-6}\cot\theta \tag{28}$$
$$\cong (N_0 - N)10^{-6}\cot B$$

15.4.2. Computation of Errors or Principal Measurements

15.4.2.1. Elevation Angle Error

In most practical applications the quantity of greatest interest is the elevation angle error. This quantity denoted by δ can be obtained from Fig. 3 by the use of the law of sines.

$$a \cos\theta_0 = \rho \cos\theta$$
$$a \cos(\theta_0 - \delta) = \rho \cos[(\theta + \epsilon) - \delta] \tag{29}$$

From (29) we get

$$\tan\delta = \frac{\sin\epsilon \tan\theta + (1 - \cos\epsilon)}{\sin\epsilon + \cos\epsilon \tan\theta - \tan\theta_0}$$

or

$$\delta = \frac{\epsilon \tan\theta + \epsilon^2/2}{\epsilon + \tan\theta - \tan\theta_0} \tag{30}$$

Omitting $\epsilon^2/2$ in the numerator of (30) results in an error of about five per cent in the troposphere for a tangentially departing ray. At higher angles of elevation or greater heights, this error becomes negligible.

It should be noted that whereas γ and ϵ, due to the passage of the ray through various layers, are directly additive, δ's are not. Thus, to evaluate δ at ionospheric heights or above, it is first necessary to combine the tropospheric and the ionospheric ϵ's or δ's and then use (30) or (31). However, it turns out that in nearly all practical cases above the troposphere $\epsilon^2/2 \ll \epsilon$ and $\epsilon \ll (\tan\theta - \tan\theta_0)$; consequently the omission of $\epsilon^2/2$ in the numerator and ϵ in the denominator usually results in less than five percent error at F region heights.

Eq. (30) may thus be approximated by

$$\delta = \frac{\epsilon \tan\theta}{\tan\theta - \tan\theta_0}$$

It is, therefore, usually justifiable to add directly the tropospheric and ionospheric δ's to obtain the total elevation angle error.

At astronomical distances all three quantities (γ, ϵ and δ) become numerically equal.

15.4.2.2. Retardation of the Signal Passing Through a Region of a Constant Refractive Gradient

Signal retardation $d\tau$ caused by a layer of thickness dp (Fig. 2) is given by

$$d\tau = \left(\frac{1}{v} - \frac{1}{c}\right) \csc B \, dp$$
$$= (c/v - 1) \csc B \, dp/c = N \times 10^{-6} c^{-1} \csc B \, dp \qquad (31)$$

where c and v are signal velocities in free space and the medium, respectively.

The range error is given by

$$\Delta r_{jk} = \int_{p_j}^{p_k} c \, d\tau = \int_{p_j}^{p_k} \frac{N \times 10^{-6} \, dp}{\sin B} \qquad (32)$$

In evaluating we found (23)

$$\gamma_{jk} = \int_{p_j}^{p_k} \frac{(dn/dp)dp}{\tan B} = \int_{p_j}^{p_k} \frac{dn}{\tan B} = \frac{(N_j - N_k) \times 10^{-6}}{\frac{1}{2}(\tan B_j + \tan B_k)} \qquad (33)$$

In other words, the value of the integral for the case of a constant radial gradient was found to be very nearly equal to the one that would have been obtained had we taken the average value of the denominator of the integrand and treated it as a constant. We are therefore tempted to treat the integral of (32) in a similar manner. Furthermore, we can argue that at low angles sine and tangent are nearly the same and at high angles the rate of change of sin is so slow that such procedure is certainly justifiable.

Thus we evaluate (32) by setting

$$\Delta r_{jk} = \int_{p_j}^{p_k} \frac{N \times 10^{-6}}{\sin B} dp = \frac{2 \times 10^{-6}}{\sin B_j + \sin B_k} \int_{p_j}^{p_k} N \, dp$$

but from (17)

$$\int_{p_j}^{p_k} N \, dp = \int_{p_j}^{p_k} \left[N_j - k(p - p_j) \right] dp$$

$$= N_j (p_k - p_j) - \frac{1}{2}(N_j - N_k)(p_k - p_j)$$

$$= \frac{1}{2} (N_j + N_k)(p_k - p_j)$$

Substituting in (32) we get

$$\Delta r_{jk} = \frac{(N_k - N_j)(P_k - P_j) \times 10^{-6}}{\sin B_k + \sin B_j} \qquad (34)$$

To compute retardation for a double passage through the layer, (34) must be doubled. The resulting final formula for Δr is:

$$\Delta r = \frac{2}{10^3} \sum_{i=1}^{m_1} \frac{|N_{i-1} + N_i|(h_i - h_{i-1})}{\sin B_{i-1} + \sin B_i} \quad \text{meters} \qquad (35)$$

In the ionosphere the formula for range propagation error is

$$\Delta r = \frac{1 + \left(\frac{f_2}{f_1}\right)^2}{10^6} \sum_{i=1}^{m} \frac{|N_{i-1} + N_i|(h_i - h_{i-1})}{\sin \theta_{i-1} + \sin \theta_i} \qquad (36)$$

where f_1 = up frequency

f_2 = down frequency

15.4.2.3 Doppler Error

Due to the refractive bending, there will generally be an error in the measurement of the radial component of the target velocity. The equation describing this can be readily derived with the aid of Fig. 3.

Let

$\underline{R}$ = station location vector in inertial coordinator

$\underline{r}$ = position venctor from earth's center to satellite in inertial coordinator

$\underline{\rho}'$ = position vector from station to satellite in inertial coordinator

$\underline{\rho}$ = position vector from station to satellite in topocentric local moving coordinates

$\underline{\Omega}$ = earth's rotation velocity vector in inertial coordinates

A = Coordinate Conversion transformation matrix

$\underline{i}', \underline{j}', \underline{k}'$ = Unit vectors, inertial coordinate system

$\underline{i}, \underline{j}, \underline{k}$ = Unit vectors, topocentric moving coordinate system

Therefore

$$\underline{r} = X\underline{i}' + Y\underline{j}' + Z\underline{k}'$$

$$\dot{\underline{r}} = \dot{X}\underline{i}' + \dot{Y}\underline{j}' + \dot{Z}\underline{k}'$$

$$\dot{\underline{R}} = \underline{\Omega} \times \underline{R}$$

$$\underline{\rho}' = \underline{r} - \underline{R}$$

$$\dot{\underline{\rho}}' = \dot{\underline{r}} - \dot{\underline{R}} = \dot{\underline{r}} - \underline{\Omega} \times \underline{R}$$

$$\underline{\rho} = A\underline{\rho}' = A(\underline{r} - \underline{R})$$

$$\dot{\underline{\rho}} = A\dot{\underline{\rho}}' = A(\dot{\underline{r}} - \underline{\Omega} \times \underline{R})$$

Let

$$\frac{\underline{\rho}'}{|\underline{\rho}'|} = \underline{i} = A_{11}\underline{i}' + A_{12}\underline{j}' + A_{13}\underline{k}'$$

$$\frac{\underline{\rho}' \times \underline{R}}{|\underline{\rho}' \times \underline{R}|} = \underline{k} = A_{31}\underline{i}' + A_{33}\underline{j}' + A_{33}\underline{k}'$$

$$\underline{R} \times \underline{i} = \underline{j} = A_{21}\underline{i}' + A_{22}\underline{j}' + A_{23}\underline{k}'$$

$$A = \begin{vmatrix} A_{11} & A_{12} & A_{13} \\ A_{21} & A_{22} & A_{23} \\ A_{31} & A_{32} & A_{33} \end{vmatrix}$$

$$\therefore \dot{\underline{\rho}} = A\dot{\underline{\rho}}' = \dot{\rho}_x \underline{i} + \dot{\rho}_y \underline{j} + \dot{\rho}_z \underline{k}$$

Where $\dot{\rho}_x$ = velocity component along the local range vector

$\dot{\rho}_y$ = velocity component normal to the local range vector in a plane determined by the transmitter beam and the earth's center

$\dot{\rho}_z$ = velocity component normal to a plane determined by the transmitter beam and the earth's center.

From the diagram the measured value of range rate is along the apparent path or along the tangent to the path at the satellite.

$\therefore$ V measured = $\dot{\rho}_x \cos(\gamma - \delta) - \dot{\rho}_y \sin(\gamma - \delta)$

V radial = $\dot{\rho}_x$

Therefore the range rate error is

ΔV_r = V radial = V measured

$$= \dot{\rho}_x - \dot{\rho}_x \cos(\gamma - \delta) + \dot{\rho}_y \sin(\gamma - \delta)$$

and since $(\gamma - \delta)$ is a very small angle

$$\Delta V_r = (\gamma - \delta)\dot{\rho}_y$$

The above quantity is doubled for a roundtrip error.

In the ionosphere, the above correction for range-rate is modified as follows

$$\Delta \dot{\rho}_r = \left[1 + \left(\frac{f_2}{f_1}\right)^2\right](\gamma - \delta)\dot{\rho}_z$$

15.4.3 Computation of Errors in Secondary Angular Measurements.

The elevation angle error, computed in the preceding section, must be transformed into the coordinate system of the secondary angular measurements in order to determine the equivalent error in these systems.

15.4.3.1 Coordinate Conversions

To convert from the azimuth angle (ϕ), elevation angle (θ) system to other systems:

From Fig 4A the following realtions hold for the 4,y angles:

$$\left.\begin{aligned} \sin y &= \cos\theta \cos\phi \\ \cos y \sin x &= \cos\theta \sin\phi \\ \cos y \cos x &= \sin\theta \end{aligned}\right\} \rightarrow \tan x = \operatorname{ctn}\theta \sin\phi$$

also from Fig 4A the following relations hold for the l,m direction cosines.

$$l = \cos\theta \sin\phi$$

$$m = \cos\theta \cos\phi$$

From Fig 4B the following relations hold for the hour angle, declination angles

$$\sin d = \sin\theta \sin\lambda + \cos\theta \cos\phi \cos\lambda$$

$$\cos d \sin h = \cos\theta \sin\phi$$

$$\cos d \cos h = \cos\theta \cos\phi \sin\lambda - \sin\theta \cos\lambda$$

$$\therefore \tan h = \frac{\sin\phi}{\cos\phi \sin\lambda - \tan\theta \cos\lambda}$$

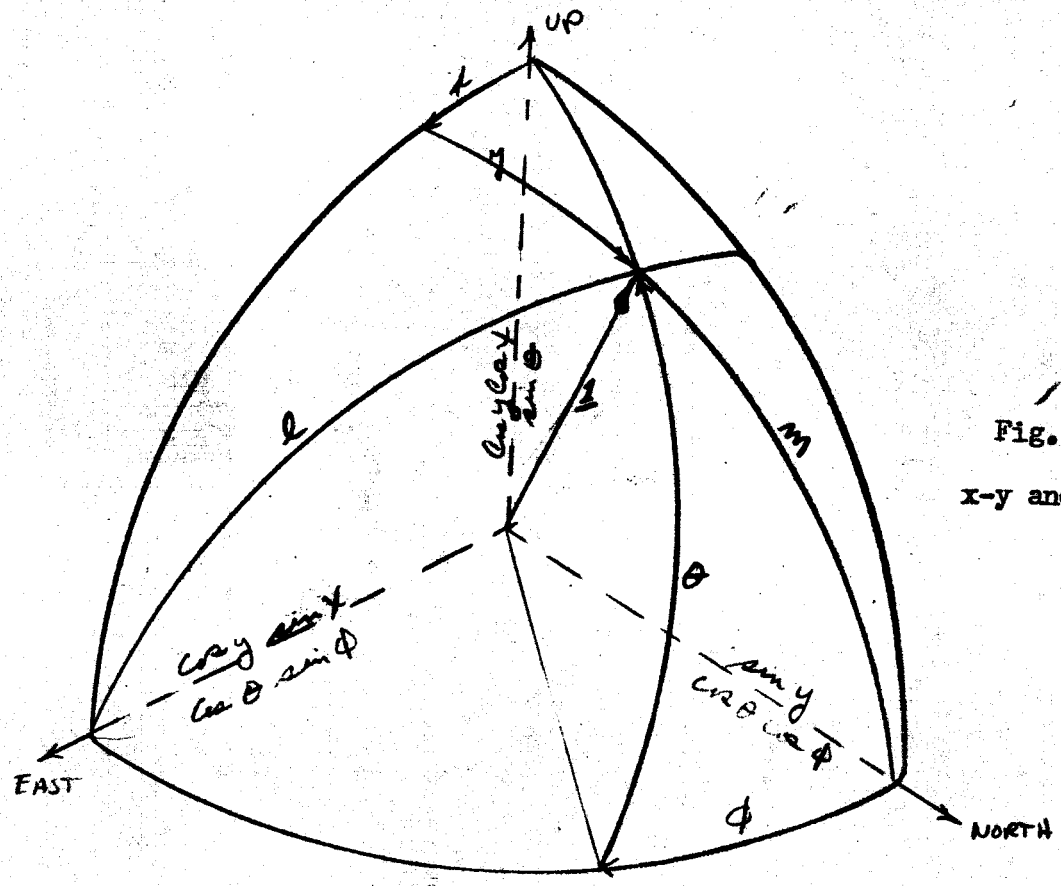

Fig. 4A

x-y and l-m System

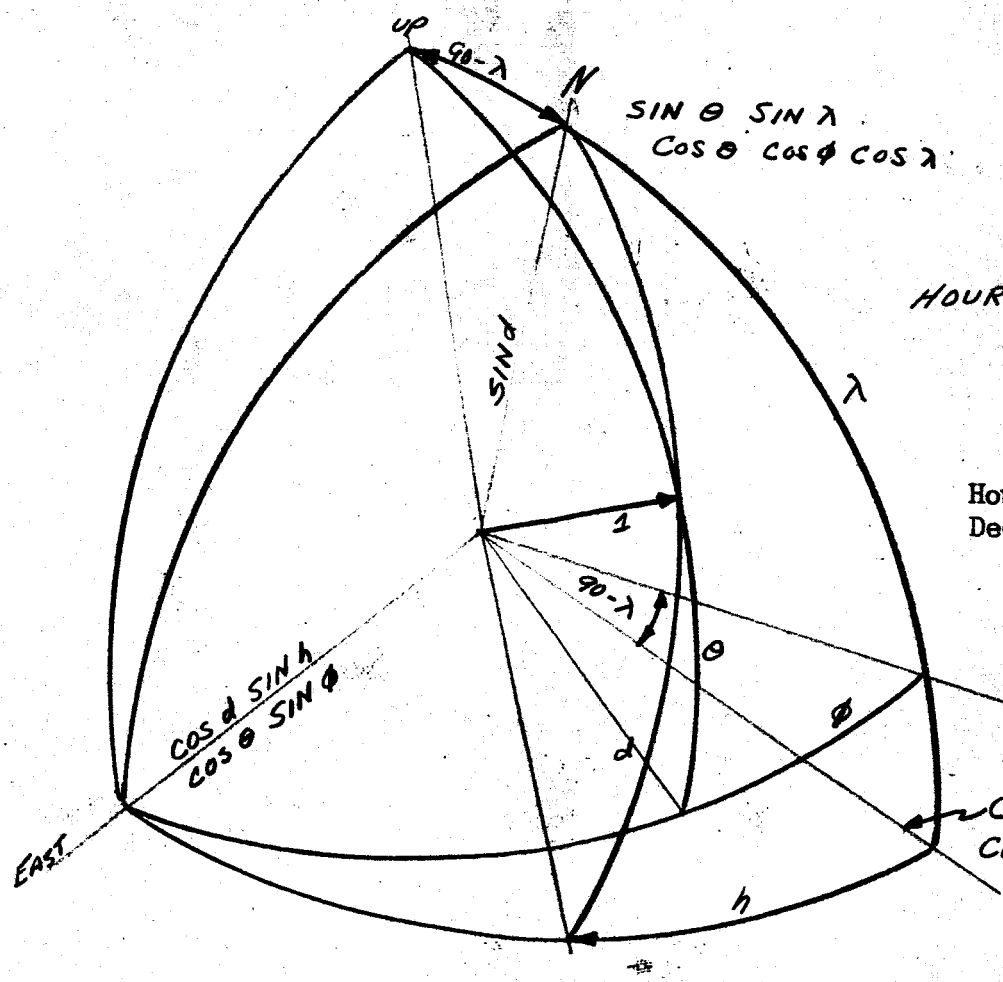

HOUR ANGLE - DECLINATION SYSTEM

Fig. 4B

Hour Angle -
Declination System

15.4.3.1 The error components

A small deviation in the elevation angle will cause a small deviation in the secondary angles. Then magnitudes can be determined by simply differentiating the previously determined coordinate conversion expressions with respect to the elevation angle.

For the x – y system

$$\frac{\partial X}{\partial \theta} = \frac{1}{SEC^2 X}(-SIN\phi\, CSC^2\theta) = \frac{-SIN\phi\, COS^2 X}{SIN^2\theta}$$

$$\frac{\partial Y}{\partial \theta} = \frac{1}{COS\, y}(-COS\phi\, SIN\theta)$$

$$\therefore \Delta X = \frac{\partial X}{\partial \theta}\delta \qquad \text{and} \qquad \Delta Y = \frac{\partial Y}{\partial \theta}\delta$$

where δ is the elevation angle error found in the preceding section.

For the l – m system

$$\frac{\partial l}{\partial \theta} = -SIN\theta\, SIN\phi$$

$$\frac{\partial m}{\partial \theta} = -SIN\theta\, COS\phi$$

$$\Delta l = \frac{\partial l}{\partial \theta}\delta \qquad \Delta m = \frac{\partial m}{\partial \theta}\delta$$

For the hour angle – declination system

$$\frac{\partial d}{\partial \theta} = \frac{COS\theta\, SIN\lambda - SIN\theta\, COS\phi\, COS\lambda}{COS\, d}$$

$$\frac{\partial h}{\partial \theta} = \frac{1}{SEC^2 h}\left[\frac{SIN\phi\, COS\lambda\, SEC^2\theta}{(COS\phi\, SIN\lambda - TAN\theta\, COS\lambda)^2}\right]$$

$$= \frac{SIN\phi\, COS\lambda\, COS^2 h}{(COS\theta\, COS\phi\, SIN\lambda - SIN\theta\, COS\lambda)^2}$$

In the preceding

ϕ is the azimuth angle

θ is the elevation angle

χ is the X-angle antenna angle

γ is Y-angle antenna angle

l is the measured l direction cosine

m is the measured m direction cosine

h is the measured hour angle

d is the measured declination

λ is the latitude of the station location

δ is the elevation angle error

References (1) S. Weisbrod and L.J. Anderson
"Simple Method for Computing Tropospheric and Ionospheric Effects on Radio Waves, Proc. of IRE Oct. 1959
pp 1770-1777.